DETERIORATION OF RC BEAMS DUE TO REINFORCEMENT CORROSION

A thesis report submitted in the partial fulfillment of the

requirements for the award of degree of

MASTERS OF ENGINEERING

IN

STRUCTURAL ENGINEERING

Submitted By

Anuj Gupta
Roll No. 801122003

Under the Guidance of

Dr. Shruti Sharma
(Asst. Professor, CED)
Thapar University
Patiala

Dr. Naveen Kwatra
(Associate Professor & Head, CED)
Thapar University
Patiala

DEPARTMENT OF CIVIL ENGINEERING, THAPAR UNIVERSITY, PATIALA-147004, INDIA JANUARY – JULY (2013)

CERTIFICATE

This is to certify that the work which is presented in this thesis report entitled "**Deterioration of RC Beams due to Reinforcement Corrosion**" being submitted by **Anuj Gupta** in partial fulfillment of requirements for the award of degree of Masters of Engineering in Structural Engineering, at Civil Engineering Department, Thapar University, Patiala, is an authentic record of the initial work carried out by him under the supervision of **Dr. Shruti Sharma, Asst. Professor**, Civil Engineering Department, Thapar University, Patiala and **Dr. Naveen Kwatra, Professor and Head of the Department**, Civil engineering Department, Thapar University Patiala.

The matter embodied in this report has not been submitted in part or full to any other university or institute for award of any degree.

SUPERVISORS

15/7/2013

Dr. Shruti Sharma

(Asst. Professor, CED)

Thapar University

Patiala

15/7/13

Dr. Naveen Kwatra

(Professor & Head, CED)

Thapar University

Patiala

COUNTER SIGNED BY

15/7/13

Dr. Naveen Kwatra

(Professor & Head, CED)

Thapar University

Patiala

Dr. S.K. Mohapatra

Dean, Academic Affairs

Thapar University

Patiala

ACKNOWLEDGEMENT

I would like to thank God for not letting me down at the time of crisis and showing me the silver lining in the dark clouds.

I wish to express my deep gratitude **to Dr. Shruti Sharma, Asst. Professor**, Civil Engineering Department, Thapar University, Patiala, and **Dr. Naveen Kwatra, Professor and Head of the Department**, Civil Engineering Department, Thapar University Patiala, for providing their uncanny guidance, support and for their patient listening of my ideas and also suggesting new ways for implementing my ideas and for the motivation and inspiration that triggered me throughout my work.

I would also like to thank all the staff members and my co-students who were always there at the need of the hour and provided with all the help and facilities, which I required for the completion of the project report.

Anuj Gupta

(801122003)

ABSTRACT

Reinforced concrete structures have not been immune to the ravages of corrosion despite the protection that concrete provides to embedded steel. Since steel corrosion remains unnoticed inside the concrete, it further accelerates and can cause loss of life and property. This report discusses the results on deterioration caused to reinforced beams due to corrosion at different levels. Five RC beams (127 x 227 x 4100) mm were casted, four of which were corroded to different levels i.e. (6days, 12days,18days & 28days) by impressed current technique, while one remain as control beam. All four beams were visually inspected at the end of their respective corrosion period for the extent of damage in the RC beams, with the increase in age of corrosion. Each beam was tested under static four-point loading and corresponding loads and deflections were recorded. The results of this experiment clearly show that there is a decrease in load carrying capacity, deflection capacity and stiffness with the increase in age of corrosion. Most importantly it was noticed that as corrosion increased the failure mode of beams shifts from predictable ductile failure to brittle failure. After the destructive testing, reinforcement was retrieved from the beams by dismantling and then cleaned to find the mass loss. The results show that there was an increase in mass loss in the reinforcement with the increase in corrosion level.

After the beam tests, bars were tested using non-destructive technique. The method used was ultrasonic testing of bars in air to detect the damages in the bars at different corrosion levels. Two ultrasonic techniques of pulse transmission and pulse echo were used to monitor the healthy and damaged bars. The signals obtained from ultrasonic testing of bars shows decrease in amplitude voltage with increasing in corrosion level, which clearly relates to the state of bars i.e. as the flaws in the bars increases amplitude signal drops. From ultrasonic test results it was also noticed that this technique is sensitive to even small damages in the bars which is of great importance.

CONTENTS

LIST OF FIGURES

Page No.

CHAPTER-1

CHAPTER-2

CHAPTER-3

CHAPTER-4

CHAPTER-5

LIST OF TABLES

CHAPTER-1

INTRODUCTION

1.1 Backround

Reinforced concrete has been used as essential materials in main load-carrying system of various structures in several countries. Reinforced concrete is recognized to be durable and capable of withstanding a variety of environment conditions. Nevertheless, failures of structures still do occur as a result of premature steel reinforcement corrosion. The corrosion of rebar in reinforced concrete, shown in Figure 1.1, deteriorates the strength of such a structure. The effects of corrosion is even more pronounced in flexural reinforced concrete member as nearly all of tension force is exerted on steel reinforcement.

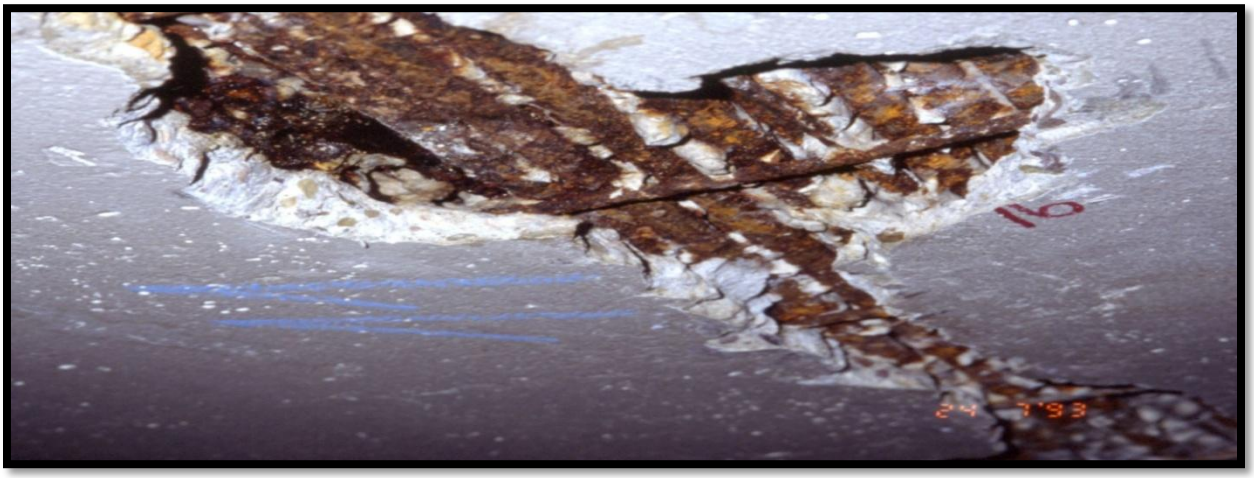

Fig 1.1 Showing corroded Steel in RC Structure (www.googleimages.com)

Corrosion of reinforced concrete was first recognized early in the twentieth century, but it has become worse in recent years with the widespread use of de-icing salts on highways and bridge decks. The corrosion of steel reinforcement in concrete greatly reduces the loading carrying capacity, shortens the service life and increases the maintenance cost of the structure. Therefore, designing against corrosion of reinforcement in concrete should be of a great concern for materials and bridge engineers, reinforced concrete corrosion specialists and those concerned with the performance of reinforced and pre-stressed concrete bridges.

It should be emphasized that the reinforcing steel is provided in reinforced concrete to resist the tensile forces, and to produce controlled cracking within that zone. However, corrosion not only deteriorates the steel bar and its function of transferring the tensile stresses, but it deteriorates the concrete by spalling of the cover. Therefore, corrosion of the reinforcement has a strong influence on the bond behavior at the interface between the steel reinforcement and concrete. As corrosion of the reinforcing steel progresses, the bond strength between the reinforcing steel and concrete diminishes progressively, and major repairs or replacement is needed. Reinforcement corrosion reduces the bond strength between steel and concrete, deteriorating the load carrying capacity of RC members. Therefore, it is very important to understand the mechanism of bond deterioration and to estimate the residual load carrying capacity of corroded RC beams.

Most national building codes aimed at ensuring that the structure being designed, constructed and operated would perform satisfactorily at the ultimate and the serviceability limit states. Therefore, a capacity reduction factor is used in the calculation of the resistance of the concrete structure for consideration of the variation of the material properties, member geometry and details, deficiencies in construction practice and quality control, and the normal variation in the applied loads. However, these considerations do not include the time-dependent behavior of loads and resistances of the concrete structures. For example, the load may change (the highway loading has increased significantly over the past several years), also, the resistance of a concrete structure will decrease due to aging of the material and the deterioration because of various environmental influences (such as corrosion of RC).

1.2 Corrosion in RC Structures

Corrosion of steel reinforcement is one of the main causes of deterioration of reinforced concrete structures. It is particularly prevalent in structures consistently exposed to aggressive environments, where deterioration often progresses at a rapid phase, resulting in severe damage to reinforcement and its surrounding concrete. While the most obvious effect of corrosion is a reduction in cross-sectional area of reinforcing bars, there are other associated effects caused by the buildup of corrosion products at the interface between the reinforcing and surrounding concrete. These corrosion products are expansive in nature and so induce radial pressures on the

surrounding concrete resulting in cracking and spalling. Furthermore, the buildup of corrosion products affects the bonding between the steel reinforcing and surrounding concrete.

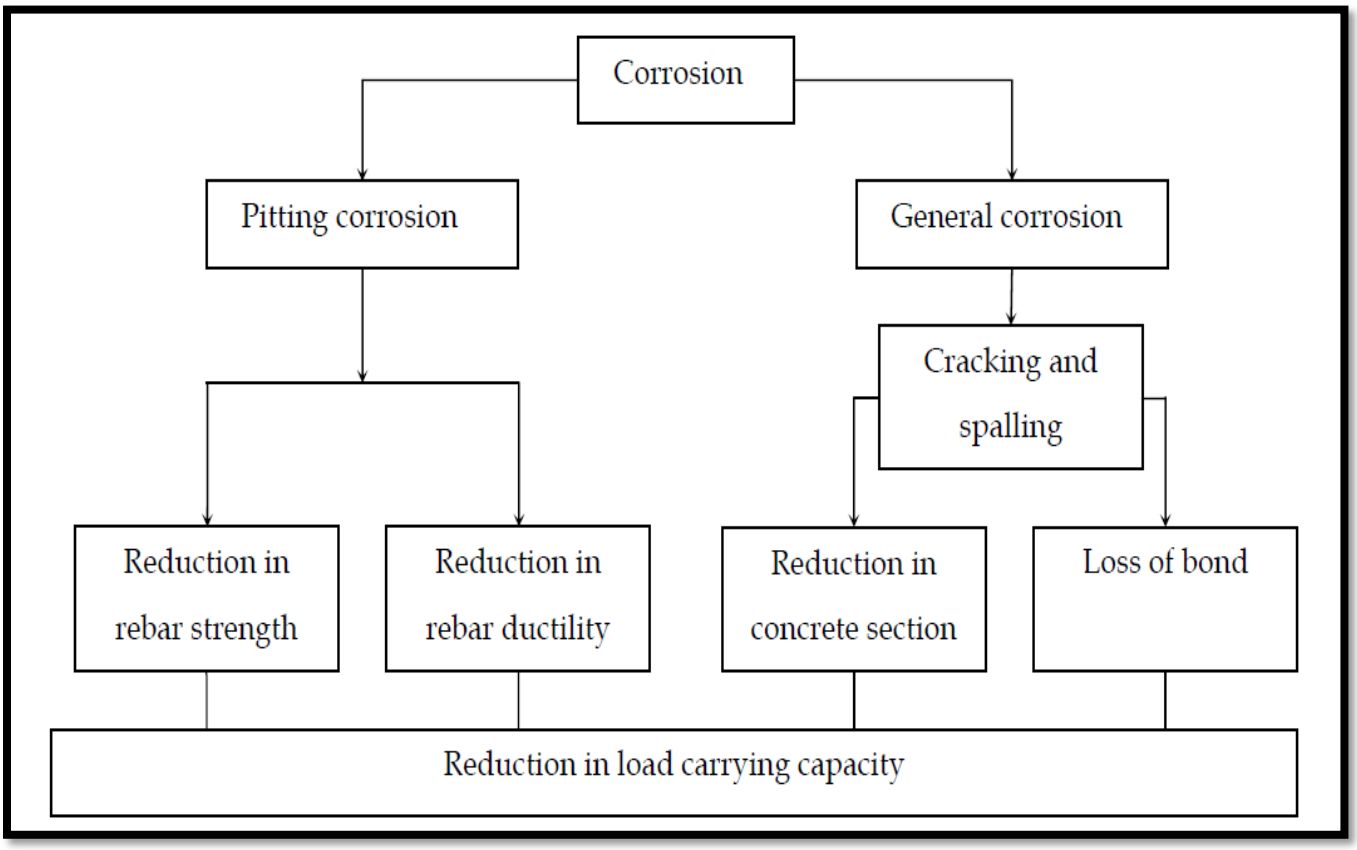

Fig: 1.2 Effects of corrosion on reinforced concrete members (www.google images.com)

1.3 Objectives and Scope of Work

The objective of this thesis is to study how progressive corrosion is detrimental to reinforced concrete beams. Specifically, the aim is to investigate both qualitatively and quantitatively the changes in flexural crack development, mode of failure and change in load-carrying capacity of RC beams under static loading subjected to corrosion at different levels. The deterioration levels are also assessed using non-destructive ultrasonic guided waves.

1.3.1 Parameters Studied

The following parameters are proposed to be measured.

- Deterioration of beams at different levels of corrosion by visual observation

- Static load-deflection behavior would be studied for beams at different levels of corrosion.
- Mass Loss of corroded beams at different levels will be measured.
- NDT of beams corroded to different levels will be studied using ultrasonic guided waves.

1.3.2 Equipments used

The equipment to be used for carrying out tests includes the following:

- Universal testing machine
- Loading frame
- LVDT for measuring deflections
- DPR 300 Pulser/Receiver for ultrasonic investigations
- PZT Cylinderical Tranducers (12mm with frequency of 1MHz)
- PC with Aquiris DAC
- Constant Voltage Supply

1.3.3 Experimental methodology

Five experimental beams of size (127 x 227 x 4100) mm were casted using M 20 grade concrete. Out of these five beams one was kept as control beam and other four beams were corroded at different levels (i.e. 6days, 12days, 18days, and 28days) using an accelerated technique. It was done by means of the impressed current technique. The successive deterioration in beams corroded to different levels was investigated using destructive (static four point loading) and non-destructive methods.

1.4 Layout of Thesis

Following the introduction to thesis, in **Chapter 1**, **Chapter 2** gives the knowledge on Corrosion in RC structures and method to monitor corrosion.

Chapter 3 discusses the Literature review i.e. the experimental work done by the people in the same field.

All the Experimental Programme along with material used and their corresponding Properties are discussed in **Chapter 4**.

Results and Discussion of the Present Study are discussed in **Chapter 5** and finally salient conclusion of the present study is given in **Chapter 6.**

In the end references cited in the entire work has be presented.

1.5 Closing Remarks

This chapter highlights the general backround of importance of RC structures and introduction to corrosion problem in these structures. It further outlines the parameters to be studied during the work and equipment required for the work.

CHAPTER-2

CORROSION IN RC STRUCTURES

2.1 Introduction

It is known that the load-carrying capacity of reinforced concrete (RC) beams is reduced with increasing corrosion. As was mentioned earlier, the degree to which performance of reinforced concrete is damaged as a result of reinforcement corrosion is a matter of great concern to those responsible for assessing and maintaining the corroded RC structures. While considerable research effort has been dedicated to the mechanisms and causes of reinforcement corrosion and to researching the durability of repair materials, considerably lower attention has been dedicated to the problem of assessing the residual strength of the corroded structure. A detailed guidance on assessment of residual strength of corrosion-damaged RC structures will be of a great importance to number of practicing and practitioners. Therefore, comprehensive knowledge (that understands and quantifies the effect of reinforcement corrosion on structural behaviour) on the effect of corrosion on structural capacity and integrity is essential for the development of effective tools for the prediction of residual service life and for the development of cost effective repair strategies. This chapter will discuss the available information on the factors that cause and control corrosion of steel in concrete, as several metals will corrode under certain conditions when embedded in concrete. Factors influencing the electrochemical process are also discussed. Hence it is very important to detect the damages in the steel caused due to corrosion. So this chapter further includes information on ultrasonic technique as non-destructive technique to detect damages in the structures.

Nondestructive testing (NDT) of civil engineering structures is a potentially valuable tool for monitoring the performance of new structures or detecting and evaluating deterioration in older structures. The inherent cost savings compared to existing destructive evaluation techniques are considerable. Currently, there are a large number of nondestructive testing techniques available for this monitoring and evaluation, though proper implementation procedures for these techniques must be developed. There is also a need to evaluate the various nondestructive testing techniques available to determine which are best suited for specific types of damage or even the absence of damage. Ultrasonic testing is a NDT method that is used to

obtain the properties of materials by measuring the time of travel of stress waves through a solid medium. The time of travel of a stress wave can then be used to obtain the speed of sound or acoustic velocity of a given material. The acoustic velocity of the material can enable inspectors to make judgments as to the integrity of a structure.

Corrosion is one of the most, if not the most, pressing durability queries of RC. The following sections report on the fundamentals of some aspects of corrosion, including the conditions that lead to corrosion and factors that influence the rate of corrosion, with the focus on corrosion initiated by chloride ions, as this was the mechanism used to initiate corrosion for the experimental.

2.2 Corrosion Mechanism

Corrosion is the process of the transformation of a metal to its "native" form, which is the natural ore state, often as oxides, chlorides or sulphates. This transformation occurs because the compounds such as the oxides "involve" less energy than pure metals, and hence they are more stable thermodynamically. The corrosion process does not take place directly but rather as a series of electrochemical reactions with the passage of an electric current. Corrosion also depends on the type and nature of the metal, the immediate environment, temperature and other related factors. The corrosion may be defined as the destructive attack of a metal by chemical or electrochemical reaction with its environment. Steel in concrete is normally immune from corrosion because of the high alkalinity of the concrete; the pH of the pore water can be greater than 12.5, which protects the embedded steel against corrosion. This alkalinity of concrete causes passivation of the embedded reinforcing bars.

Fig: 2.1 Concrete as a protective layer around steel in RC Structures (www.googleimages.com)

A microscopic oxide layer, which is the "passive" film, forms on the steel surface due to the high pH, which prevents the dissolution of iron. Furthermore, the concretes made using low water-cement ratios and good curing practices have a low permeability, which minimizes the penetration of the corrosion inducing ingredients. In addition, low permeability is believed to increase the electrical resistivity of the concrete to some degree which helps in reducing the rate of corrosion by retarding the flow of electrical currents within the concrete that accompany the electrochemical corrosion. Consequently, corrosion of the embedded steel requires the breakdown of its passivity.

Once the passive layer on the reinforcing steel has been disrupted and corrosion is activated, the chemical reactions are similar whether the corrosion was initiated by chloride attack or by carbonation. The principal cause of steel corrosion is the presence of chlorides during the preparation of the concrete. In several places close to shore, even sea sand is used as an aggregate. Some chemical admixtures, as accelerators, can contain high percentage of chlorides. De-icing salts used during winter time can introduce chlorides to the reinforced steel. The corrosion process caused by chlorides in steel is shown below in figure: 2.2.

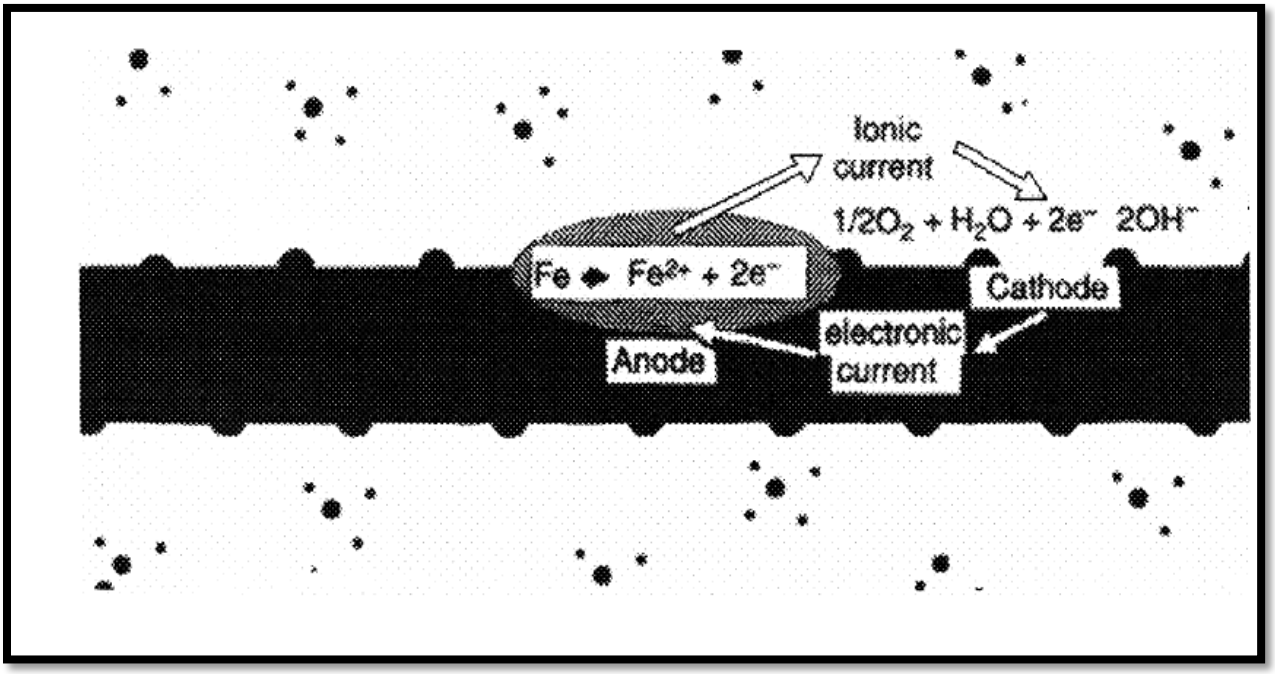

Fig: 2.2 (a) the anodic and cathodic reactions (Broomfield, 1997)

Ferrous hydroxide forms as the 2Fe++ ions at the anode combine with the hydroxide ions flowing from the cathode. In the presence of oxygen and moisture, the ferrous hydroxide

converts to ferric oxide i.e. rust. The quantity of iron that reacts (rusts) is proportional to the corrosion current and time in accordance with Faraday's law. This law is used in many of the tests described in the following sections.

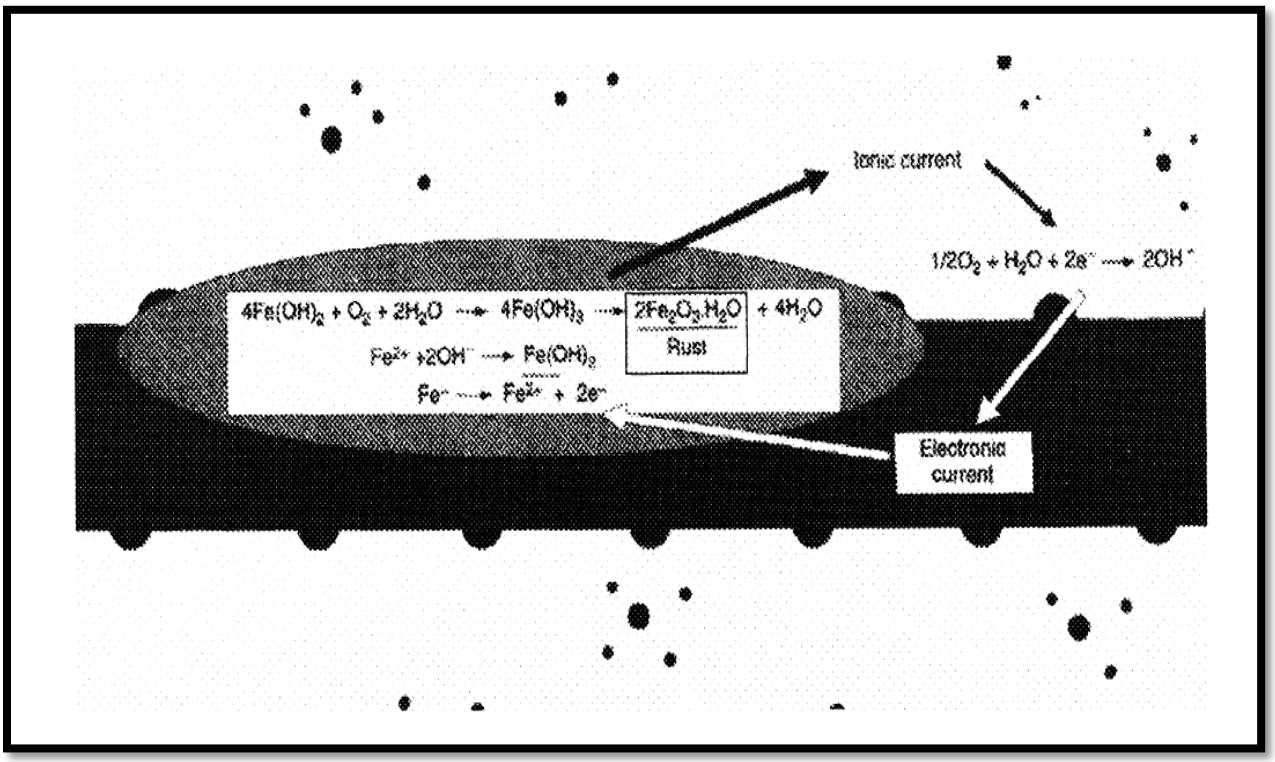

Fig: 2.2 (b) Anodic and Cathodic reactions on steel (Broomfield, 1997)

When unhydrated, ferric oxide is dense and has a volume of around twice that of the steel it replaces. When it becomes hydrated (takes in water) it swells and becomes porous. This swelling can lead to a volume increase of between two to four-fold at the steel-concrete interface.

This gives the flaky red/brown rust on the reinforcing bar and can cause cracking (and spalling) of the cover concrete. Some of the rust will be accommodated in the concrete pore structure adjacent to the corroding bar. Corrosion is the loss of iron at the anode, whilst rust is the product formed at the cathode. The effects of various parameters on the corrosion process are summarized in Table 2-1.

Table 2.1 Parameters affecting the corrosion process (Webster, 2000)

Table 2-1: Parameters affecting the corrosion process

Parameter	*Effect*
Moisture	Moisture is required initially for the cathodic reaction and then for rust formation at the anode. Without sufficient moisture, the rate of corrosion will be negligible.
Oxygen	Oxygen is required initially for the cathodic reaction and then for rust formation at the anode. It is possible that chloride-induced corrosion will be controlled by oxygen availability as chlorides typically enter with moisture. With low levels of oxygen, the rate of corrosion will be negligible.
Resistivity	The higher the resistivity, the lower the corrosion current will be. Resistivity increases with temperature, and decreases with increasing moisture content (RH).

2.3 Effect of Corrosion on Structural Capacity

There are three broad types of corrosion experienced by reinforcing bars namely, **Pitting**, **General** and **Macro-cell** corrosion. The factors governing these types of corrosion are discussed below.

- **Pitting corrosion**

Pitting corrosion is most likely to occur in concrete with good conductivity, a high content of alkali (i.e. non-carbonated) and a moderate level of chloride (or chloride reaching only isolated areas of the reinforcement). The chloride ion breaks down the passive film locally in those areas where the concentration is high or the passive film is weak. A localized corrosion cell is formed with adjacent areas of passive steel acting as a cathode, where oxygen is reduced, and the anodic dissolution of iron taking place only at the small central anode. Several factors then maintain or aggravate the development of the existing pit rather than to spread the corrosion or nucleate new pits. Acid is produced at the anode (pit site) due to hydrolysis reactions and alkali at the cathode due to the reduction of oxygen. Under the acid conditions present, the corrosion products formed

are soluble. Therefore, considerable amounts of corrosion can occur without spalling of the concrete. In pitting corrosion access of oxygen is the major factor in determining the total amount of corrosion. However, with the large cathode/anode area ratio, intense pitting can result even with limited oxygen supply.

- **General corrosion**

General corrosion may result from carbonation or due to the presence of large amounts of chlorides, so a large number of closely situated pits are formed. Both anodic and cathodic processes take place everywhere on the surface, and the pH shifts associated with each of these processes cancel each other.

This means that the anodic dissolution takes place in a near neutral or alkaline environment, where oxygen has access. The corrosion product, in this case, is solid rust, which occupies about 4 times the volume of the metal that has been corroded. The buildup of corrosion products on the steel reinforcing bars exerts tensile forces on the concrete cover resulting in cracking and spalling.

In practice, general corrosion caused by carbonation or by chlorides has different characteristics. In cases, where carbonation has penetrated deeply, the concrete is likely to be rather permeable and semi-dry, and the rate of corrosion, once it starts, is probably controlled by the relatively high resistivity and lack of water rather than the diffusion of oxygen. The 'time-of wetness', known to be an important factor in atmospheric corrosion, is an appropriate measure of corrosion rate under these conditions.

Conversely, corrosion in chloride-rich concrete is more often found where water is abundant and resistivity of the concrete is low. Under these conditions the diffusion of oxygen through the water-filled pores is the rate determining factor.

- **Macro-Cell Corrosion**

Under certain conditions, it is possible for the anodic and cathodic sites to be significantly remote from each other so that the reaction products from the anode and cathode reactions do not interact. Such conditions can exist if some of the steel is in anaerobic conditions and if the concrete is sufficiently conductive (ie. low resistivity, 12 kΩcm or less) to carry the macro-cell corrosion current. Typically this occurs in a concrete member with its lower parts permanently

immersed in sea-water and extending upwards through the tidal and splash zones. This may include bridge and wharf piles, and skirting panels for wharves or promenades. Under conditions of macro-cell corrosion, the cathode reaction occurs in the oxygen-rich tidal or splash zones, with no noticeable effect on the concrete.

The steel, however, dissolves at the anode which will be the immersed lower part of the member, saturated with sea-water but with little or no available oxygen. The ferrous ions react with anions present in sea-water (chlorides, sulphates, hydroxides) to produce ionic compounds which form a sticky black/green colloidal paste within the concrete, often referred to as "black rust". Since this is not an expansive reaction, the colloidal corrosion products will opportunistically occupy available spaces such as voids and pores, or fracture planes if cracking is present from other causes. The colloid can slowly migrate to the surface where, if oxygen is more abundant, it may form conventional brown/orange rust stains, or it may simply be lost in the sea-water. Since there are few outward signs of this mechanism, and although this process is generally slow, significant loss of metal can occur over time with subsequent loss of structural integrity and possible sudden, catastrophic failure. Even concrete of high quality and density can corrode by this mechanism. General corrosion cycle of uncoated steel bar in concrete is shown in Fig: 2.3.

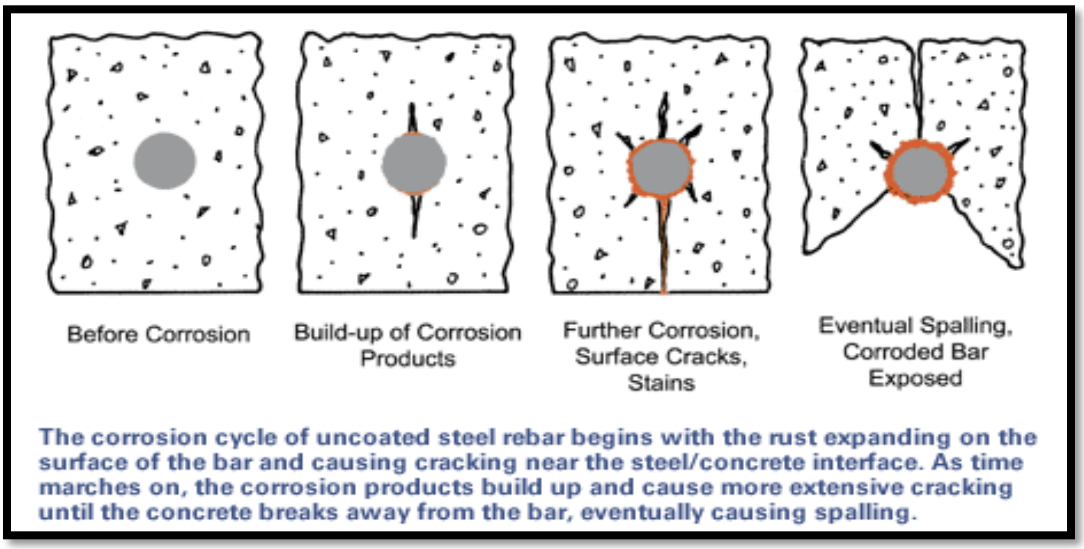

Fig: 2.3 Corrosion Cycle in Reinforced Concrete (www.googleimages.com)

2.3.1 Effect on Steel

In the case of general corrosion, bond is more likely to affect structural capacity than is loss of tensile strength of reinforcement. Experiment results indicated that the level of reinforcement corrosion does not influence the tensile strength of steel bars (calculated on the actual area of cross-section), but reinforcing steel bars with more than 12% corrosion indicates a brittle failure (Almusallam A. A., 2001). It's concluded that the strength ratio and elastic modulus of reinforcement are not significantly affected by corrosion and consequently the strength and modulus of elasticity of non-corroded bars can be adopted in practice (Du et al. 2005).

2.3.2 Effect on Concrete

The corrosion products have higher volume than the original steel. With the increase of corrosion level, the volume expansion of excessive rust products on the surface of steel induces radial compression pressure and hoop tensile pressure on the surrounding concrete after corrosion products fill the pores in concrete. When the hoop tensile stress exceeds the tensile strength of concrete, the concrete will crack. Hence, properties of cracked concrete should be considered to demonstrate the behavior the RC member after concrete cracks.

2.4Electrochemical Methods to measure Corrosion

As a result of the development of the fundamental understanding of corrosion electrochemistry, fast and accurate potentiostats, and computer technology, a suite of electrochemical techniques exists for the study of corrosion. These techniques provide the technologist with the ability to monitor corrosion rates in service, giving early warning of conditions that could adversely affect performance and integrity. They also provide the experimentalist with the ability to determine corrosion rate with high sensitivity, assess rate controlling mechanisms, and in some cases make life predictions.

Electrochemical methods are used to evaluate corrosion activity of steel reinforcement. As is the case with other nondestructive test methods, an understanding of their underlying principles and inherent limitations is needed to obtain meaningful results. In addition, an understanding of the factors involved in the corrosion of steel in concrete is essential for reliable interpretation of data from this type of testing. Three commonly used methods are:

(1) Half-cell potential;

(2) Concrete resistivity; and

(3) Polarization resistance.

- **Half-Cell Potential**

When there is active corrosion, current flow (ion migration) through the concrete between anodic and cathodic sites is accompanied by an electric potential field surrounding the corroding bar. The equipotential lines intersect the surface of the concrete and the potential at any point can be measured using the half-cell potential method. By mapping equipotential contours on the surface, those portions of the structure where there is a high likelihood of corrosion activity are identified by their high negative potentials.

- **Concrete Resistivity**

The half-cell potential method provides an indication of the likelihood of corrosion activity at the time of measurement. It does not, however, furnish direct information on the rate of corrosion of the reinforcement. As has been discussed, after a bar loses its passivity, the corrosion rate depends on the availability of oxygen for the cathodic reaction. It also depends on the electrical resistance of the concrete, which controls the ease with which ions migrate through the concrete between anodic and cathodic sites. Electrical resistance, in turn, depends on the microstructure of the paste and the moisture content of the concrete. Thus, measurement of the resistivity of the concrete is useful in conjunction with a half-cell potential survey. The resistivity is numerically equal to the electrical of resistance (in ohms) times length.

- **Polarization Resistance**

The polarization resistance technique is a well-established method for determining corrosion rate by using electrolytic test cells. The technique basically involves measuring the change in the open-circuit potential of the short-circuited electrolytic cell when an external current is applied to the cell. For a small perturbation about the open-circuit potential, there is a linear relationship between the change in voltage ΔE and the change in applied current per unit area of electrode Δi. The ratio $\Delta E/\Delta i$ is called the polarization resistance Rp. Because the current is expressed per unit area of an electrode that is polarized, the units of Rp are ohms times area.

Each method provides distinct information related to the corrosion status. The half-cell potential provides an assessment of the likelihood that there is active corrosion in the structure. It does not, by itself, provide information on the corrosion rate. One of the controlling factors for corrosion rate is the concrete resistivity, and measurement of concrete resistivity is a useful complement to the half-cell potential survey. The polarization resistance technique allows measurement of half-cell potential along with the actual corrosion current. The latter can be used to estimate the rate of section loss of the bar. It is emphasized that any of these measurements represent the conditions at the time of testing.

2.5 Ultrasonic Testing

The term “ultrasonic” refers to sound waves having a frequency above the human ear's audibility limit, which is about 20,000 Hz. Ultrasonic testing has been used to successfully evaluate the quality of concrete for approximately 60 years. This method can be used for non-intrusively detecting internal defects in concrete. Some of these flaws include deterioration due to sulfates or other mineral attack, and cracking and changes due to freeze-thaw cycling.

Nondestructive material testing with ultrasonic is more than 40 years old. From the very first examinations, using ultrasonic oscillations for detection of flaws in different materials, it has become a classical test method based on measurements with due regard to all the important influencing factors. Today it is expected that ultrasonic testing, supported by great advances in instrument technology, give reproducible test results within narrow tolerances. This assumes exact knowledge of the influencing factors and the ability to apply these in testing technology.

2.5.1 Ultrasonic Principles

The UT scope mainframe generates ultrasonic vibrations and sends them through the test object in a beam of short bursts of energy. Any discontinuity in the path of the ultrasonic beam, as well as the far side of the test object, reflects the vibrations back to the instrument. The time required for the initial pulse to travel through this material and subsequently return as an echo is displayed on a cathode ray tube (CRT) as a thickness or distance measurement.

The sound waves are generated as recurrent changes in electrical voltage occurring at an ultrasonic rate, since it is above the audible range. Ultrasonic vibrations of lower frequencies act in essentially the same manner as audible sound waves. Ultrasonic waves of the higher

frequencies behave somewhat like light waves. Ultrasonic vibrations have two basic characteristics:

a. They are reflected by discontinuities occurring in the medium through which they are traveling and,

b. They tend to travel in a straight line, as do light waves, due to the shortness of the wave length employed.

Ultrasonic Testing requires following units:

1. Transducers
2. Pulser/Receiver
3. Display Devices
4. Coupling Agent

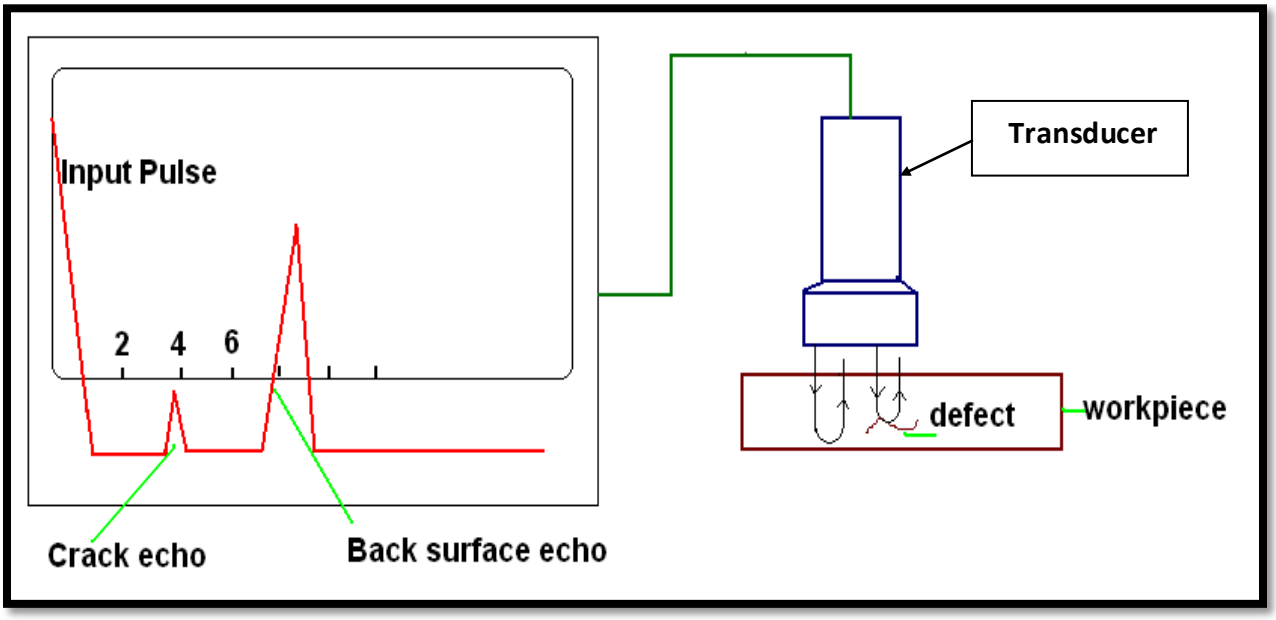

Fig: 2.4 General Ultrasonic Inspection Principles (www.googleimages.com)

- **Transducers**

Ultrasonic transducers perform according to two main parameters: resolution and sensitivity. The resolution of a particular transducer is denoted by its ability to discern between two discontinuities that are on top of one another. A transducer with sufficient resolution will stop ringing, or vibrating, from the first discontinuity before receiving the echo from the second discontinuity. If the ceramic does not stop ringing before the second echo is received, the second

echo is masked from the test system. Sensitivity of an ultrasonic transducer refers to the ability to detect small discontinuities. Reference blocks with standard sized defects are used to gauge the sensitivity of a particular transducer.

The frequency of the transducer is chosen based on the required sensitivity and depth of penetration. Remember that the higher the frequency, the better the sensitivity, but lower penetration depth.

- **Pulser/Receiver (P/R)**

These devices provide the high-voltage pulse required by the ultrasonic transducer as well as signal conditioning before the analog signal is passed to the digitizer. For use within an automated test system, the P/R should be computer programmable via a standard PC bus. The devices are typically programmed one time at the beginning of the test to set the pulse voltage level, pulse repetition frequency, damping, band pass filtering settings, and several other parameters. After these parameters are set, these devices are passive and do not send any information back to the PC during operation.

- **Display**

The signal received by the ultrasonic test equipment is typically displayed digitally with modern equipment. The results consist of a direct reading of display time on an x-y coordinate system. The x-axis becomes the time trigger and the y-axis represents the mechanical energy received. The display units can also illustrate defect or anomaly locations and sizes, depending on the type of data requested by the user.

- **Coupling agent**

A coupling agent is usually required to ensure the efficient transfer of mechanical energy between the transducer and the tested material. The purpose of placing the coupling material between the transducer and test specimen is to eliminate air between the respective surfaces. Typically, coupling agents consist of viscous liquids such as grease, petroleum jelly, or water-soluble jelly.

2.5.2 Ultrasonic Waves

In solids, sound waves can propagate in four principle modes that are based on the way the particles oscillate. Sound can propagate as longitudinal waves, shear waves, surface waves, and in thin materials as plate waves. Longitudinal and shear waves are the two modes of propagation most widely used in ultrasonic testing. The particle movement responsible for the propagation of longitudinal and shear waves is illustrated below.

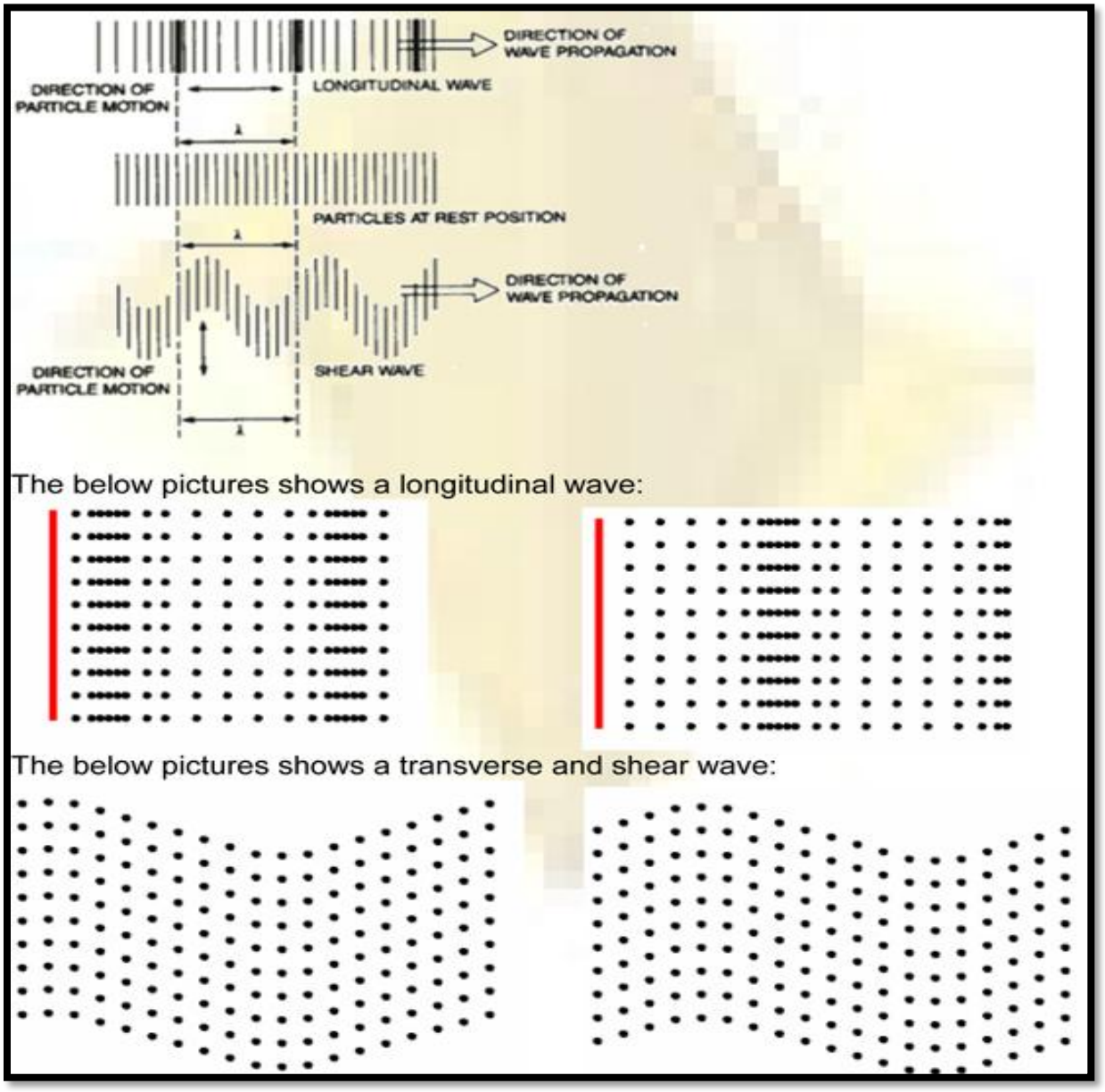

Fig: 2.5 General View of Propagation of waves (www.googleimages.com)

Longitudinal, or compression, waves exist when the motions of the particles of a medium are parallel to the direction of wave travel. It is the type used when employing the straight beam technique of testing. This type wave is most often used in ultrasonic testing, since it will travel in liquids or solids, and is easily generated and detected.

When shear waves are generated in a material, the movements of the particles in that medium are at right angle to the direction of the wave propagation. They usually travel in a form of a beam of small cross section. Shear waves have a velocity that is approximately one-half that of the longitudinal waves. The shear wave is the type that is generated when using the angle beam technique of testing.

2.5.3 Main applications of Ultrasonic Testing

- Ultrasonic Testing (UT) is used to locate surface and subsurface defects in many materials including woods and plastics.

- Ultrasonic Testing (UT) is used to measure thickness of materials.

- Ultrasonic Testing (UT) measures characteristics of materials based on sound velocity and attenuation measurements.

2.5.4 Methods of Ultrasonic Testing

Ultrasonic Testing (UT) uses high frequency sound waves (typically in the range between 0.5 and 15 MHz) to conduct examinations and make measurements. Besides its wide use in engineering applications (such as flaw detection/evaluation, dimensional measurements, material characterization, etc.), ultrasonics are also used in the medical field (such as sonography, therapeutic ultrasound, etc.). In general, ultrasonic testing is based on the capture and quantification of either the reflected waves (*pulse-echo*) or the transmitted waves (*through-transmission*). Each of the two types is used in certain applications, but generally, pulse echo systems are more useful since they require one-sided access to the object being inspected

- **Pulse Echo Method**

The single transducer (pulse-echo) technique is the simplest and most common form of flaw detection. Sound waves from the instrument are transmitted through the test object by a transducer and reflected back by the far side surface of the test object. The Initial Pulse (IP) appears on the left hand side of the cathode ray tube (CRT) screen. The back reflected pulse from the far side of the test object appears on the right hand side of the CRT screen. Presence of a flaw shows up as a reduced amplitude pulse anywhere between the initial pulse and the back reflected pulse. When a flaw is large enough to intercept the sound wave completely, there is no back-reflected pulse from the far side of the test object displayed on the CRT.

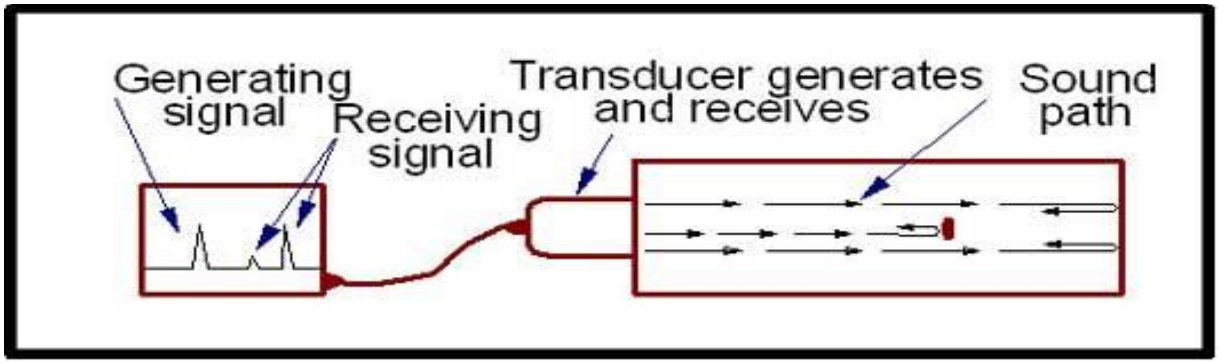

Fig: 2.6 Typical Ultrasonic setup in pulse/echo mode (www.google images.com)

- **Pulse Transmission Method**

The thru-transmission technique requires two transducers; one operating as a transmitter, the other as a receiver, with each positioned at opposite sides of the test object. This technique is used where the geometry or internal condition of the test object prevents a round trip of the sound wave as described for the pulse echo technique. The initial pulse appears on the left hand side of the CRT screen and the received pulse appears at the right side of the screen. The presence of a flaw within the test object causes a reduction in amplitude of the sound wave pulse intercepted by the receiving transducer. Complete lack of a received sound wave pulse indicates that the flaw is large enough to block (or absorb) the transmitted sound wave completely.

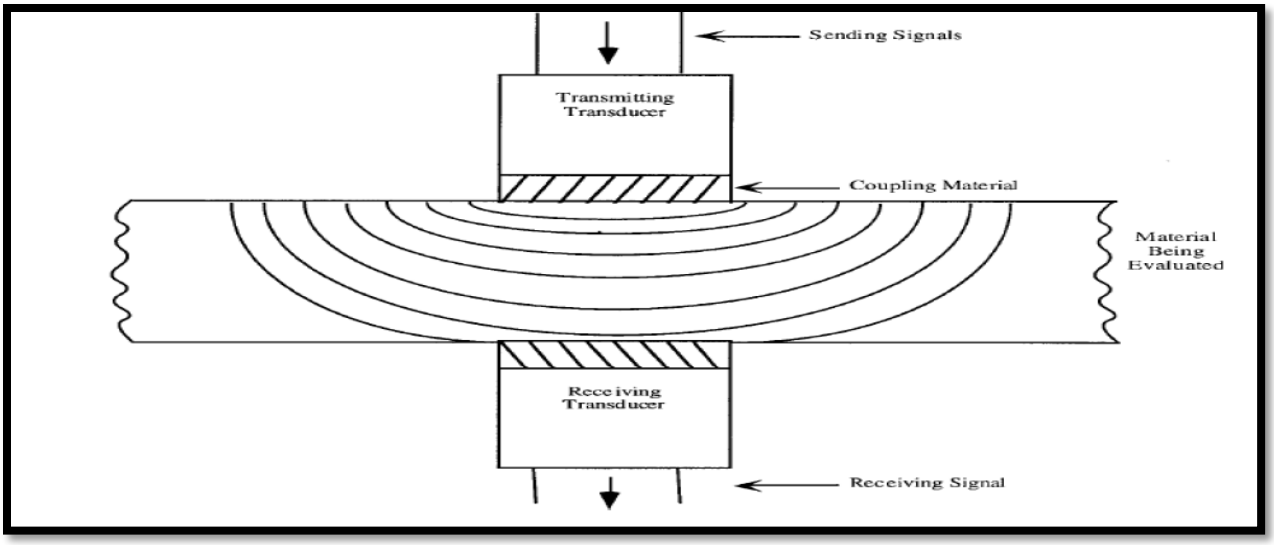

Fig: 2.7 Principle of through transmission of Ultrasonic Testing (Vermani, 2008**)**

2.5.5 Advantages of Ultrasonic Testing (UT)

- Ultrasonic Testing (UT) requires minimal part preparation is required for material to be tested.
- Ultrasonic Testing (UT) is sensitive to both surface and sub-surface discontinuity.
- The depth of penetration for flaw direction or measurement is superior to other NDT methods.
- Only single sided access is needed when the pulse-echo technique is used.
- Electronic equipments provide instantaneous results.
- Detailed images can be produced with automated systems.
- Ultrasonic Testing (UT) has other uses as thickness measurement, in addition to flaw detection.
- Ultrasonic Testing (UT) provides fast, reliable measurement and testing.
- Ultrasonic Testing (UT) can be used for any type of material type.

- Instruments used for Ultrasonic Testing (UT) are portable for ready to use and transport.

2.5.6 Disadvantages of Ultrasonic Testing (UT)

- Surface must be accessible
- Ultrasonic Testing (UT) is highly sensitive to surface roughness
- Ultrasonic Testing (UT) requires coupling mechanism
- Linear defects which are parallel to sound beam may be undetected/unnoticed.
- Coarse grain particles are difficult to inspect for Ultrasonic Testing (UT)

The most successful application of ultrasonics has been in the detection and location of the presence of discontinuities in concrete specimens and structures. Ultrasonic testing has been proven to be capable of detecting various anomalies including rebar, prestressed tendons, conduit delaminations, voids, and cracks. The reliability of ultrasonic tests has been confirmed when applied to the testing of concrete and masonry structures.

2.6 Effectiveness of Impressed Current Technique to Simulate Corrosion of Steel Reinforcement in Concrete

Accelerated corrosion by means of the impressed current technique is widely used in concrete durability tests. The impressed current technique in accelerated corrosion studies is used so that tests can be completed within a reasonable amount of time. Corrosion is induced by applying an electrochemical potential between the reinforcing steel anode and cathode. The potential applied is varied, in order to achieve a constant applied current density. The majority of previous studies have used current densities that are from 3 to 100 times greater than the maximum current densities reported from field studies (Andrade et al. 1990, 1993; Broomfield 1997). The applied impressed current densities have typically ranged from 200 to 3,000 mA/cm2, with a maximum of 10,400 mA/cm2 (Almusallam et al. 1996b0 and a minimum of 45 mA/cm2 (Bonacci et al., 1998). A summary of some of the previous accelerated corrosion tests on reinforced-concrete members is presented in Table2.2. Although accelerated corrosion using an impressed current is typically used, there is little information in the literature on the influence

of varying the current density level on the effects of reinforcement corrosion in concrete structures.

Table 2.2 Sumary of Some Previous Accelerated Corrosion Tests (El Maaddawy et al. 2003)

Table 1. Summary of Some Previous Accelerated Corrosion Tests

Study	Specimen type	Applied current (mA)	Current density ($\mu A/cm^2$)	Cathode type	Corrosion environment
Uomoto et al. (1984)	Beams	167	200–630	External copper plate	Constant immersion, 5% NaCl solution
Tachibana et al. (1990)	Beams	1,000[a]	500	External copper plate	Constant immersion, 3.3% NaCl solution
Al-Sulaimani et al. (1990)	Beams	Varies	2,000	External stainless steel plate	Constant immersion, salted solution[c]
Lee et al. (1996)	Beams	1,000	2,000[a]	External copper plate	Constant immersion, 3% NaCl solution
Lee et al. (1997)	Beams	672	230[a]	External copper plate	Constant immersion, 3% NaCl solution
Phillips (1991)[b]	Slabs	1,800 (average)	600 (average)	External steel mesh	Constant immersion, 3% NaCl solution
Almusallam et al. (1996a)	Slabs	2,000	3,000	External stainless steel plates	Specimen soffits in contact with 5% NaCl solution
Tachibana et al. (1990)	Bond pull-out	32	500	External copper plate	Constant immersion, 3.3% NaCl solution
Al-Sulaimani et al. (1990)	Bond pull-out	Varies	2,000	External stainless steel plate	Constant immersion, salted solution[c]
Almusallam et al. (1996b)	Bond pull-out	400	10,400[a]	External stainless steel plate	Constant immersion, 3% NaCl solution
Bonacci et al. (1998)[b]	Columns	150 (average)	45 (average)[a]	Internal stainless steel bar	2.5 day dry, 1 day immersion cycle in 3% NaCl solution. Concrete cast with 2% NaCl by weight of cement

2.7 Closing Remarks

This chapter highlights the fundamentals of corrosion. It briefly describes the corrosion mechanism i.e how the corrosion originates in the structures, it main types and factors which avail the condition for corrosion in reinforced concrete structures. It further describes the electrochemical methods involved in monitoring of corrosion. And this chapter gives a brief detail about the ultrasonic testing of bars as an non-destructive technique to detect damages in RC structures. It also gives introduction on the impressed current technique, to corrode steel steel in short duration so as to carry out durability tests.

CHAPTER-3
LITERATURE REVIEW

It is known that the load-carrying capacity of reinforced concrete (RC) beams is reduced with increasing corrosion. Reinforced concrete structures have a limited service life. The durability of concrete structures depends on the resistance of the concrete against chemical and physical factors and its ability to protect the embedded reinforcement against corrosion. So it is very important to monitor the amount or severity of damage caused due to corrosion which actually is a serious problem. So some non-destructive techniques like Ultrasonic testing are there which encounters the extent of damage in the material without destructing it. This chapter explains the work of some researchers on various effects of corrosion on the health of reinforced concrete structures and how to monitor these damages using ultrasonic techniques.

3.1 Effect of Corrosion on Performance RC Structures

Yoon et al., **(2000)** involved testing RC specimens of dimensions 100x150x1170 mm. The beams were tested whilst under a sustained load using a mechanical loading frame shown in Fig. 3.1, in the absence of a sustained load but having been previously loaded and in the absence of a sustained load with no previous loading. Loading on the beams tested under a sustained load was induced by hanging weights on a lever beam and the load was then transferred to the test beams by a load distribution beam. A lever arm was employed to amplify the load from the applied weights. The frame applied tensile stresses at the top part of the beams so that they were tested with the tensile face up. The arrangement to test inverted beams was mainly done to enable a plastic dam of NaCl solution to be built at the top of the beams. This arrangement also exposed the tensile face of the beams where the severest level of corrosion was expected and repair of damaged concrete would often be carried out.

.

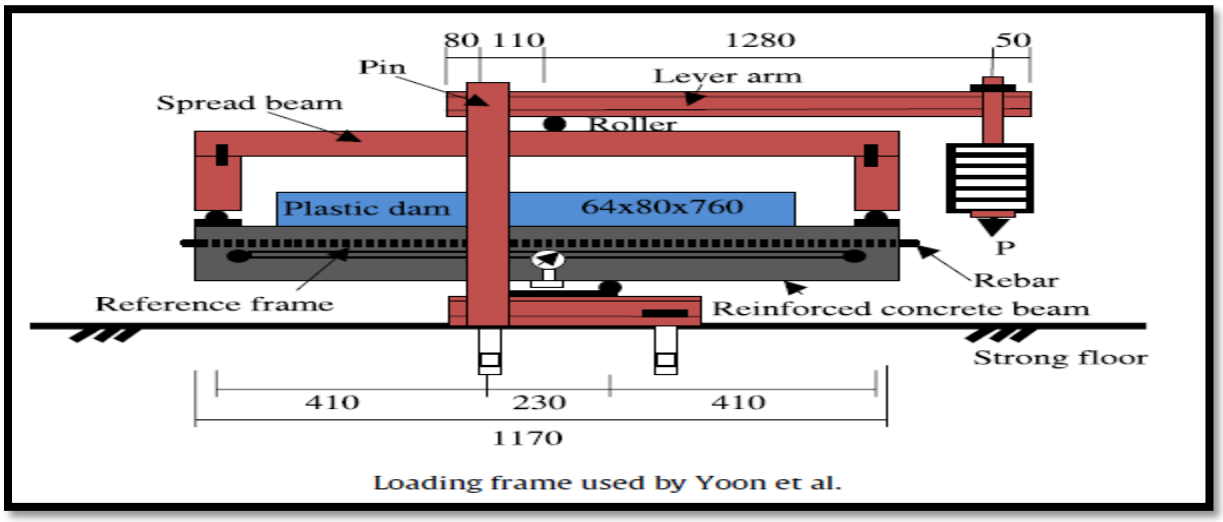

Fig: 3.1 loading Frame used by Yoon et al., 2000

The overall configuration of the loading system was that specimens were tested over a span of 1050 mm using a 4-point bending configuration with a constant moment region of 230 mm at the middle part of the beams. They were tested under sustained load levels equivalent to 0%, 20%, 45%, 60% and 75% of the ultimate capacity of a virgin beam. For specimens tested under 0%, 45% and 75% sustained loads and under previous loads, the testing process was divided into two stages; corrosion initiation stage; and corrosion propagation stage. Other specimens were only tested under the corrosion propagation stage. During the corrosion initiation stage, beams were subjected to cycles of four days wetting with 5% solution of NaCl and three days drying in natural air. A half-cell potential was used to monitor corrosion initiation during this stage. The results indicated that beams that were previously loaded to high loads had shorter corrosion initiation periods (2 days and 4 days for beams previously loaded to 75% and 45% loads respectively). The results also showed that beams with high sustained loads had shorter corrosion initiation periods (3 days, 10 days and no corrosion initiation after 30 days for beams tested under 75%, 45% and 0% loads respectively).

Central deflections of specimens that were corroded under a sustained load were continuously monitored during the test. As expected, during the corrosion initiation stage, all specimens illustrated increased deflections with decreasing rates overtime due to creep effects, with the higher loaded specimens exhibiting increases in both initial and long-term deflections. During the corrosion propagation stage, a constant voltage was applied on the tensile steel bars to accelerate the corrosion process. Deflections suddenly increased at the application of the voltage and reached a plateau after a certain level of corrosion. The sudden increase in deflections after applying voltage shows that there

was no gain in the bond between the steel and the concrete at the early corrosion stages. Furthermore, increase in deflections when applying the voltage after 50 days of testing beams at very high sustained loads (up to 75% of the ultimate capacity) clearly indicates that it is the corrosion that controls deflections of beams corroded whilst under a sustained load and not the creep. The author attributed the increased deflections to the loss in the stiffness due to cracking of the cover concrete.

The results showed that beams subjected to high levels of sustained loads and high previous loads had higher corrosion rates. These rates were found to generally increase with the duration of electrolysis and at an increasing rate.

Castel et al., (2000) studied the mechanical behaviour of RC beams with corroded reinforcement. They conducted two separate experimental studies; the first one consisted of four beams, which were naturally corroded in a salt fog environment for 14 years in an attempt to mimic actual field conditions, with dimensions of 150 x 280 x 3000 mm. Beam ultimate strength were determined by using three-point loading tests. The average reported degree of corrosion was 10% and the reduction in flexural strength was 20% with a 70% reduction in ductility. They concluded that the decrease in stiffness was due to the reduction of both the steel cross -sectional area and bond strength. This was attributed to the fact that the average maximum cross -section loss near the centre of the beam was 20%, which would theoretically result in a stiffness decrease of 15%. However, the total stiffness loss for one of the beams tested was 35%; hence, there was a 20% difference in loss that was unaccounted for, which the researchers suspected to be the result of bond deterioration (Castel et al., 2000). They also said that the concrete cracks resulting from compression reinforcement corrosion have an insignificant effect on the global behavior of RC beams.

Ballim and Reid., (2003) tested beams having dimensions of 100 x160 x1500 mm. The beams were tested under load over a span of 1050 mm in a 4-point bending configuration with a constant moment region of 350 mm in the middle span. The load on the beams was applied using a compressed spring and then transferred to the test specimens via a load distributor as shown in Fig. 2. The bottom supports of the beams and underside of the beams (tensile region) were placed inside a tank containing a 3% solution of NaCl. Corrosion of tensile steel bars was accelerated by impressing current of 300mA.

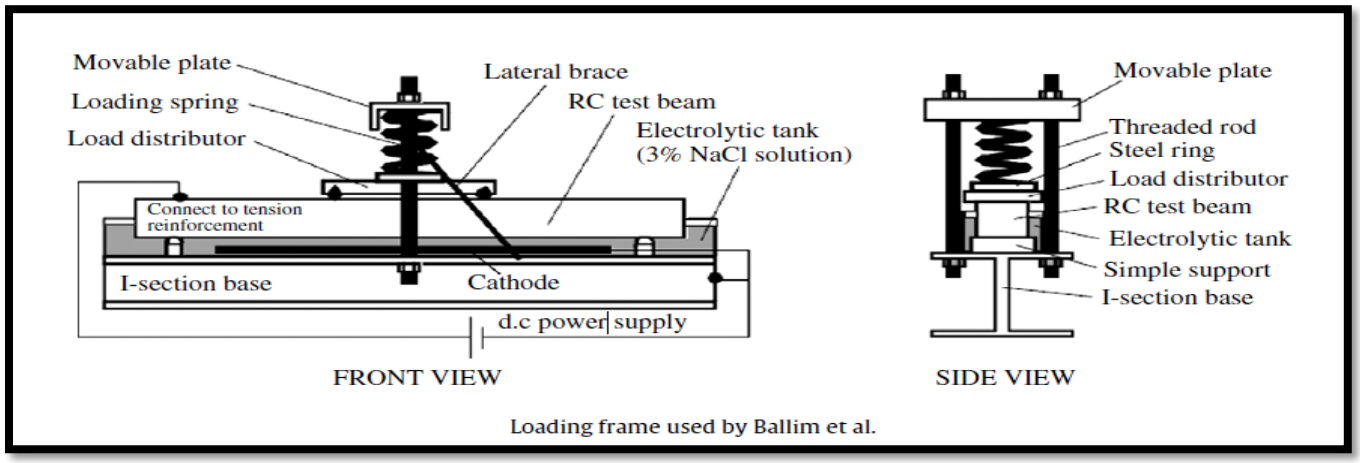

Fig: 3.2 loading Frame used by Ballim et al (2003)

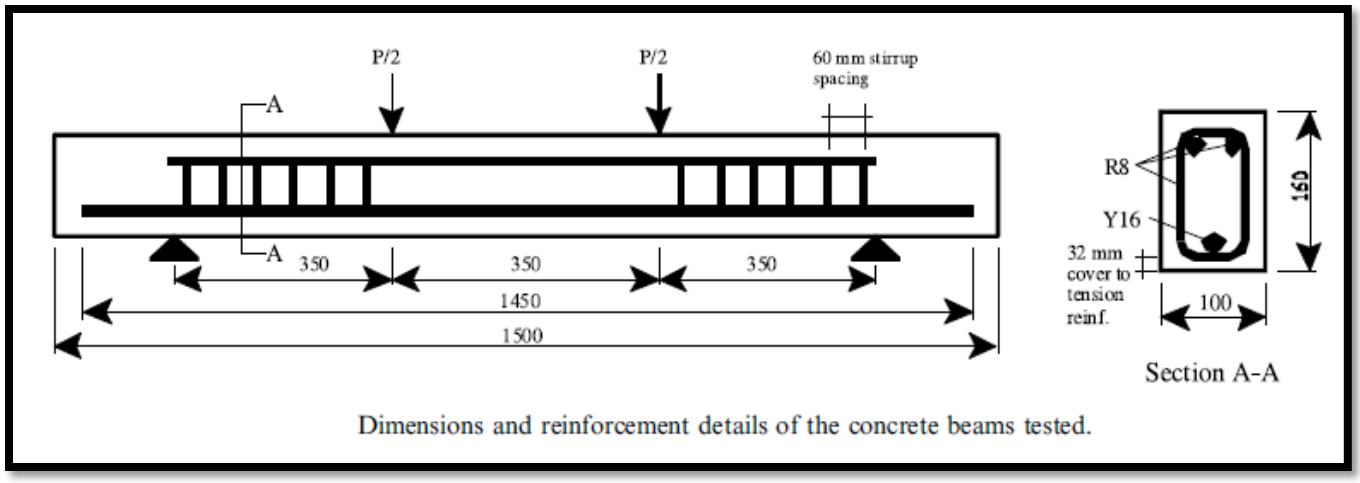

Fig: 3.3 Dimensions and reinforcement details of the concrete beams tested (Ballim et al 2003)

This work was divided into two main sets; set 1 beam were tested under a load equivalent to 23% of the ultimate load; and set 2 beams were tested under a load equivalent to 34% of the ultimate capacity of beams. Central deflections were measured on the beams, and after testing the beams to failure, corroded bars were retrieved from the concrete, cleaned and weighed to determine the gravimetric mass loss. As expected beams corroded under high load levels were found to exhibit larger deflections. Surprisingly however, after 30 days of testing, a beam corroded under a load equivalent to 23% of the ultimate capacity had a comparable deflection as an uncorroded beam that was subjected to a sustained load equivalent to 34% of the ultimate capacity of the beam. This indicates that corrosion of beams had a significant impact on the deflections of the beams. Furthermore, the ratio of deflections calculated as deflection of a corroded beam to the deflection of corresponding uncorroded beam

overtime, was found to be highest for beams corroded under a high load. It is therefore evident that deflections were more sensitive to the level of corrosion on beams corroded under a high load. In addition, this ratio was found to constantly increase with the level of corrosion which indicates that at higher levels of corrosion (especially for beams corroded under high loads), the majority of measured deflections would be from the corrosion and not the creep.

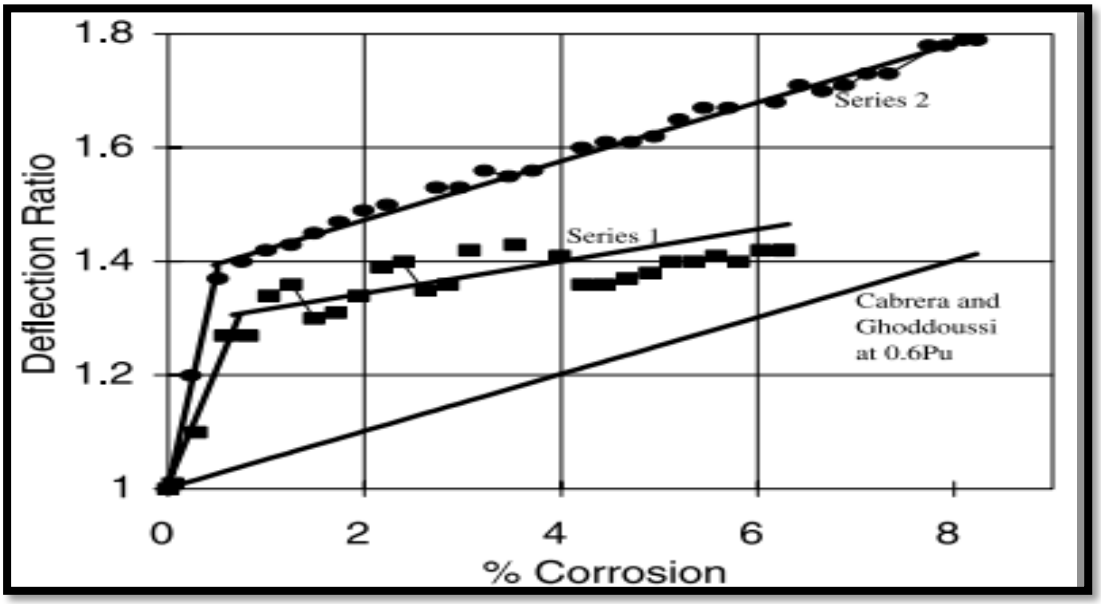

Fig: 3.4 Effect of corrosion on the deflection ratio of RC beams. Series I – loaded to 0.23Pu (Ballim and Reid, 2003)

Fig. shown above summarizes the deflection ratios that were observed by Ballim and Reid (2003), which were calculated by dividing the average deflections of the corroded beams with those of the control beams. This graph indicates that the deflection increased as corrosion propagated, particularly at the early stages. The researchers attributed this initial increase in deflection to early crack formation, as the crack creation and widening progressed at a slower rate after a certain point.

El-Maaddawy et al., (2003) studied the influence of varying the impressed current density level between 100 and 500 mA/cm2 on the actual degree of steel reinforcing bar corrosion as well as on the concrete strain behavior due to expansive corrosion products was experimentally investigated. Twelve reinforced-concrete prisms (150x250x300mm) were used. The prisms were reinforced by two No. 10 reinforcing bars. Corrosion was induced by means of impressed current using electric power supplies. To depassify the steel reinforcement, 5% NaCl by weight of cement was added to the concrete

mix. The strain response due to the expansion of corrosion products was measured at each face of the prisms.

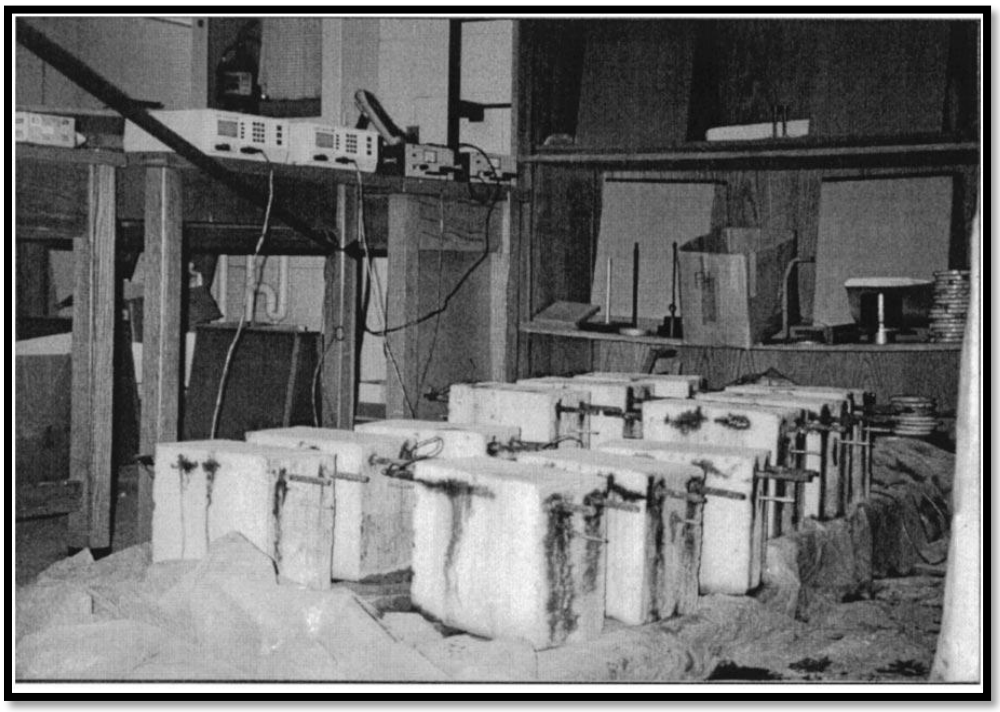

Fig: 3.5 General view for accelerated corrosion (El-Maaddawy et al., 2003)

At the end of the corrosion phase, all the corroded reinforcing bars were removed, cleaned according to the ASTM G1-90 standard, and weighed to get the actual degree of mass loss. The results showed that, up to 7.27% mass loss, accelerated corrosion using the impressed current technique was effective in inducing corrosion of the steel reinforcement in concrete. With respect to Faraday's law, the use of different current densities has no effect on the percentage of mass loss. However, increasing the level of current density above 200 mA/ cm2 results in a significant increase in the strain response and crack width due to corrosion of the steel reinforcement.

Acosta et al., (2004) studies the influence of corrosion on structural stiffness of reinforced concrete beams. This work presents an experimental investigation that correlates the stiffness changes of reinforced concrete beams with the amount of steel cross section loss and concrete cover cracking morphology due to localized corrosion of the embedded steel. Ten concrete beams (100 by 150 by 1,500 mm) with the central portion contaminated by chlorides placed during mixing of the concrete were used in this investigation. In addition, two beams without chloride contamination were used as

controls. Corrosion was further accelerated in the chloride contaminated beams by impressing an anodic current to the single no. 3 steel reinforcement bar (10 mm diameter.

To determine the effect of corrosion-induced stiffness deterioration, a loading-unloading technique was used. This technique was based on applying gradually (in steps) a vertical force at the beam center and measuring the corresponding displacement. Three loading-unloading cycles were performed on each beam at a time every week during the entire acceleration corrosion process.

Crack widths and lengths were recorded for all beams every other week. All beams, where accelerated corrosion was induced, developed surface concrete cracks. The cracks were parallel to the rebar. Most of the corroding beams (7 out of 10) presented only one crack parallel to the rebar at the concrete surface closest to the rebar (bottom surface).

The results in Table 3.1 show a marked decrease in the flexure stiffness for all types of corroding beams with general corrosion (GC), localized corrosion (LC), and highly localized corrosion (HLC).

Table: 3.1 Decrease in Flexural Stiffness Acosta et. al., (2004)

	Experimental Values of $K(t)_{EQ}$ in KN/mm[A]											
Time (days)	V01[B]	V02[B]	V03	V04	V05	V06	V07	V08	V09	V10	V11	V12
8	4.57	7.04	5.96	5.97	5.98	6.94	7.29	6.91	6.03	4.89	5.72	5.71
15	4.19	5.94	5.58	4.97	5.22	6.46	6.80	6.64	5.54	5.14	5.55	5.56
22	4.45	7.05	5.71	5.78	5.46	6.76	6.75	6.59	6.18	5.80	5.53	5.74
29	4.52	7.16	5.81	5.01	5.39	5.85	6.52	6.07	5.59	4.74	5.41	5.39
36	4.56	6.73	5.88	5.23	5.24	6.22	7.25	6.01	5.27	4.77	5.53	5.39
42	4.56	6.27	5.35	5.39	5.41	6.06	7.54	6.40	5.39	5.13	5.23	5.21
50	4.30	5.88	4.73	4.51	4.81	6.91	5.85	5.65	4.72	4.99		
57	3.99	6.27	5.24	4.96	5.33	5.83	5.74	6.22	5.21	4.89		
64	4.03	6.30	5.21	4.90	5.22	5.79	5.83	6.10	5.20	4.85		
71	4.23	6.56	4.75	4.38	5.36	5.88	5.56	5.95	5.85	4.95		
77	4.30	6.46	4.87	4.20	5.06	5.96	5.86	5.56	6.20	4.94		
88	4.15	6.46	4.76	3.91	5.43	5.48			5.26	4.52		
92	4.01	6.38	4.91	4.36	4.65	5.17			4.74	4.49		
98	4.52	6.46	4.36			4.65			4.40	4.43		
114						4.87				4.40		
128						4.47				4.24		
142						4.47				4.15		
156						1.41				3.99		
172						4.24				3.99		
181						3.82				3.99		
SL_{END}(%)[C]	1.09	8.24	26.84	26.97	22.24	44.96	19.62	19.53	27.03	18.4	8.57	8.76

[A] $K(t)_{EQ}$ = equivalent stiffness (slope obtained from the load-displacement experimental results) at time t.
[B] Control beam: beam in which there was no chloride added and no externally applied anodic current.
[C] $SL_{END} = 100 \times [K(181)_{EQ} - K(8)_{EQ}] / K(8)_{EQ}$.

The results obtained showed decreases as high as 32% in the flexure stiffness when only 14% of rebar radius was lost due to localized corrosion, for similar rebar radius loss due to corrosion (about 10%) the stiffness decreased 19.6%, 24.6%, and 26.9%, for HLC, LC, and GC, respectively.

El-Maaddawy et al., (2005) studied the flexural behaviour of corroded RC beams under combined effect of corrosion and sustained loads. Test results showed that the presence of a sustained load and associated flexural cracks during corrosion exposure significantly reduced the time to corrosion cracking and slightly increased the corrosion crack width. For example they found that crack width would propagate 22% faster in loaded conditions. They observed that with 8.9% and 22.2% mass loss, strength losses of 6.4% and 20.0%, respectively. It was also observed that the presence of flexural cracks during corrosion exposure initially increased the steel mass loss rate and, consequently, the reduction in the beam strength. El-Maaddawy et al. (2005) concluded that at low corrosion levels, the effect of bond loss can be ignored and that the ultimate load carrying capacity of the beam is affected only by the loss on steel reinforcement.

Toongoenthong and Maekawa., (2005) investigated the effect of fractured stirrups on the shear strength of reinforced concrete beams. The beam specimens were 350 mm deep, 250 mm wide, and 3000 mm in length and were simply supported over a clear span of 2.0 m. Fig: 3.6 below shows the specimen setup, dimension and reinforcement details. The tension and compression reinforcement consisted of 4-19mm high strength deformed bars. The shear stirrups were 6mm U shaped spaced at 100mm c/c. The fractured stirrups were considered the replicas of stirrups damaged by corrosion or alkali-aggregate reaction of concrete. The fractured stirrups were simulated by removing the bond near the edges of stirrup legs. A 50 mm strip of vinyl tape was used to eliminate the bond near the edges of the stirrup legs. The beam specimens were tested in three-point bending with a shear span to depth ratio of 3.2.

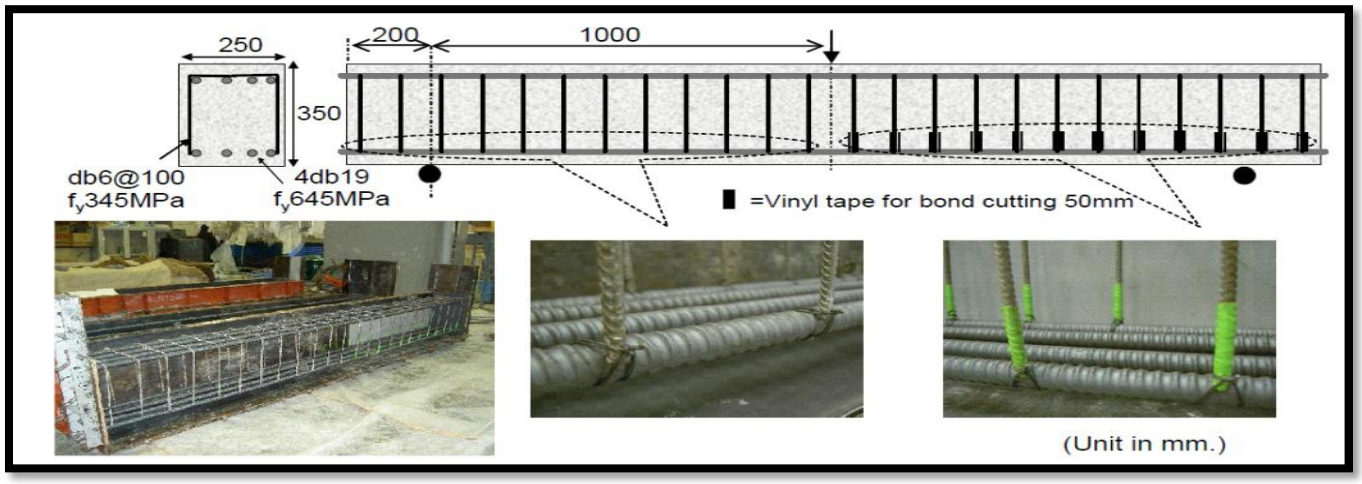

Fig: 3.6 Details of Specimens (Toongoenthong and Maekawa, 2005)

Fig: 3.7 below shows the load deflection curves of the damaged beam with the fractured stirrups and the undamaged reference beam. The results showed that the damaged beam experienced 37% reduction in shear capacity compared to the undamaged beam. It was also observed that beams having stirrups without proper anchorage experienced longitudinal cracking along the main reinforcement before inclined cracking, which leads to the ineffectiveness of stirrups. The load carrying mechanism was changed from a truss mechanism to a tied-arch action leading to anchorage failure of the main reinforcement.

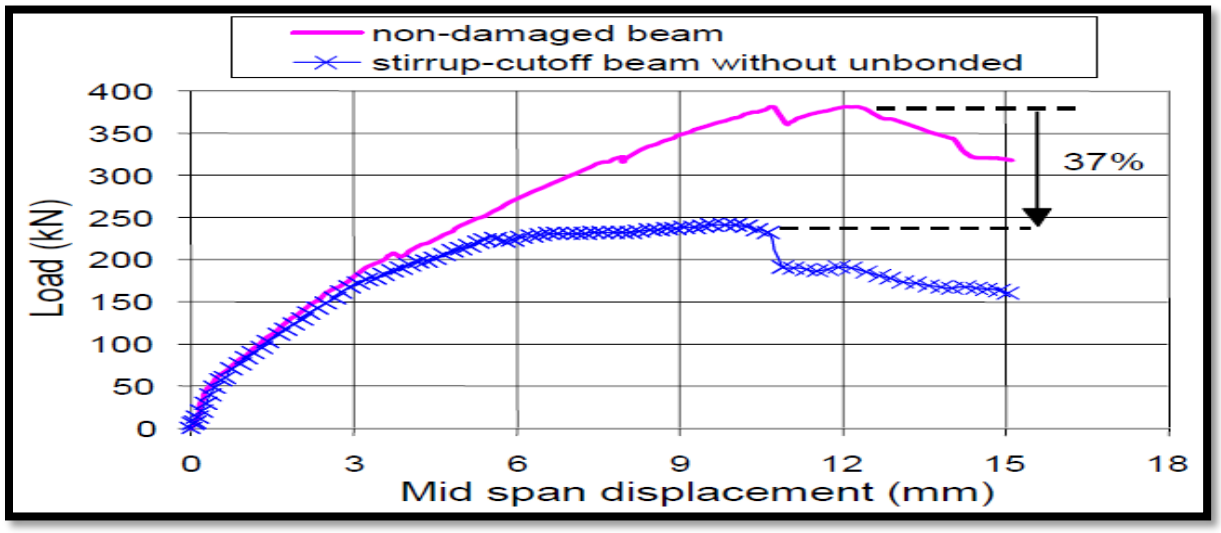

Fig: 3.7 Load ~ Deflection Curve (Toongoenthong and Maekawa, 2005)

Smith, (2007) conducted experimental investigation into the effects of corrosion on the structural behavior of RC beams. The experimental results of beam tests indicated that the failure mode shifted from predictable ductile flexural failures at mid-span, to more brittle failures at supports. The load carrying capacity decreased with increasing levels of corrosion. Pull-out tests were also conducted by Smith (2007), and the experimental results showed a gradual bond strength loss with increasing corrosion levels.

Acosta et al., (2007) used specimens of concrete beams with 100 mm × 150 mm cross section and 1500 mm in length casted with chlorides to investigate the flexural capacity loss with steel cross-section loss due to generalized corrosion of the embedded steel. The specimens were tested in flexure under three point loading. The experimental values of maximum load were used to estimate the residual load capacity ratio **RLCcor**. An empirical equation was formulated according to the test data as:

$$RLC_{COR} = -0.8596 \cdot \left(\frac{PIT_{MAX}}{r_0}\right) + 0.9707$$

where

PIT_{MAX} = maximum pit corrosion depth;

r_0 = rebar radius.

It was observed that the flexural load capacity decreased 60% with only 10% **Xavr/ro** of the ratio, which is the ratio of average corrosion depth to the rebar radius. **PIT max/ro** rather than **Xavg/ro** ratio was the most important parameter affecting flexural load capacity reduction, because pitting corrosion greatly decrease the cross sectional area of the steel at a certain location and change the steel from ductile behavior to brittle behavior.

Joyce, (2008) carried out experiments to study the effect of corrosion on the flexural behavior of reinforced concrete (RC) beams. The corrosion of the steel was isolated in the flexural region in order to eliminate contributions from stirrup corrosion and loss of bond within the development length. It was determined that the flexural capacity of reinforced concrete beams decreased as the rate of corrosion increased.

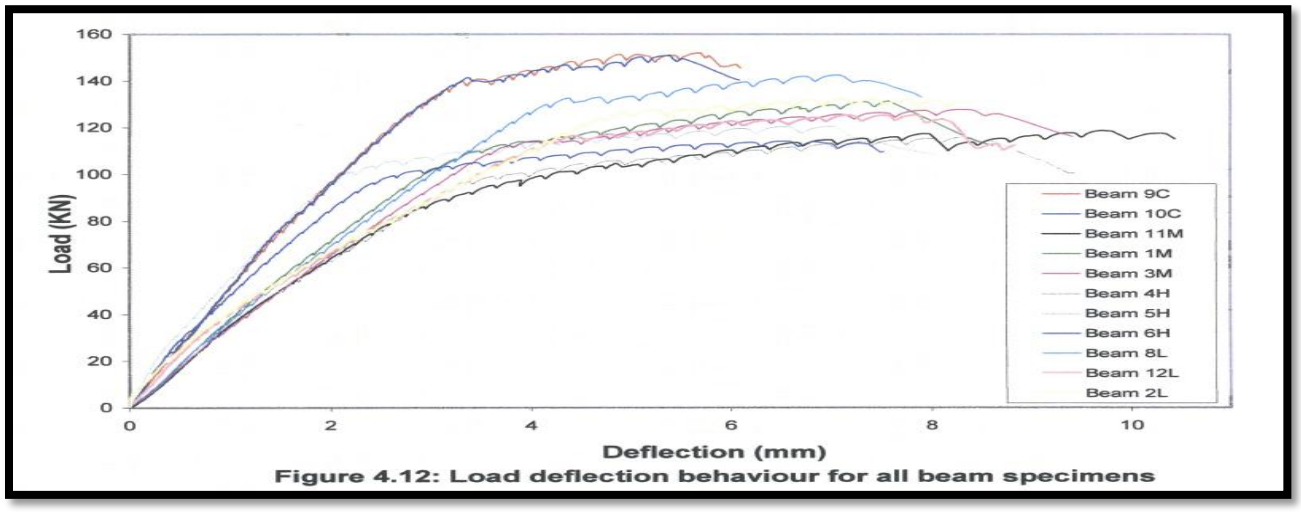

Fig: 3.8 Load Deflection Behavior for all beam specimens Joyce, 2008

In addition to the study of flexural capacity, the prediction of the flexural behavior of corroded beams was studied through the stiffness effects of reinforcement corrosion. The stiffness study indicated a sharp drop in stiffness at relatively low degrees of corrosion, followed by a slower decline at increasing levels of corrosion. Mass loss, crack width and chloride ion content were examined as indicators of degree of corrosion.

Kitjapat Phuvoravan presents the effect of steel corrosion level on flexural behavior of RC beams by performing nonlinear finite element analysis which has been verified with experimental results. Concrete was modeled as three dimensional solid elements while all steel reinforcement was represented by truss elements having nonlinear property for both materials. Nonlinear springs were used to model bonding between steel and concrete. The objective is to investigate the effect of steel corrosion level and the location of corrosion in main reinforcement on the load carrying capacity of the beams. The results from this research lead to the preliminary evaluation of the remaining flexural strength for RC beam under corroded condition.

Three-dimensional finite element analysis (FEA) was employed to investigate the effect of steel corrosion on flexural strength of RC beams. The bond-slip between the steel and the concrete was represented by non-linear spring. The spring having no dimension connected the nodes of steel elements and concrete elements. The load exerted on the springs and the deformation of the springs which characterized the load-deformation pattern was obtained by converting the maximum bond stress into force.

The results of experimental study (Maaddawy *et al.*, 2005) were chosen to investigate the corrosion effect in his paper. Two main case studies are RC beam with reinforcement corrosion in the middle portion, and RC beam with reinforcement corrosion for the whole length.

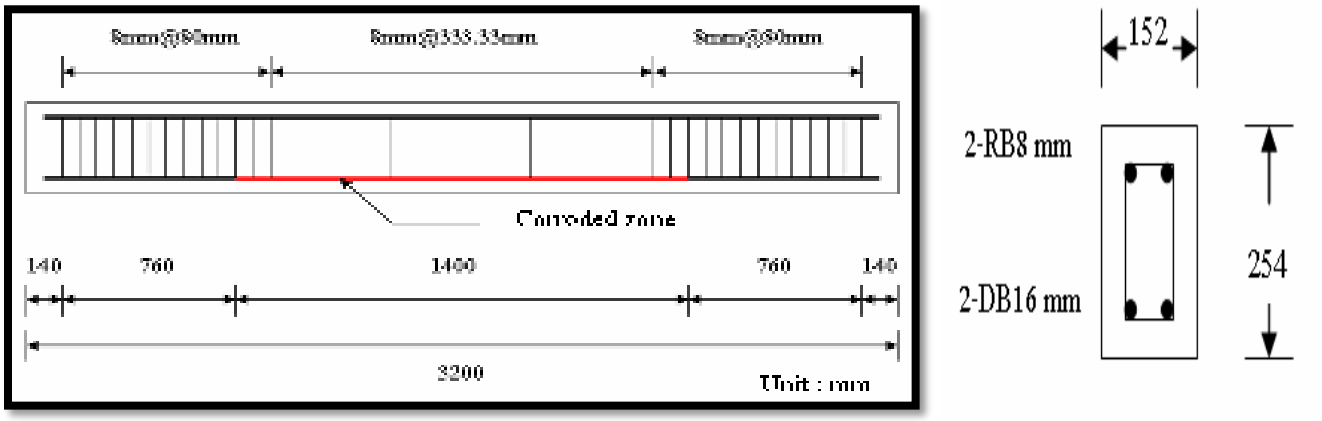

Fig: 3.9 Beam Reinforcement Details for Case Study no. 1 (Phuvoravan)

For the first case study, corrosion was restricted to the tensile steel placed in the middle 1400 mm of the beams as shown in Fig: 3.9 The corrosion induced was divided into four levels, i.e., 0%, 8.9%, 14.2%, and 22.2% corrosion.

For the second case study, corrosion was activated on bottom main reinforcement for the whole length of RC beam as shown in Fig: 3.10. The corrosion induced was divided into three levels, i.e., 0%, 8.8%, and 14% corrosion.

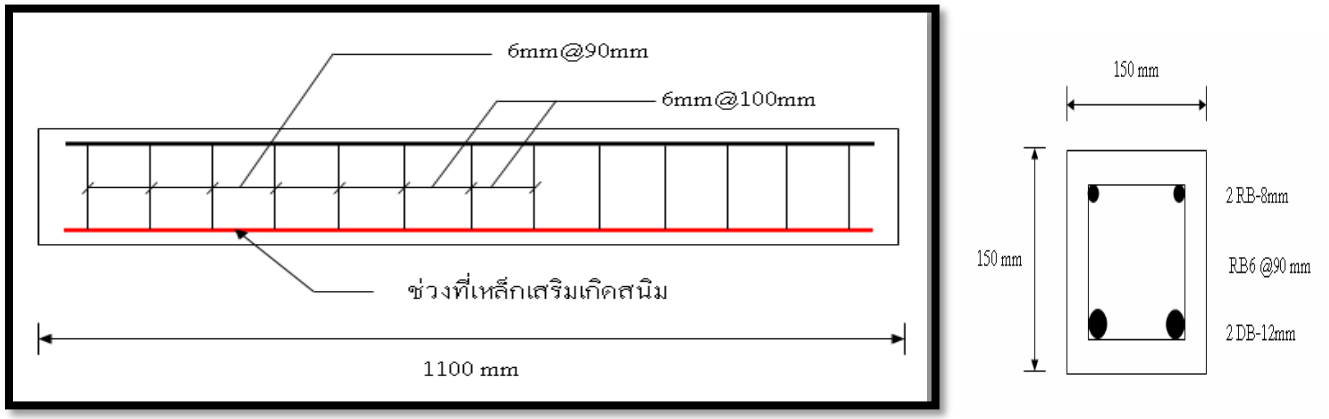

Fig: 3.10 Beam Reinforcement Details for Case Study no. 2 (Phuvoravan)

The relationship between applied loads and mid-span deflection derived by FEA give a good agreement comparing to the results obtained from the structural tests.

For case study no.1 where corrosion of reinforcement in the middle portion of RC beam, the study showed that bond-slip contributed relatively smaller effect than did the reduction of the cross-sectional steel area. When the degree of corrosion increased, the ultimate load and the yield load decreased accordingly. Immediately after first crack at the middle portion of the beam, additional flexural cracks occur at interval within constant moment region. At the ultimate load capacity, diagonal tensile crack occurs at the shear region near support, and the compressive crushing occurs at the top fiber of the beam.

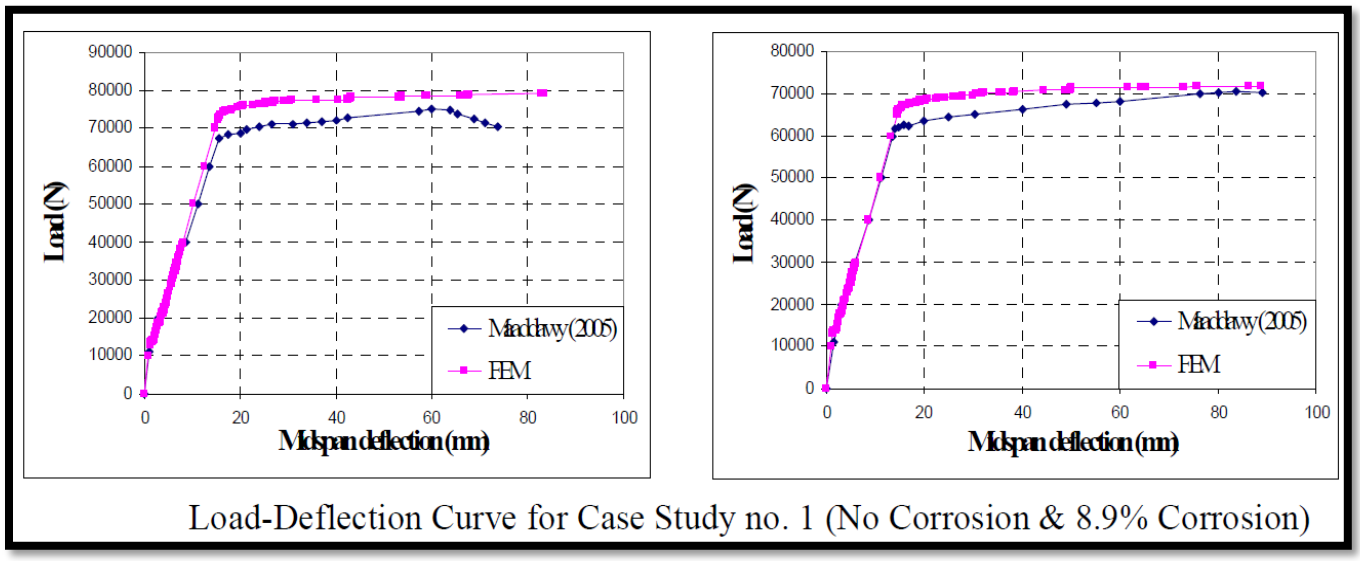

Fig: 3.11 Load-Deflection Curve for Case Study no. 1 (No Corrosion & 8.9% Corrosion) (Phuvoravan)

It was noted that, as the level of corrosion increased by 8.9%, the ultimate-moment decreased in the order of 9.17% and the loss of the ultimate flexural moment could be as great as 22.65% when the corrosion level reached 22.2%.

For case study no. 2 where corrosion of reinforcement for the whole length of RC beam, bond-slip behavior plays a important role in the flexural behavior of the beam. When the degree of corrosion increased, the ultimate load and the yield load decreased rapidly. At first cracking state, flexural cracking is concentrated at the middle bottom portion of the beam. At the ultimate load capacity, diagonal tensile crack occurs at the shear region near support, the compressive crushing occurs at the top fiber of the beam, and cracking spreads throughout the beam.

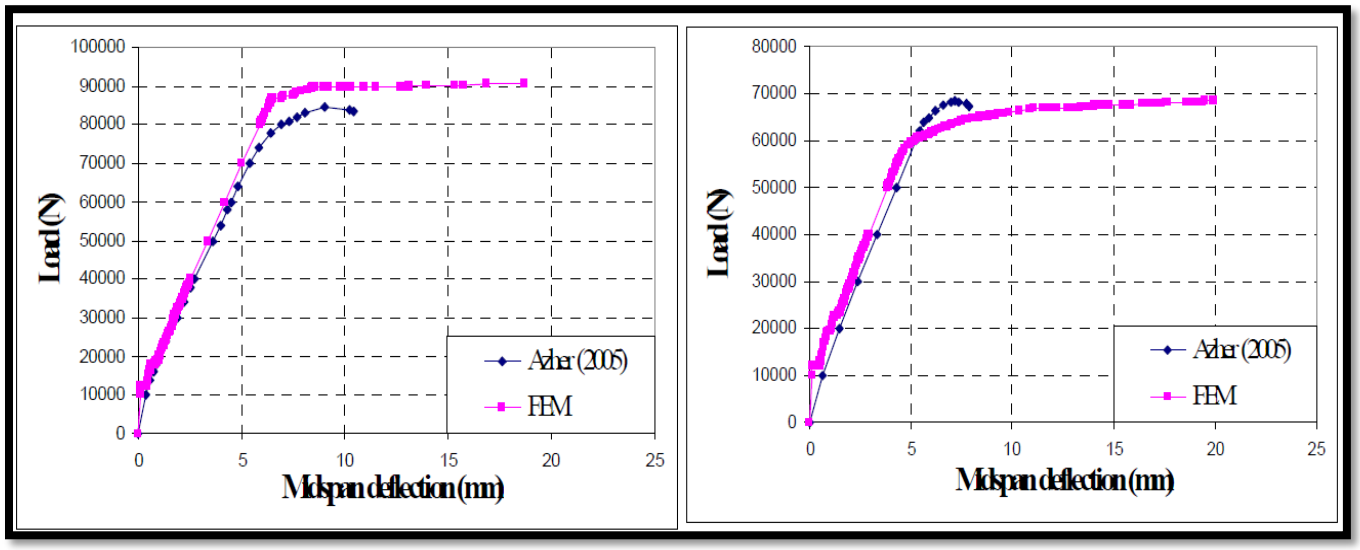

Fig: 3.12 Load-Deflection Curve for Case Study no. 2 (No Corrosion & 8.8% Corrosion) (Phuvoravan)

It was noted that the level of corrosion increased by 8.8%, the ultimate moment decreased by 24.45% and the loss of the ultimate flexural moment could be as great as 37.88% when the corrosion level reached 14%.

Okude et al., (2009) presents an experimental investigation on the flexural failure behavior of RC beams having different weight loss of 0, 5, 10 and 30% due to corrosion. Acoustic Emissions (AE) was also monitored during the loading tests of the deteriorated concrete beams. They conclude that as corrosion levels represented by weight loss increased, load carrying capacity of the beams decreased dramatically.

In experimental setup they uses beam specimens measuring 140 x 80 x 1460 mm for bending tests. All stirrups were wrapped with polyvinyl tape to prevent corrosion of stirrups themselves. In order to induce rebar corrosion, an accelerated corrosion test was carried out for the beam specimen. The specimens were placed on a copper plate in a chamber filled with NaCl solution (concentration: 3%), and current of 0.6 A (0.907 mA/cm2) was applied to rebar in each specimen. The weight loss was controlled by total applied current.

Fig: 3.13 below shows the longitudinal crack width measured at bottom surface that is close to a rebar. Basically, crack width became wider with increasing of corrosion levels that represented by

weight loss. In severe corrosion case (10 % and 30 % cases), crack width along a specimen axis was not so constant that it indicates that corrosion was occurred locally.

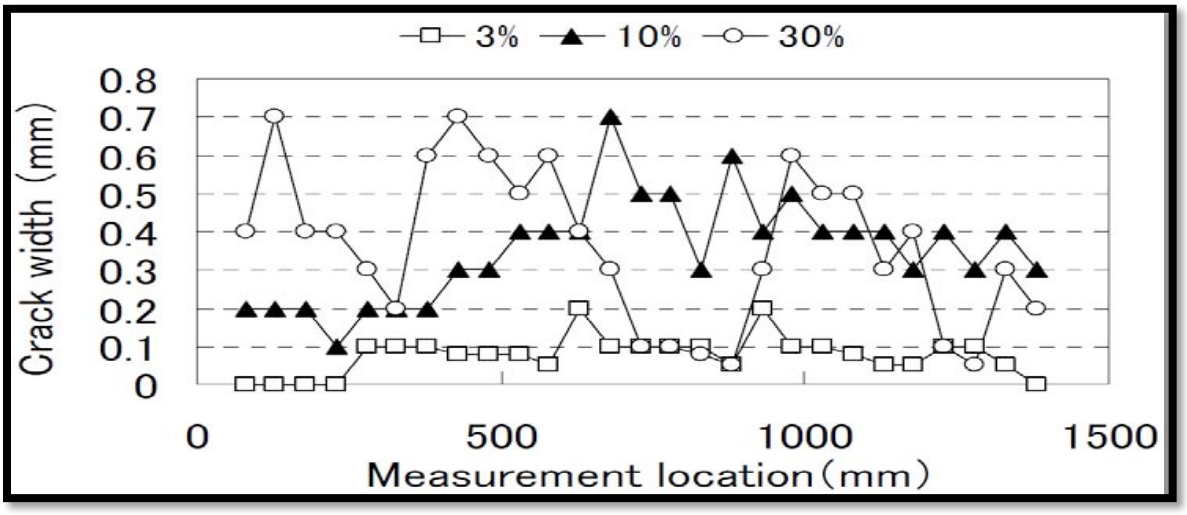

Fig: 3.13 Crack width Okude et. al., (2009)

Fig: 3.14 shown below indicates the diameter of rebar measured in longitudinal direction at an interval of 50 mm. Nominal diameter of the rebar used in this test was 13 mm. Significant decrease of rebar diameter was observed locally, especially in the case of severe corrosion (30%).

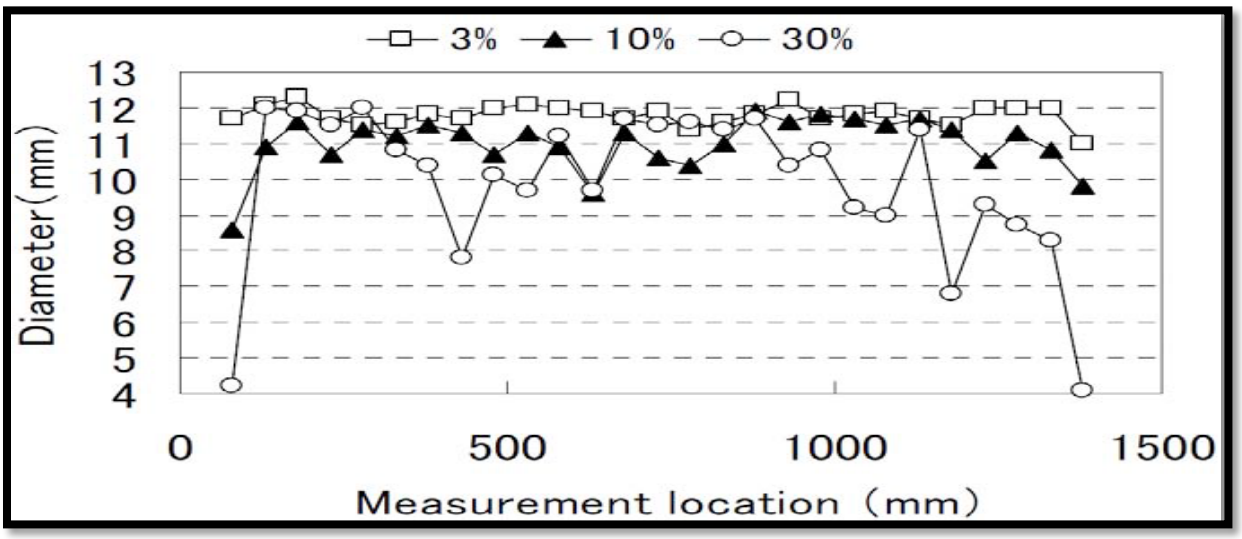

Fig: 3.14 Diameter rebar measured in longitudinal direction Okude et al., (2009)

Four-point bending tests were conducted with a constant moment length of 280 mm and total span length of 1260 mm. In this test, load and displacement at loading points were measured by a load cell with a capacity of 100 kN (sensitivity: 33 N) and LVDT with a capacity of 50 mm (sensitivity: 0.01 mm), respectively. Fig: 3.15 shown below represent the crack patterns after the loading tests. In the case of no corrosion, more than five cracks were observed. Decrease in the number of cracks, which normally represents lower bond property, was observed in only 30% case.

Fig: 3.15 Crack patterns after loading tests Okude et. al., (2009)

Fig: 3.16 below shows the measured load-displacement curves in all series. There was no significant difference in 0% and 3% cases. In other cases, however, the yielding and maximum loads became lower with increasing corrosion levels (weight loss). Especially in the case of 30%, rebar was finally broken.

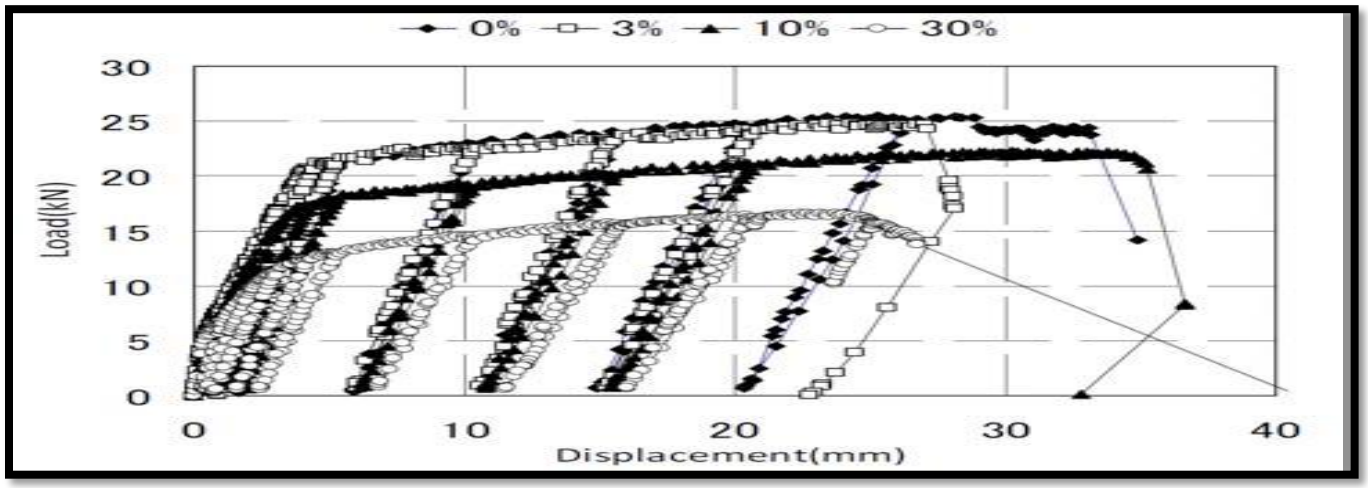

Fig: 3.16 Load Vs Displacement curve Okude et al., (2009)

Malumbela et al. (2009) studied the flexural behaviour of corroded RC beams under combined effect of corrosion and constant sustained loads. An accelerated corrosion process using a 5% solution of NaCl and a constant impressed current induced corrosion on tensile steel bars. They tested four RC beams, each with a width of 153 mm, a depth of 254 mm and a length of 3000 mm.

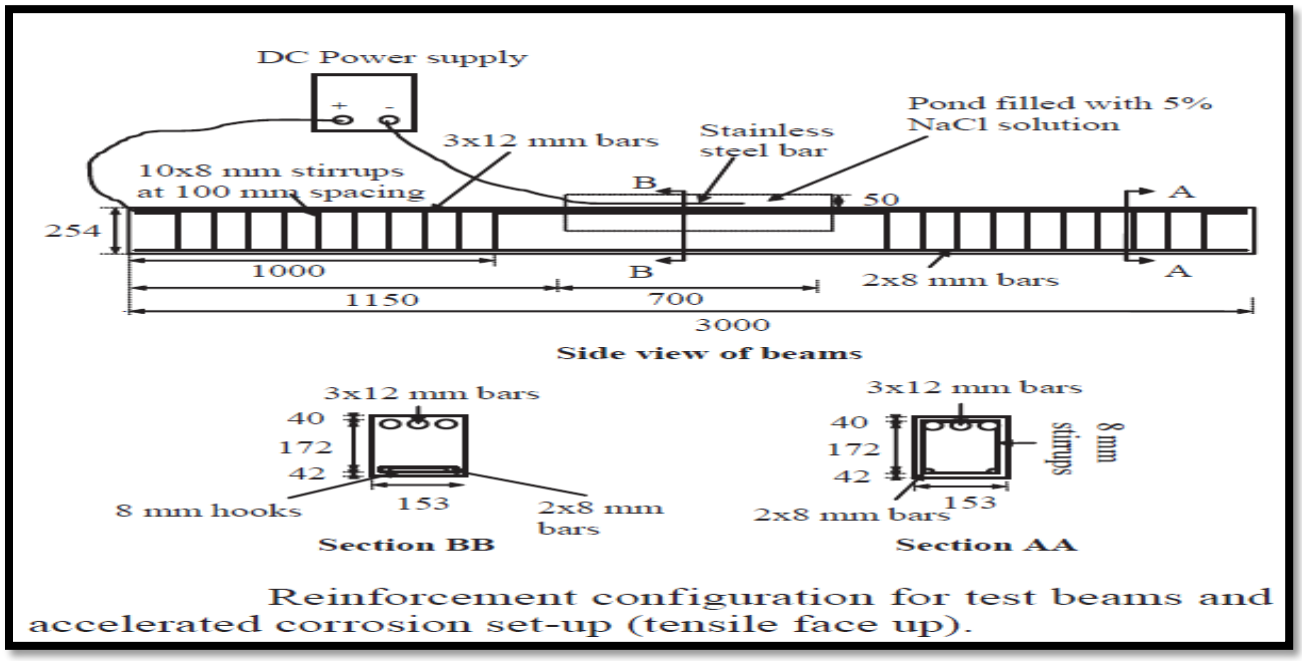

Fig: 3.17 Reinforcement configuration for test beams and accelerated corrosion set-up (tensile face up).
Malumbela et al., 2009

Four beams were used in the test programme. Beam 1 was tested under self-weight; Beam 2 was tested under a constant sustained load that was equivalent to 10% of the ultimate load capacity of the beam (uncracked condition); and beams 3 and 4 were tested under a constant sustained load that was equivalent to 33% of the ultimate load capacity of the beam (cracked condition). Beams 1 to 3 were corroded under their respective loading systems whilst beam 4 was not corroded.

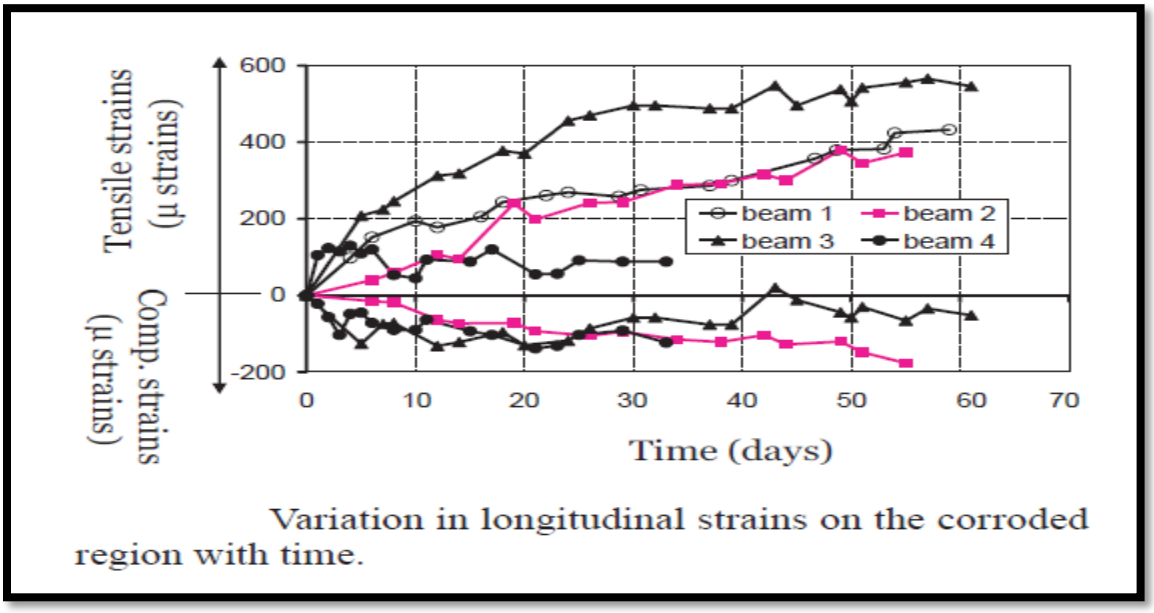

Fig: 3.18 Variation in longitudinal strains on the corroded region with time.
Malumbela et al., 2009

Fig: 3.18 above shows that longitudinal tensile strains on a beam that had transverse cracks from applied load (beam 3) are higher than strains on corroded beams without flexural cracks (beams 1 and 2). After 55 days of corrosion, tensile strains on beam 3 were about 1.5 times higher than strains on beams 1 and 2. Unexpectedly, tensile strains on beams 1 and 2 were almost the same but significantly higher than strains on beam 4. Measured strains indicate that;

1. Longitudinal tensile strains are influenced by the applied load but mostly by the level of corrosion of steel bars.
2. Longitudinal tensile strains of corroded beams increase monotonically with time at a decreasing rate.

Fig: 3.19 below shows that depth of the neutral axis is independent of the level of corrosion for beams free from flexural cracks and beams free from corrosion but significantly reduces with an increase in degree of corrosion for corroded beams with flexural cracks as shown below.

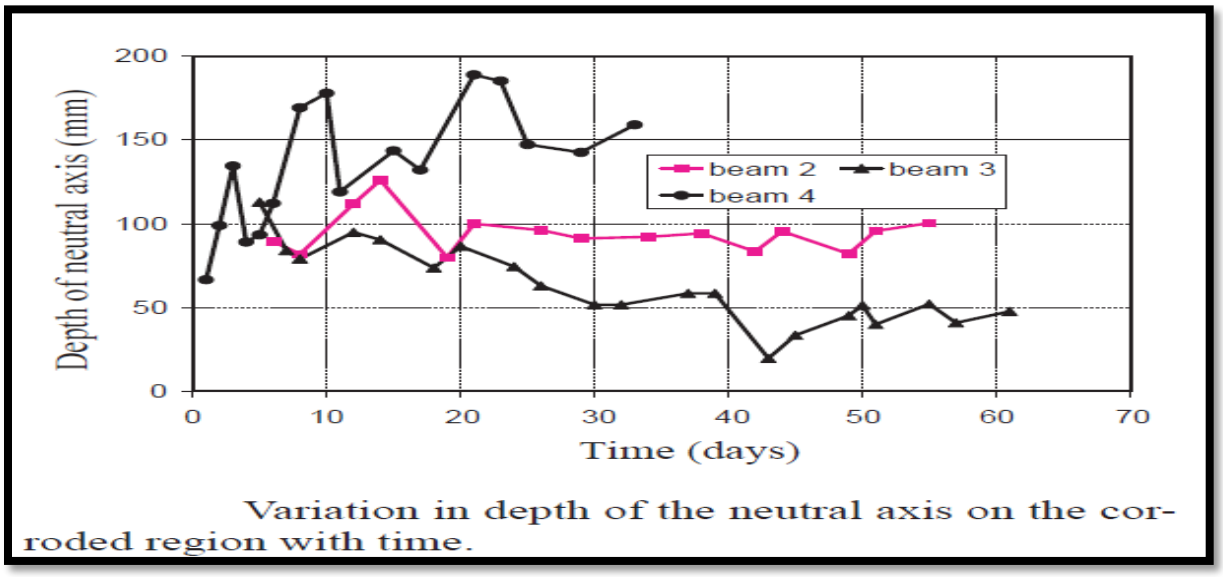

Fig: 3.19 Variation in depth of the neutral axis on the corroded region with time. Malumbela et al., 2009

Fig: 3.20 below shows that curvatures of corroded beams increase monotonically with degree of corrosion but at a decreasing rate.

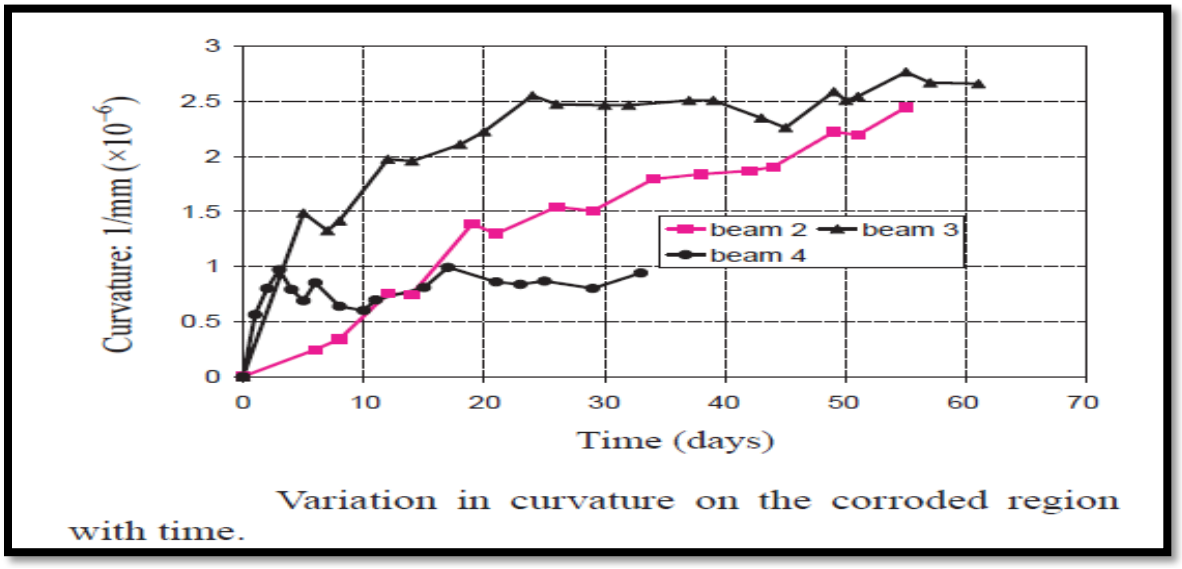

Fig: 3.20 Variation in curvature on the corroded region with time. Malumbela et al., 2009

Fig: 3.22 shown below conclude that:

1. The effective moment of inertia of corroded beams decreases monotonically with time of electrolysis but at a decreasing rate.
2. For corroded beams, the effective moment of inertia of beams with flexural cracks is almost the same as the effective moment of inertia of beams free from flexural cracks

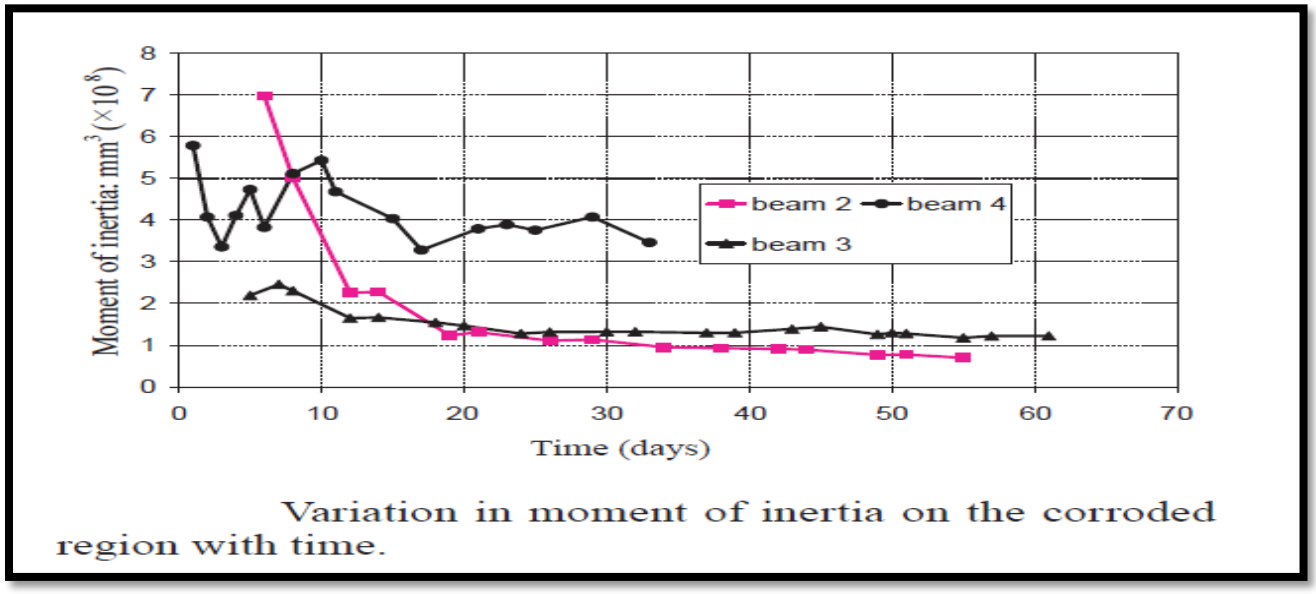

Fig: 3.21 Variation in moment of inertia on the corroded region with time. Malumbela et al., 2009

At the end it is said that the longitudinal strains, depth of the neutral axis and curvature depend on both the level of corrosion and the applied load whilst the moment of inertia only depends on the level of corrosion.

Malumbela et al., (2010) experimentally studied the rate of widening of corrosion cracks with the pattern of corrosion cracks as well as the level of steel corrosion for RC beams (153 × 254 × 3000 mm) that were corroded whilst subjected to varying levels of sustained loads. Steel corrosion was limited to the tensile reinforcement and to a length of 700 mm at the centre of the beams. The rate of widening of corrosion cracks as well as strains on uncracked faces of RC beams was constantly monitored during the corrosion process, along the corrosion region and along other potential cracking faces of beams using a demec gauge.

The experimental programme involved testing eleven quasi-full-scale RC beams (153 × 254 × 3000 mm) under four different levels of sustained loads: 0%, 1% (low deflections), 8% (high deflections but no flexural cracks) and 12% (high deflections and flexural cracks) of the ultimate load capacity of a virgin beam. The accelerated corrosion process was induced by impressing a constant direct current of 150 mA on the tensile steel bars to corrode the beams. It was limited to the tensile reinforcement and to a length of 700 mm at the centre of the beams by building a NaCl pond on the extreme tensile face of the beams. In this programme, lateral strains were measured using a 100 mm demountable mechanical (demec) strain gauge with a range of ± 10 to ± 5000 micro strains. A minimum strain of 10 micro strains recorded from the gauge is therefore equivalent to a lateral expansion or a crack widening of 0.001 mm. to contaminate only the region to be corroded.

During the corrosion process, RC beams in this programme exhibited three main types of corrosion crack patterns namely; crack pattern A, crack pattern B and crack pattern C. In crack pattern A, a single crack that propagated parallel to the corroded steel bars was observed on the extreme tensile face of the beam as shown in Fig: 3.22.

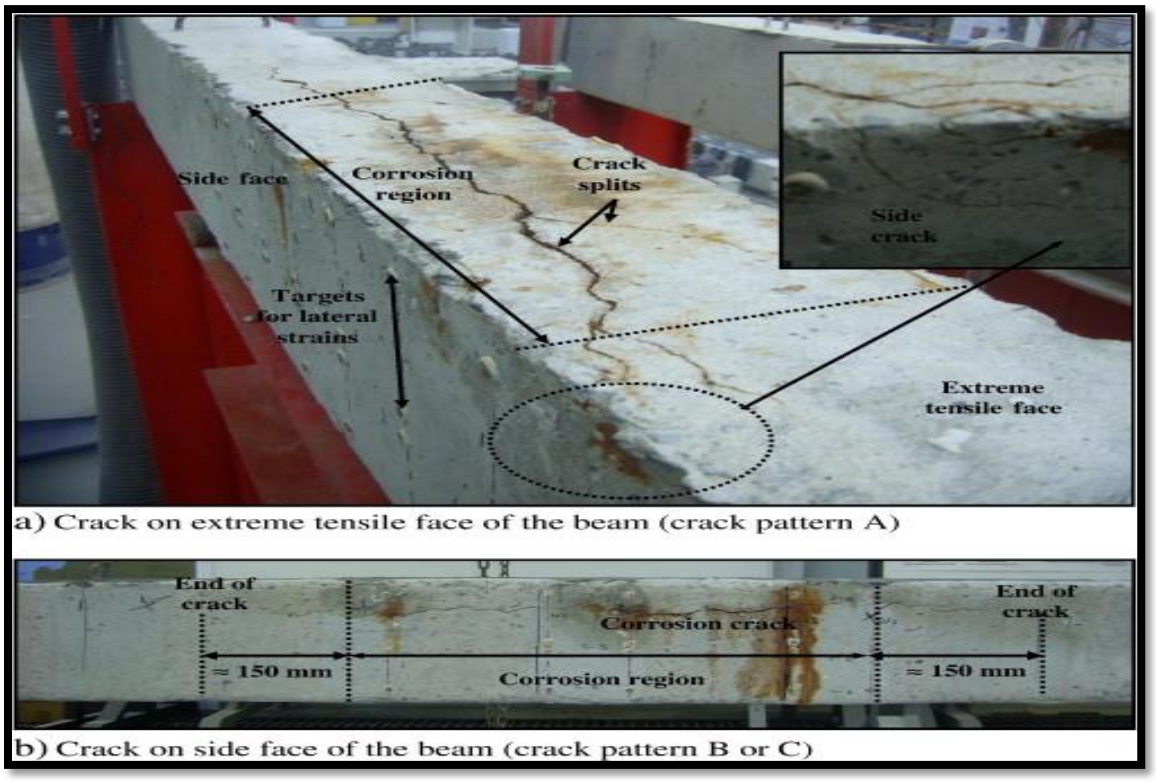

Fig: 3.22 Corrosion Crack Patterns Malumbela et al., 2010

In crack pattern B, the beam initially cracked on its extreme tensile face as in crack pattern A. However, as the level of corrosion increased, another crack was observed on one side face of the beam whilst the other side face remained uncracked. In crack pattern C, the beam initially cracked on its extreme tensile face followed by a single crack on each side face as the level of corrosion progressed. In this pattern, the crack on the extreme tensile face ended in the middle of the face (at a distance of about 150 mm beyond the end of the corrosion region) and did not diverge to the side edges of the beam as in the other crack patterns.

They also studied the average percentage mass loss of steel for every measured section (50 100 mm) along the corroded length. They observed the max mass loss at the centre of corrosion region. and the level of mass loss of steel and its variation along the beam were independent of the level of the sustained load and probably most importantly, were independent of the pattern of corrosion cracks.

It was shown in this programme that a corrosion crack width of 0.3 mm which is one of the criteria for end of service life of corroding RC structures was observed at about the same time for various beams used in the programme. If however, a corrosion crack width of 1 mm was to be used as a criterion for end of service life then similar beams were found to have significantly varying times for end of service life depending on their pattern of corrosion cracks. The rate of loss of steel was however found not to be dependent on the crack patterns. It was shown that to reach a crack width of 1 mm, the beams were likely to have mass losses of steel ranging from 8% to 50%. It was therefore recommended that for beams that exhibit cracks on the extreme tensile face as well as on the near side face, the maximum crack width should be taken as the sum of the maximum cracks for each face of the beam. If the recommendations in this programme are followed then a maximum crack width of 0.8 mm is reached at a mass loss of steel ranging from 8% to 19%. To be conservative, a mass loss of steel of 1% corresponds to a maximum corrosion crack width of 0.04 mm.

3.2 Ultrasonic Testing Methods to Monitor Corrosion in RC Structures

Liang et al., (2001) studied the detection of the corrosion damage of rebar in concrete using impact-echo method. They used three electrochemical methods; that is open-circuit potential (OCP), direct current (DC) polarization, and alternating current (AC) impedance. The result of this study indicates that the impact-echo method can certainly detect the development of microcrack in the concrete blocks. With respect to predicting corrosion damage, the displacement spectrum obtained from the impact-echo method should be transferred as acceleration spectrum. Thus, the degree of corrosion

damage can be predicted from relative amplitude obtained from acceleration spectrum. The OCP method can evaluate the corrosion state of steel in concrete. However, it is not useful in predicting the corrosion damage of the interior of the specimen. Both the DC polarization and AC impedance methods can predict the corrosion rate. The corrosion thickness of specimen obtained from integrating the corrosion rate can directly evaluate corrosion damage.

Iyer et al., (2002) proposed ultrasonic C-scan imaging to detect corrosion and voids in post-tensioning tendons. Investigation on post-tensioned specimens using ultrasound C-scan imaging technique have proved to be promosing for future applications in the evaluation of corrosion and voids in post-tensioned tendons, but further investigations are also needed to upgrade the technique.

Jones et al., (2006) investigates the interaction of ultrasonic waves and structural damage, i.e., cracking and corrosion. It is shown that cracking and corrosion damage produces a diffraction pattern that resembles that associated with the traditional physics of wave motion. The extension of this hypothesis implies that it may be possible to use a simple ripple tank to investigate how to best detect/sense and size a given damage state, e.g., corrosion. They also find that cracking, and corrosion damage, has a significant effect on both the amplitude and period of the waveform and also on the local (apparent) refractive index of the material and that these effects have the potential to be used as damage indicators.

Sharma and Mukherjee., (2010) studied longitudinal waves for monitoring chloride corrosion in reinforcing bars in concrete. They investigate the effect of local loss of material and loss of bond on the propagation of ultrasonic waves. Simulated pitting effects were created by notches on the surface of the bar in varying percentages of its cross-sectional area. Simulated debond was generated by wrapping a double sided tape of varying length on the bar embedded in concrete. Then an experiment is carried out to create accelerated actual corrosion in RC samples.

RC beam specimens of dimensions (150mm x 150mm x 700mm) were casted and 25mm diameter plain mild steel bar of 1.2m length was embedded in the center of cross section of the beam at the time of casting. The bar projected out by 250mm on each side of beam. Bars were subjected to two different types of damages, simulating different aspects of corrosion phenomenon in the form of notches representing pits and debonding representing delamination between steel and surrounding concrete. In one set of specimens, notches with symmetrical 0%, 20%, 40%, and 60% diameter

reduction are introduced in the middle of the bar before casting them in concrete. Two samples of each specimen were tested to examine the repeatability and precision of the results. In another set of specimens, delamination is simulated by wrapping a double sided tape on the steel bar to different extents of 0%, 6.25%, 12.5%, 25%, 50%, and 75% representing different extents of debonds and then embedded in concrete.

In this paper, longitudinal guided ultrasonic waves have been utilized to monitor notch and debond defects in steel bars in concrete simulating pitting and delamination phenomena caused by corrosion. Two ultrasonic techniques of pulse transmission and pulse echo were used to monitor the healthy and damaged specimens. The developed methodology is successfully applied for real time monitoring of RC beam specimens undergoing accelerated chloride corrosion. The ultrasonic signals effectively relate to the state of reinforcing bars.

Sharma and Mukkherjee., (2011) has worked on monitoring corrosion in oxide and chloride environments using ultrasonic guided waves. Ultrasonic guided wave monitoring with specific core- and surface-seeking modes successfully identifies the type of corrosion mechanism in chloride and oxide environments in a bar embedded in concrete. In general, pitting and nonuniform area loss highlighted by severe signal attenuation that marks CC, identified well by the core-seeking mode. With surface-seeking mode, the signal strength initially rises followed by the drop. This indicates that CC starts with delamination followed by local loss of material. In OC, the rate of corrosion is slow and localized marked by initial drop in signal due to pressure build up by formation of corrosion products and then slow bond deterioration as depicted by gradual rise in signal strength in surface-seeking mode. Pitting is insignificant as manifested by very slow signal fall in core-seeking mode in OC. Thus, through a judicious selection of ultrasonic modes the mechanism and rate of corrosion in oxide and chloride environments in RC structures can be successfully monitored.

Ye Lu et al., (2013) investigated the propagation properties of ultrasonic waves in rebar-reinforced concrete beams for purpose of damage detection. Two types of piezoelectric (PZT) elements were used in experiments in which PZT disks were attached on the surfaces of concrete beams to observe wave propagation in concrete before and after a four-point bending test, while rectangular PZT patches were attached at the exposed ends of the rebar to monitor wave transmission along the rebar with and without simulated corrosion in the form of partial material removal from the rebar.

Six concrete beams were prepared with the same dimensions and configuration of reinforcement rebar (two pieces of rebar in each concrete beam) as described above, except that the diameter of the rebar was increased to 12 mm. Before casting 12 pieces of rebar in concrete beams, simulated damage in the form of material removal of 1/3 in depth and 75 mm in length, at a position 600 mm away from one end, was introduced in two pieces of rebar. Damage with the same depth and position but 150 mm in length was introduced in another two pieces of rebar. These four pieces of damaged rebar were cast separately in four concrete beams, each paired with a piece of intact rebar. The other four pieces of intact rebar were cast in another two concrete beams. As a result, a total of 12 pieces of rebar (four damaged and eight intact) in six concrete beams were characterized individually in this study.

Comparison of wave signal with and without cracking was done and it was notice that there is a decrease in amplitude for the cracked specimens. This decrease in amplitude clearly predicts the damage in specimen.

Experimental testing demonstrated that the surface-attached PZT disks were capable of detecting the change in material properties due to the existence of cracking. It was concluded that slim piezoelectric elements can activate and sense bulk and surface waves propagating in concrete with a good signal-to-noise ratio at frequencies below 100 kHz. A decrease in the dynamic Young's modulus of concrete beams due to concrete cracking can be evaluated by the change in the velocity of bulk waves propagating in the concrete. The presence of surrounding concrete significantly dissipates the propagation of guided waves through the embedded rebar, indicated by decreases in wave magnitude and velocity.

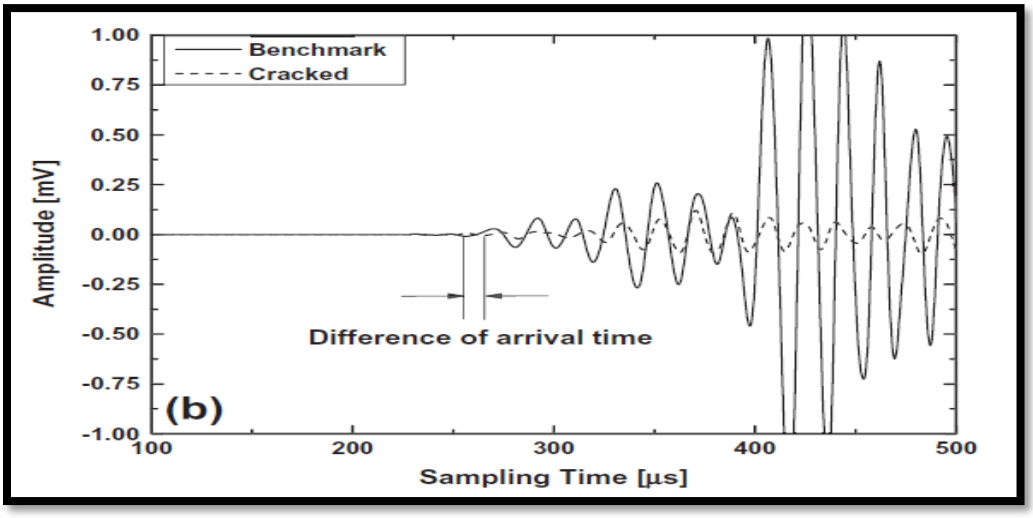

Fig: 3.23 Comparison of wave signals with and without cracking damage (Ye Lu et al., 2013)

In consideration of the inevitable discrepancies in different concrete beams due to specimen preparation and sensor installation, principal component analysis (PCA) based on statistical parameters extracted from wave signals was applied to highlight the difference between benchmark and damaged rebar. It was found that PCA is capable of reducing the dimension of a complex set of original data, whose characteristics can be represented and highlighted by the first few mapped principal components. The different rebar conditions can be classified with the assistance of PCA, in terms of the existence of damage and its corresponding severity.

3.3 Closing Remarks

This chapter highlights the work done by some researchers on effect of corrosion on RC structures. They explain that RC structures exposed to corrosion environment results in its deterioration. It decreases its service life by introducing early cracks and spalling of concrete. Their works predicts that as the corrosion level increases the load carrying capacity of RC structure decreases. And the structures fail earlier than to its design life. So corrosion is a very serious problem which needs to be monitor.

Further this chapter explains the work on Ultrasonic testing as a non-destructive technique to monitor defects in the RC structures.

CHAPTER 4

EXPERIMENTAL STUDY OF RC BEAMS SUBJECTED TO CORROSION

4.1 Introduction

Main objective of the thesis was to monitor the effect of corrosion on reinforced concrete beams at different levels of corrosion and its effect on load carrying capacity of RC beams subjected to different levels of corrosion. To carry out the investigation, five real size beams were cased. Out of these five beams, one beam was taken as control beam and tested to failure to find out the load carrying capacity and other four beams were corroded at different levels. All four beams were corroded using impressed current technique for 6 days, 12 days, 18 days, and 28 days respectively reprenting varying degree of corrosion. The change in the crack pattern due to corrosion and load (P)-deflection (Δ) behavior of beams subjected to static load, which were corroded at different levels were studied experimentally. After the destructive testing, beams were dismantled using jack hammer and reinforcement was taken out to determine the mass loss in the steel subjected to varying levels of corrosion. The state of extracted corroded bars were also measured using ultrasonic pulse echo P/E and pulse transmission method P/T method to relate to different levels of corrosion.

4.2 Test Program

The test program was planned as below.

1. Determinations of basic properties of constituent materials namely cement, sand, coarse aggregates and steel bars as per relevant Indian standard specifications.
2. Five real size beams (127 x 227 x 4100mm) were casted using M 20 grade concrete.
3. Initially, control beam was tested to failure to determine its P-Δ behavior and subsequently other beams are corroded at different levels.
4. Out of five beams, all the four beams were corroded at different levels using accelerated corrosion technique.

5. After the corrosion process was completed all the four beams were also tested under static loading, to relate the effect of varying corrosion with the load-deflection behavior of RC beams.
6. Levels of corrosion were ascertained by calculating the mass loss of longitudinal reinforcement.
7. Degradation due to corrosion was also measured by non-destructive technique of ultrasonics.

4.3 Materials

Cement, fine aggregates, coarse aggregates, reinforcing bars are used in casting of beams. The specifications and properties of these materials are as under:

4.3.1 Cement

Portland pozzolana cement 43 grade cement from a single lot was for the study. The physical properties of cement as obtained from various tests are listed in Table 4.1. All the tests are carried out in accordance with procedure laid down in IS: 8112-1989.

Table 4.1: Physical Properties of Cement used

Sr. No	**Characteristics**	**Value obtained Experimentally**	**Value specified by IS: 8112-1989**
1	Standard consistency	33	-
2	Fineness of cement as retained on 90 micron sieve	1.0	<10%
3	Setting time 1. Initial 2. Final	 2hrs 5 hours	 >30 mins <10 hours
4	Specific gravity	3.05	-

4.3.2 Fine Aggregate

The sand used for the experimental program was locally procured and conformed to grading zone II. The sand was first sieved through 4.75 mm sieve to remove any particles greater than 4.75 mm and then was washed to remove the dust. The fine aggregates were tested per Indian Standard Specifications IS: 383-1970. Properties of the fine aggregate used in the experimental work are tabulated in Table 4.2 and Table 4.3.

Table 4.2: Sieve analysis of fine aggregate

S. No.	Sieve No.	Mass Retained (g)	Percentage retained	Percentage passing	Cumulative %age retained
1.	4.75 mm	1	.1	99.9	.1
2.	2.36 mm	21.5	2.15	97.75	2.25
3.	1.18 mm	204	20.4	77.35	22.65
4.	600 µm	190.5	19.05	58.3	41.7
5.	300 µm	298	29.8	28.5	71.5
6.	150 µm	225	22.5	6	94
7.	Pan	60	6	ΣF	**232**

Table 4.3: Properties of fine aggregates

S. No.	Characteristics	Value
1.	Type	Uncrushed (natural)
2.	Specific gravity	2.67
3.	Total water absorption	4.9 %
4.	Fineness modulus	2.32
5.	Grading zone	II

4.3.3 Coarse Aggregates

Crushed stone aggregate (locally available) of 20mm and 10mm are used throughout the experimental study. The physical properties and sieve analysis of coarse aggregate are given in Table 4.4 and Table 4.5 and Table 4.6.

Table 4.4: Sieve analysis of 10mm aggregates

S. No.	Sieve No.	Mass retained (kg)	Percentage retained	Percentage passing	Cumulative %age retained
1.	80 mm	-	0.00	100	0.00
2.	40 mm	-	0.00	100	0.00
3.	20 mm	-	0 .00	100	0.00
4.	10 mm	1.005	33.5	66.5	33.5
5.	4.75 mm	1.572	52.4	14.10	85.9
6.	Pan	0.423	14.1	ΣC	**119.4**

Fineness Modulus of Coarse aggregate (10 mm) = ΣC+500/100 = (119.4+500)/100 = 6.194

Table 4.5: Sieve analysis of 20 mm aggregates

S. No.	Sieve No.	Mass retained (kg)	Percentage retained	Percentage passing	Cumulative %age retained
1.	80 mm	0	0.00	100	0.00
2.	40 mm	0	0.00	100	0.00
3.	20 mm	19	.633	99.367	.633
4.	10 mm	2.92	97.32	2.047	97.953
5.	4.75 mm	.035	1.17	.877	99.123
6.	Pan	.025	.833	ΣC	**197.709**

Fineness Modulus of Coarse aggregate (20 mm) = ΣC+500/100 = (197.709+500)/100 = 6.9771

Table 4.6: Physical Properties of Coarse Aggregates

SNo.	Characteristics	Value	
		20mm	10mm
1.	Type	Crushed	Crushed
2.	Specific gravity	2.63	2.60
3.	Total water absorption	1.7%	2.29%
4.	Fineness modulus	6.97	6.194

4.3.4 Water

Fresh and clean water is used for casting the specimens in the present study. The water is relatively free from organic matter, silt, oil, sugar, chloride and acidic material as per Indian standard.

4.3.5 Reinforcing Steel

HYSD steel of grade Fe-415 of 10mm and 8mm and 6mm diameters were used as longitudinal steel. 10mm Ø bars are used as tension reinforcement and 8mm Ø bars are used as compression steel. 6mm Ø bras are used as shear stirrups. The properties of these bars are shown in Table 4.7

Table 4.7 Physical Properties of Steel Bars

Sr. No.	**Diameter of bars/ mesh wire**	**Yield-strength (N/mm^2)**	**Ultimate strength**	**Percentage Elongation**
1.	10mm	440.55	515.2	14.9
2.	8mm	555.5	638.23	22.5
3.	6mm	459.2	614.8	31.5

4.3.6 Concrete Mix

It was decided to use ***M20*** grade concrete mix design as per IS code method using the properties of materials as discussed above i.e. Table 4.1 to Table 4.6 the water-cement ratio used in the design is ***0.5***. The mix proportion of the concrete to be designed was calculated as ***1:1.8:3.3*** (cement: sand: aggregate). Total six cubes of size (150 x 150) mm were casted for the compressive strength test of designed concrete mix. Three cubes very tested after seven days of curing and rest after 28 days and the average values were recorded at which concrete cubes break

and compressive strength of materials after 7 days and 28 days comes out to be 16 and 28.5 KN/mm² respectively.

4.4 RCC Beam Design

The beam used for experimental study is designed using limit state method (IS-456-2000). It is designed as under-reinforced section. The beam is reinforced with 2 bars of 8mm at compression face and 2 bars of 10mm at tension face. 6mm stirrups were spaced at 150mmc/c. Longitudinal section and cross-section of beam are shown in Fig 4.1.

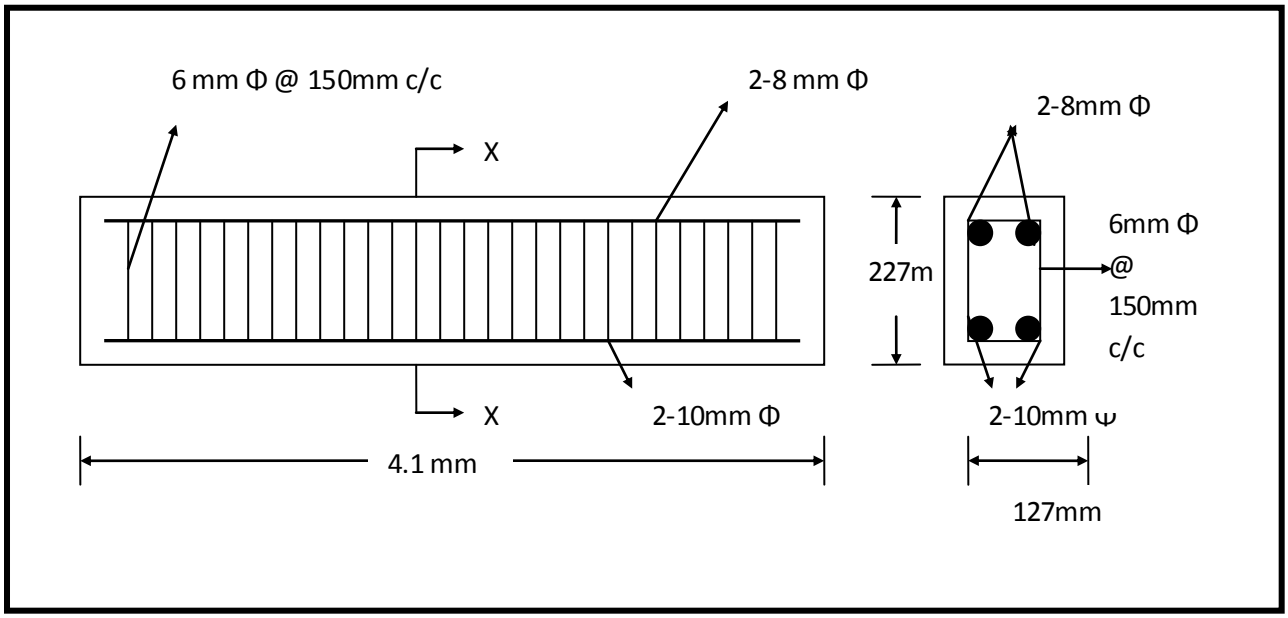

Fig 4.1 Longitudinal and Cross-Section of Beam

4.5. Casting of Composite Beams

The casting of beams was done in single stage. The beams were cast in mould of size 127 x 227 x 4100 mm. Entire beam mould is first oiled so that the beam can be easily removed from the mould after 24 hours. Spacers of size 25mm are used to provide uniform cover to the reinforcement. When the bars have been placed in position as per design, concrete mix is poured in the mould and the beam is vibrated using a needle vibrator, to ensure the proper compaction. The vibration is done until the mould is completely filled and there is no gap left. The beams are then removed from the mould after 48 hours. After demoulding the beams are cured for 28days using jute bags. Fig. 4.2 shows the beams before and after casting.

Fig. 4.2 Beams Before and After Casting

4.6. Inducing Corrosion in RC Beams

Out of all five beams, four beams were corroded using impressed current technique for 6 days, 12 days, 18 days, and 28 days respectively. Initially from the above selected four RC beams which are to be corroded at different levels of corrosion, one control beam was subjected to the accelerated corrosion until the longitudinal crack spread in the whole length of the beam, this took 28 days. And then the test matrix for the corrosion was further decided. So, rest three beams were subjected to 6 days, 12 days, & 18 days of corrosion representing different levels of corrosion. The corrosion of reinforcing steel was accelerated by impressing a constant anodic current of 0.8A. This was done through an integrated system incorporating a DC rectifier with a built-in ammeter to monitor the current and voltage to control the current intensity. Scientech Dual Power Supply with a maximum output of 2A at 30V was used (Fig: 4.3). This method of corrosion was employed to reach advanced stages of deterioration in a relatively short time. At a time two beams were connected in series for corrosion process. Central 1.5 m portion of concrete beams were subjected to corrosive environment. It was done by continuous sprinkling of 3%

NaCl solution. This type of arrangement was selected to assure that the corrosion product formed is not washed away and cracks are formed in the concrete specimens. The direction of the current was adjusted so that the reinforcing steel became an anode and a stainless steel wire mesh wrapped all around concrete beams at centre 1.5m served as a cathode as shown in Fig:4.4.

Fig: 4.3 Scientech Dual Power Supply Source

Fig: 4.4. Cathode

4.7 Study of Load-Deflection Characteristics

After all the beams were corroded to different levels of corrosion, load-deflection behavior of beam was study to relate the effect of corrosion on RC beams. All the five beams were tested under simply supported end conditions. Ultimate load ***P-Δ tests*** were performed in the laboratory to determine the load-carrying capacity of the beam specimens. The loading arrangement used was four-point loading, as shown in Figure 4.5. This arrangement allows for a central region having virtually constant moment without any shear force. The testing of beams is done with the help of hydraulic operated jack connected to load cell as shown in Fig: 4.6.

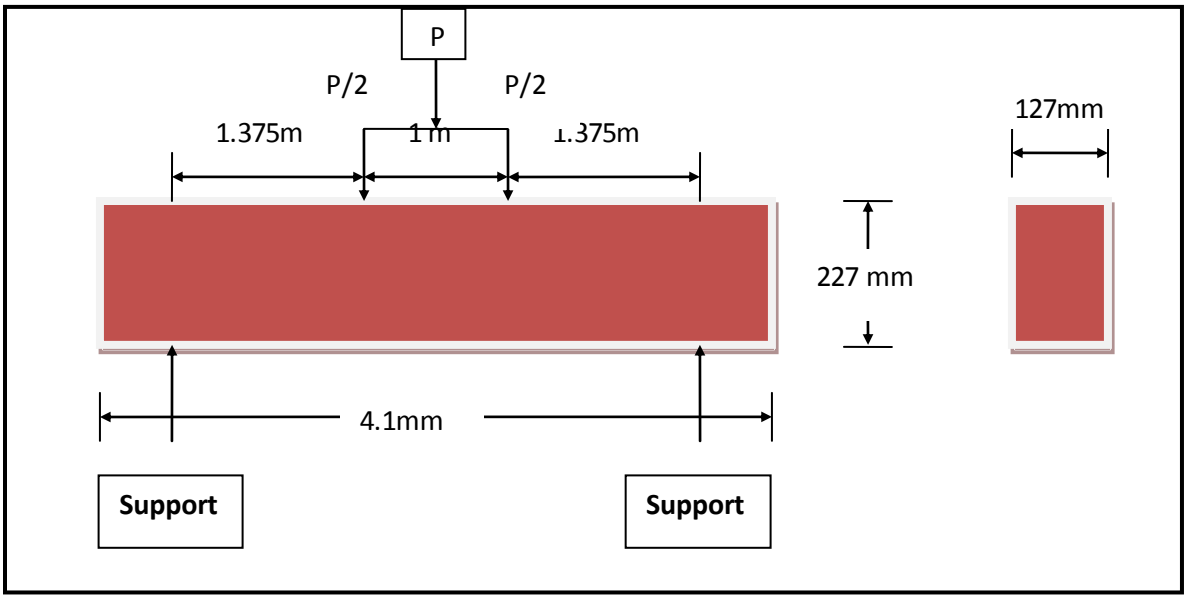

Fig. 4.5 Loading System of Beam

Fig: 4.6 Hydraulic Operated Jack

The load is applied to the beam with the help of load cell and load value is obtained from the data acquisition system, which is attached with the load cell as shown in Fig 4.7.

Fig: 4.7 Load Cell

Two LVDT's are placed at the center and at a distance of span/4 from the end of beams to record the deflection against the loading as shown in Fig.4.8.

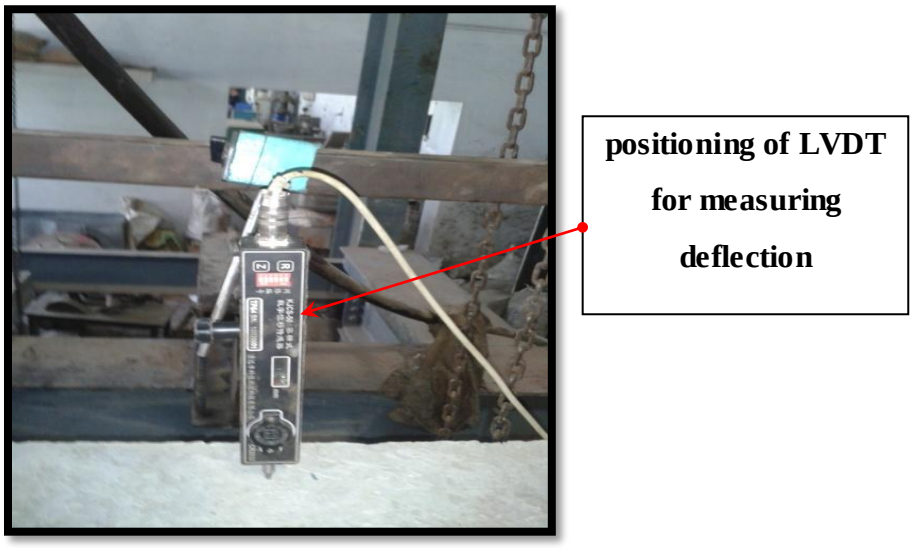

Fig: 4.8 LVDT

4.8 Other tests

After studying the load-deflection characteristics of all five beams (C-0 to C-28) as discussed above mass loss in the steel reinforcing bars which were subjected to varying levels of corrosion was determined.

4.8.1 Mass Loss Determination

Following the structural and subsequent destructive tests, the reinforcement was removed from each beam by dismantling the beams using jack-hammer as shown in Fig: 4.9 and the corrosion products were cleaned using a wire brush. The corroded reinforcing bars were characterized by percent mass loss (ML), which was calculated by **eq: 4.1** where *m* denotes mass and the subscript "i" represents the initial or reference mass and "cor" represents the residual mass. The reference mass of reinforcement was measured using healthy bar. For residual mass calculations middle 1.5m portion of reinforcement was cut from the cage which was taken out after dismantling of corroded beams.

$$ML = \frac{mi - mcor}{mi} X\ 100 \qquad \text{- eq. 4.1}$$

Where,

mi = Initial or Reference Mass

mcor = Residual mass

Fig: 4.9 Jack-hammer used for dismantling of RC Beams

4.8.2 Ultrasonic Testing Arrangement

After finding the percent mass loss in reinforcement due to corrosion at different levels, ultrasonic testing was done on reinforcing bars in air corroded to different levels.

A typical Ultrasonic Testing (UT) system is used as shown in Fig: 4.12 to detect the damages in the bars. It consists of a pulser/receiver(DPR 300, JSR Make) as shown in Fig: 4.10, transducers (Karl Deutsch Make) of 12mm having frequency 1MHz as shown in Fig: 4.11, and display devices. Driven by the pulser, the compressional transducer generates ultrasonic pulse that propagates through the bar. Full experimental set for ultrasonic is shown in Fig: 4.12 . Two

ultrasonic techniques of pulse transmission and pulse echo were used to monitor the healthy and damaged bars.

In pulse echo, when there is an interface such as a crack, void, or flaw in the wave path, part of the energy is reflected back from the interface and received by the same transmitting transducer. In pulse-transmission method, an ultrasonic transmitter introduced the wave from one end of the bar and a receiver is placed at the opposite end to record the transmitted pulse. By measuring the relative change of amplitudes of the input and the received signals, the relative severity of the damage is assessed. The results were reported in the form of voltage-time curves.

Fig: 4.10 pulser/receiver (DPR 300, JSR Make)

Fig: 4.11 Contact Transducers

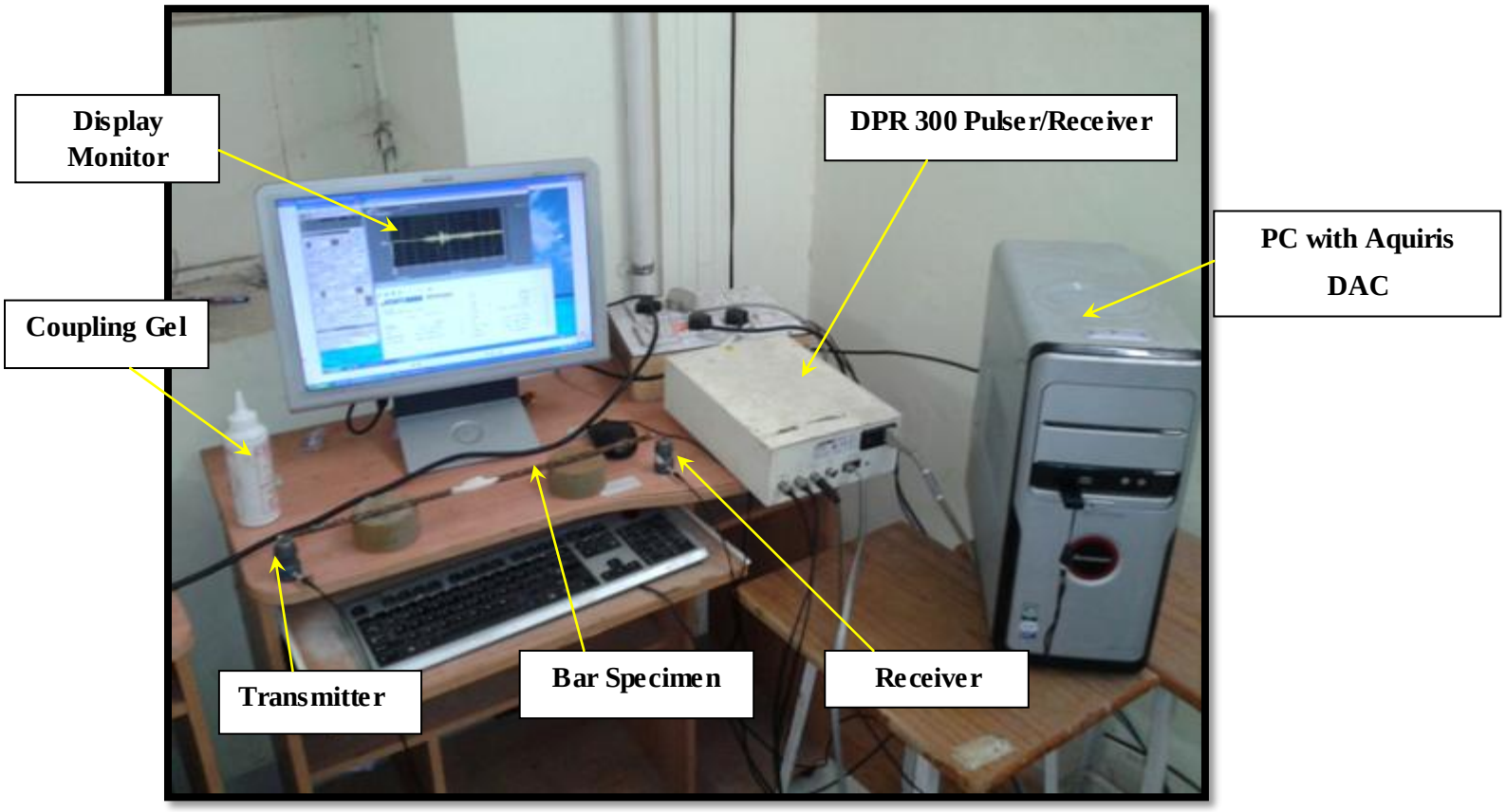

Fig: 4.12 Experimental Set up of Ultrasonic Testing

4.9 Closing Remarks

This chapter highlights the experimental procedure adopted in this research work. Firstly this chapter gives a brief introduction about the concrete mix adopted for casting of RC beams. It mainly covers the description of properties of the materials like cement, sand, aggregates and water. And based on this knowledge design mix was done. M20 grade concrete was adopted. Further this chapter covers the information about the designed section adopted for RC beams and briefly describes the casting procedure of RC beams. This chapter also highlights the devices used for inducing corrosion in RC beams and for study of load deflecting behavior of RC beams. It also gives information about the devices used for ultrasonic testing.

CHAPTER-5

RESULTS AND DISCUSSION

5.1 Introduction

In this work, deterioration in RC beams subjected to varying degree of corrosion was studied by measuring the effect on load carrying capacity of beams, variation in crack pattern and effect on deflections under static four point loading. The different levels of corrosion were related to percent mass loss and change in ultrasonic signals with varying corrosion.

5.2 Visual Observations

Visual inspection refers to evaluation by means of eyesight, either directly or assisted in some way. The visual inspection of a structure is the "first line of defense" and typically involves the search for large-scale deficiencies and deformities.

As discussed earlier, initially one control beam was subjected to the accelerated corrosion until the longitudinal crack spread in the whole length of the beam, this took 28 days. And then the test matrix for the corrosion was further decided. So, rest three beams were subjected to 6 days, 12 days, & 18 days of corrosion representing different levels of corrosion. So results of visual observation are discussed in same order.

5.2.1 Beam corroded to 28 Days (C-28)

Beams undergoing corrosion for 28 days shows dark reddish brown corrosion products with reddish brown liquid oozes out from the cracks on all faces of the beam at centre 1.5m portion. Corrosion products formed in C-28 beam was in large volume than in other cases. At the top surface of C-28 beam continuous longitudinal crack was observed throughout the centre 1.5m portion of the beam as shown in Fig: 5.1. At the front side face also longitudinal crack was observed throughout the centre 1.5m portion along the tension bar as shown in Fig: 5.2. At the back side face small vertical and horizontal cracks were observed as shown in Fig: 5.3. At the bottom face of beam large corrosion products were noticed but no crack generated. It was noted that deterioration of C-28 beam due to corrosion was more than the other beams.

Fig: 5.1 (a) Top surface of C-28 beam

Fig: 5.1 (b) Longitudinal Crack on top surface of C-28 beam

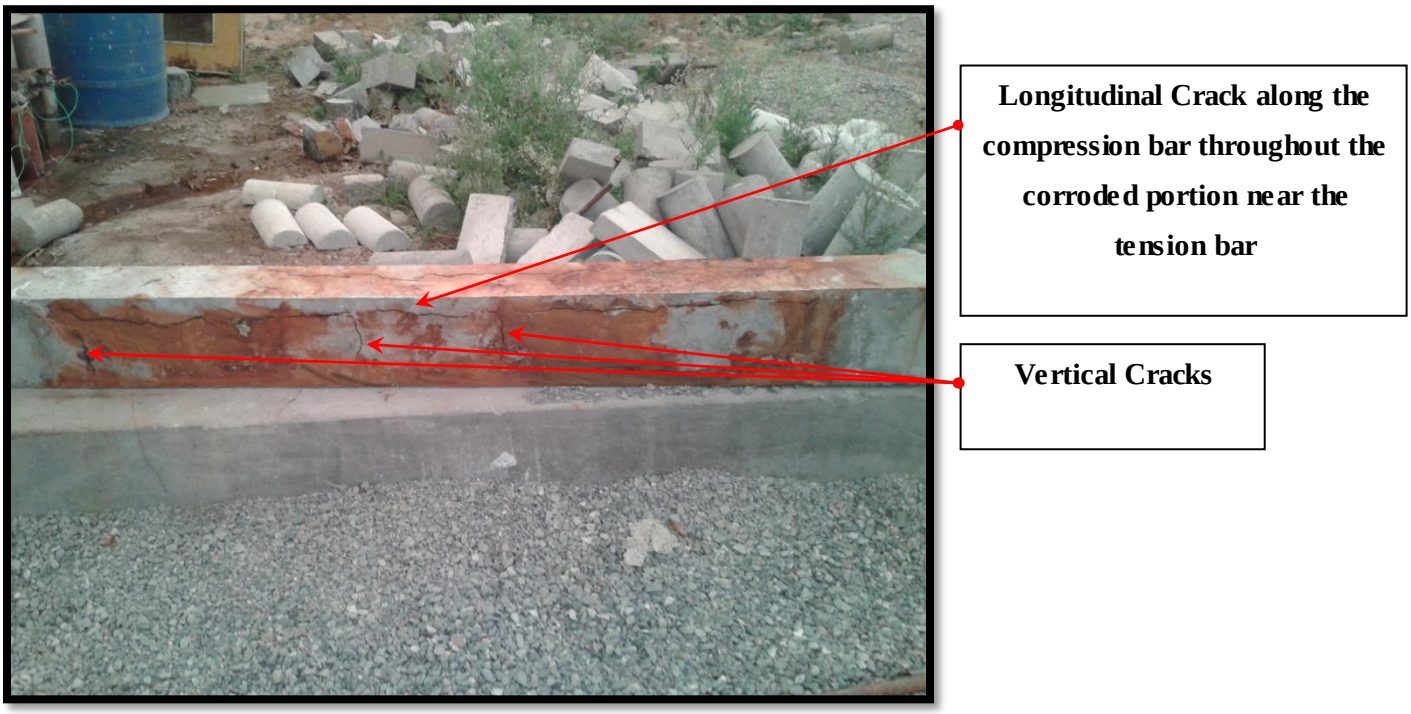

Fig: 5.2 Front Side Face of C-28 Beam

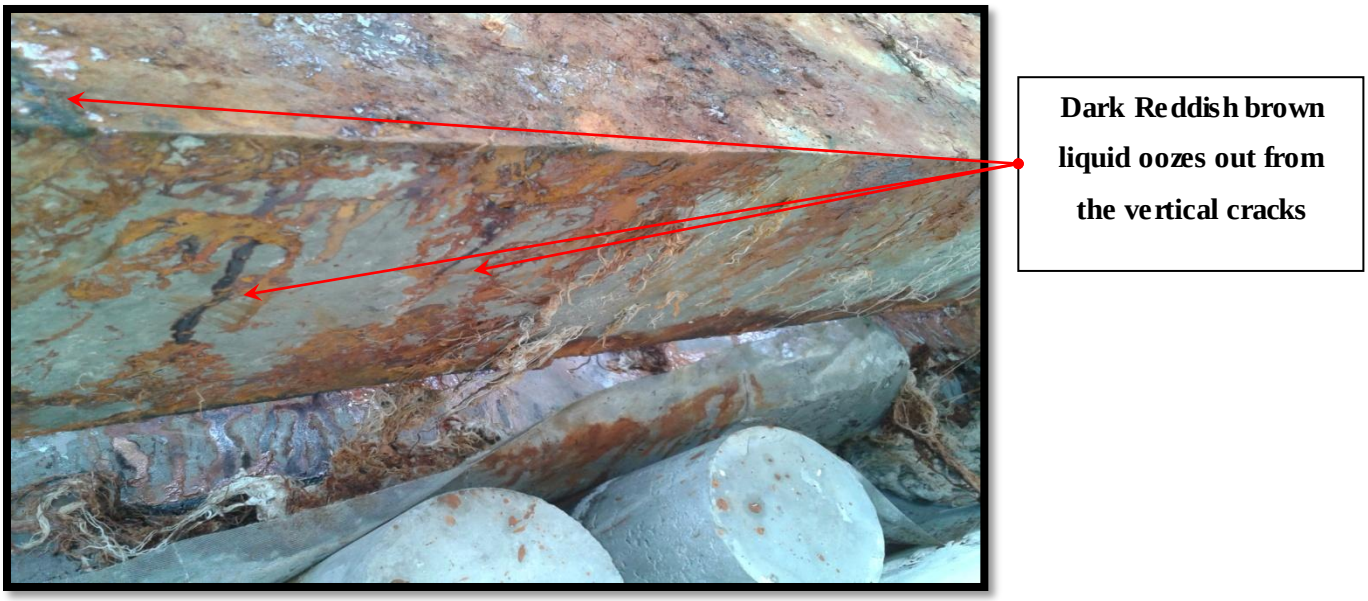

Fig: 5.3 (a) Back Side Face of C-28 beam.

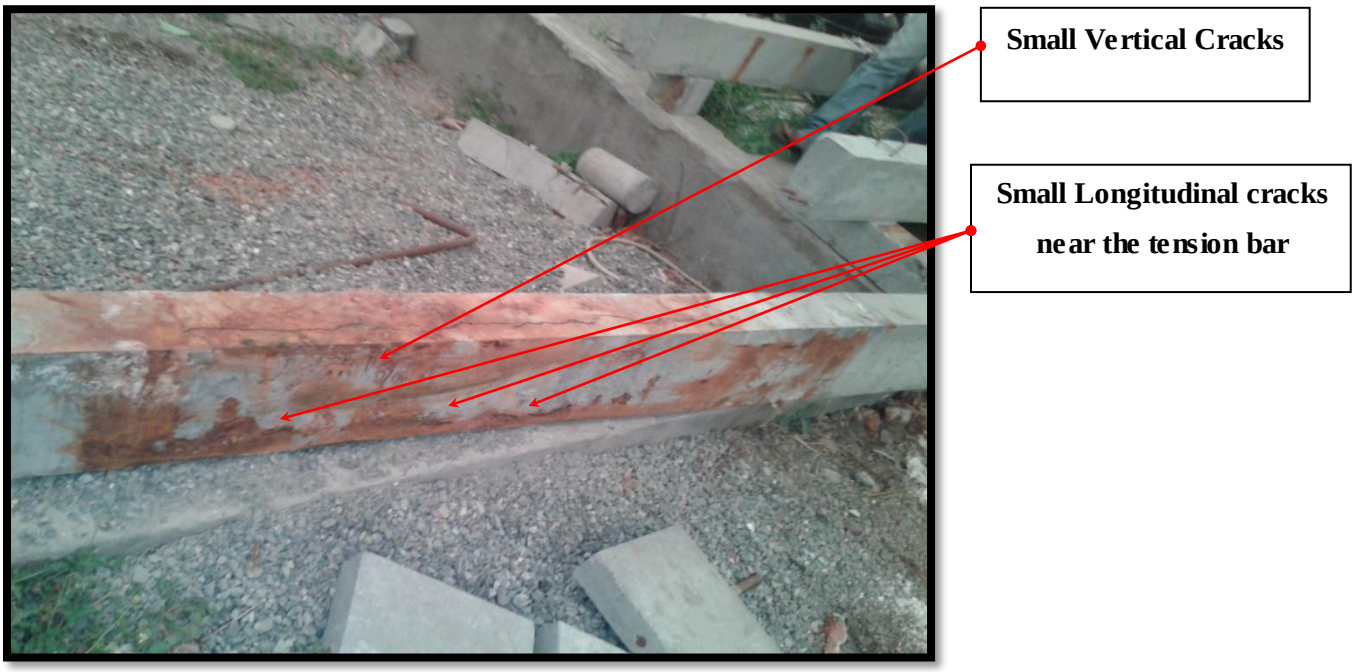

Fig: 5.3 (b) Back Side Face of C-28 beam

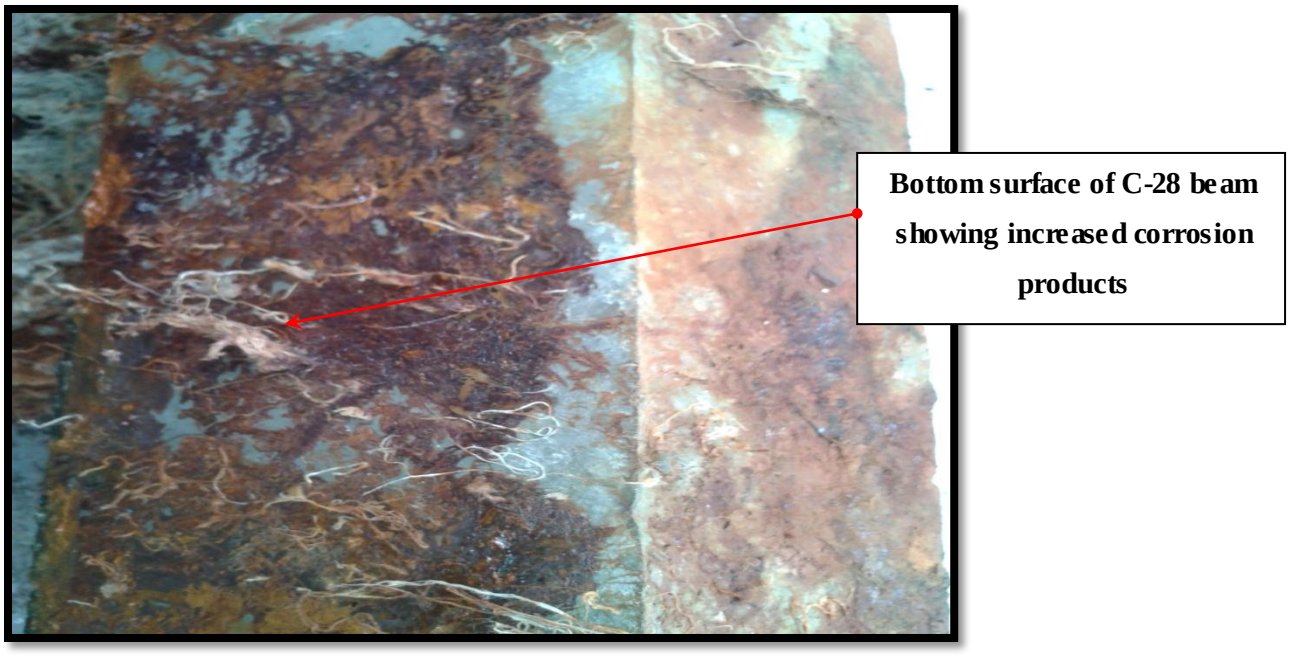

Fig: 5.4 Bottom Face of C-28 beam

5.2.2 Beam Corroded to 6 Days (C-6)

A beam undergoing accelerated corrosion for 6 days shows reddish brown patches of corrosion product on the all four sides of beam at centre 1.5m portion of beam as shown in Fig: 5.5 to 5.7. It was noted that no cracks was generated on surface of beam after 6 days corrosion. It was observed that 6 days corroded beam shows small corrosion products and no cracks as compared to other beams.

Fig: 5.5 Top surface of C-6 Beam

Fig: 5.6 Front Side face of C-6 beam

Fig: 5.7 back Side face C-6 beam

5.2.3 Beam Corroded to 12 Days (C-12)

Beam undergoing corrosion for 12 days shows reddish brown patches along with cracks. Small longitudinal cracks were generated on all sides of beam as shown. In addition to this small vertical cracks on right side from the centre on front side face of the beam as shown in Fig: 5.9. And small longitudinal cracks of shorter length near the compression face of the beam on right side of the centre on back face of the beam as shown in Fig: 5.10. But no cracks were observed on the bottom side except reddish brown corrosion patches were seen.

Fig: 5.8 Top Surface of C-12 beam

Fig: 5.9 Front Side Face of C-12 beam

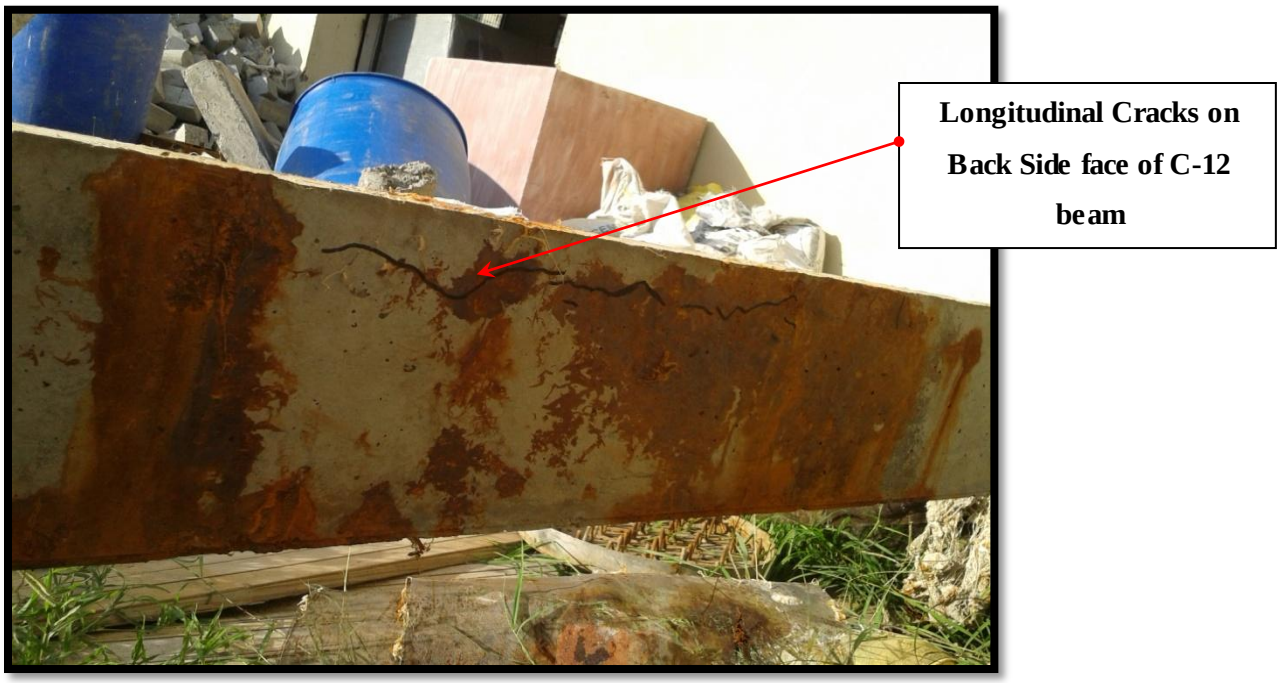

Fig: 5.10 Back Side Face of C-12 beam

5.2.4 Beams corroded to 18 days (C-18)

Beam undergoing corrosion for 18 days shows reddish brown patches on four sides at centre 1.5m portion of the beam along with cracks on top and side faces. At the top of the C-18 beam longitudinal crack was observed with increased length and width than C-12 beam at centre as shown in Fig: 5.11. At the front side face of the beam vertical cracks were observed originating from tension face towards compression face as shown in Fig: 5.12. At the back side face of the beam it was observed that full centre 1.5m portion of the beam was covered with reddish brown patches, an increase in volume of corrosion product was observed in C-18 beam than in C-6 and C-12 beams and longitudinal crack was observed on the surface throughout the centre 1.5m portion of the beam as shown in Fig: 5.13. A reddish brown liquid oozes out from cracks on the back side face of the beam as shown in Fig: 5.14

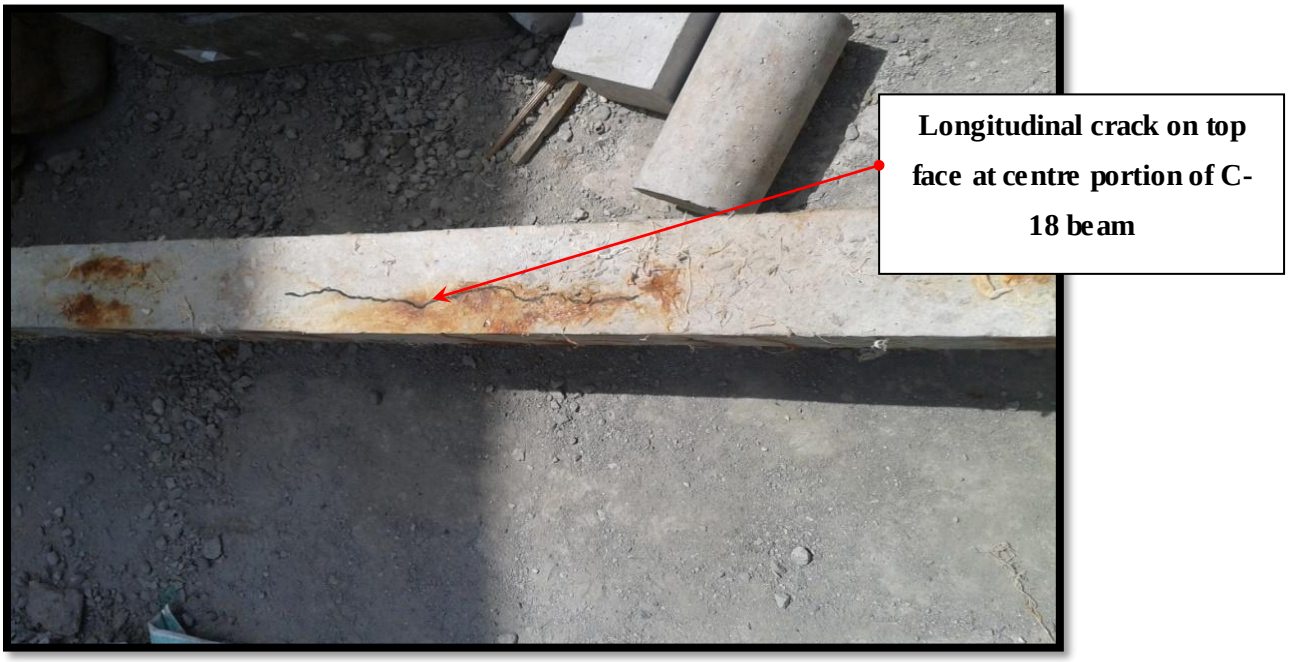

Fig: 5.11 Top Surface of C-18 beam

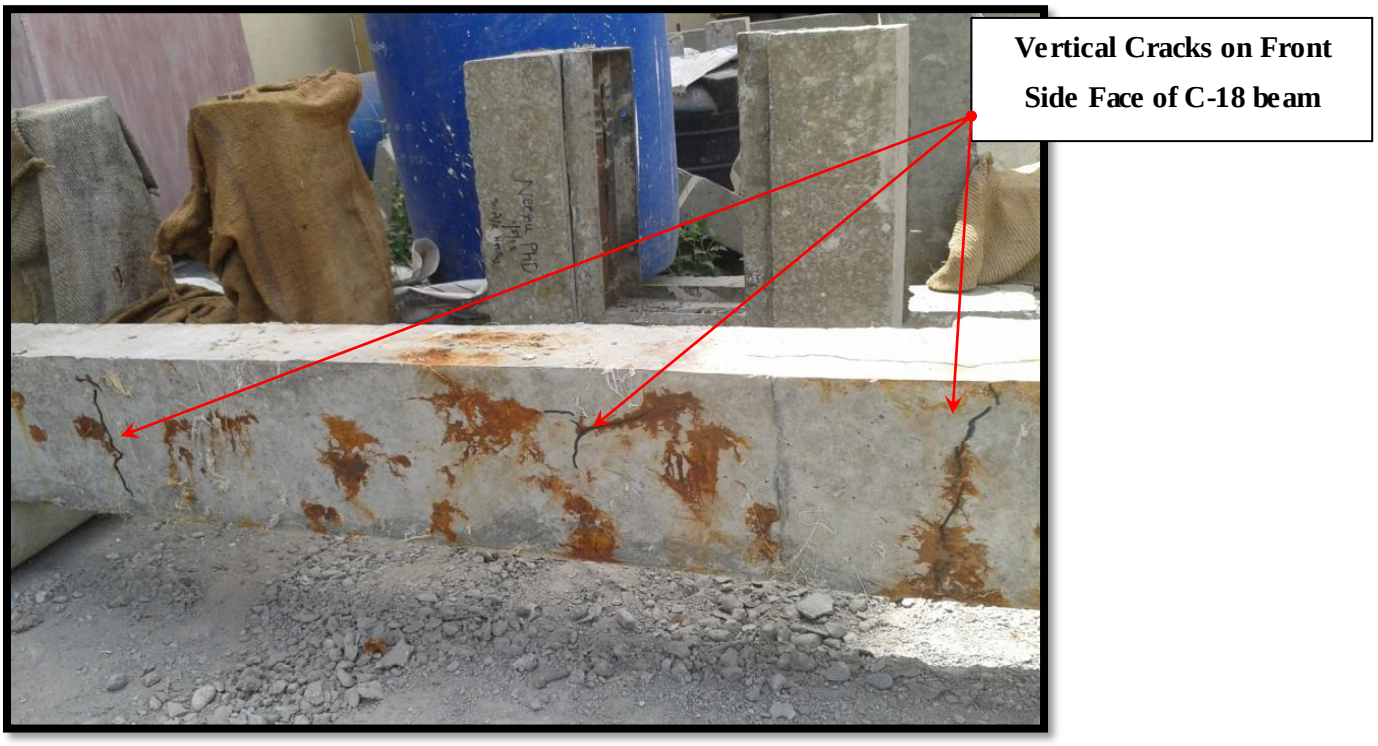

Fig: 5.12 Front Side Face of C-18 beam

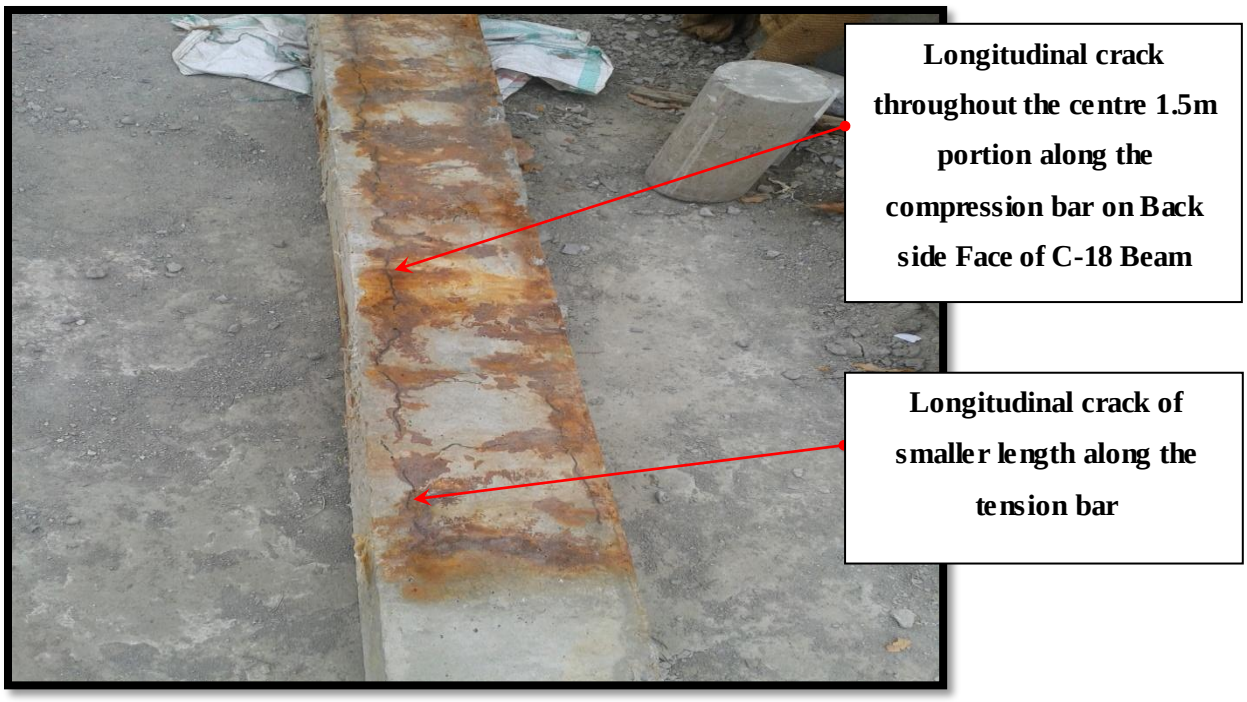

Fig: 5.13 Back Side Face of C-18 beam

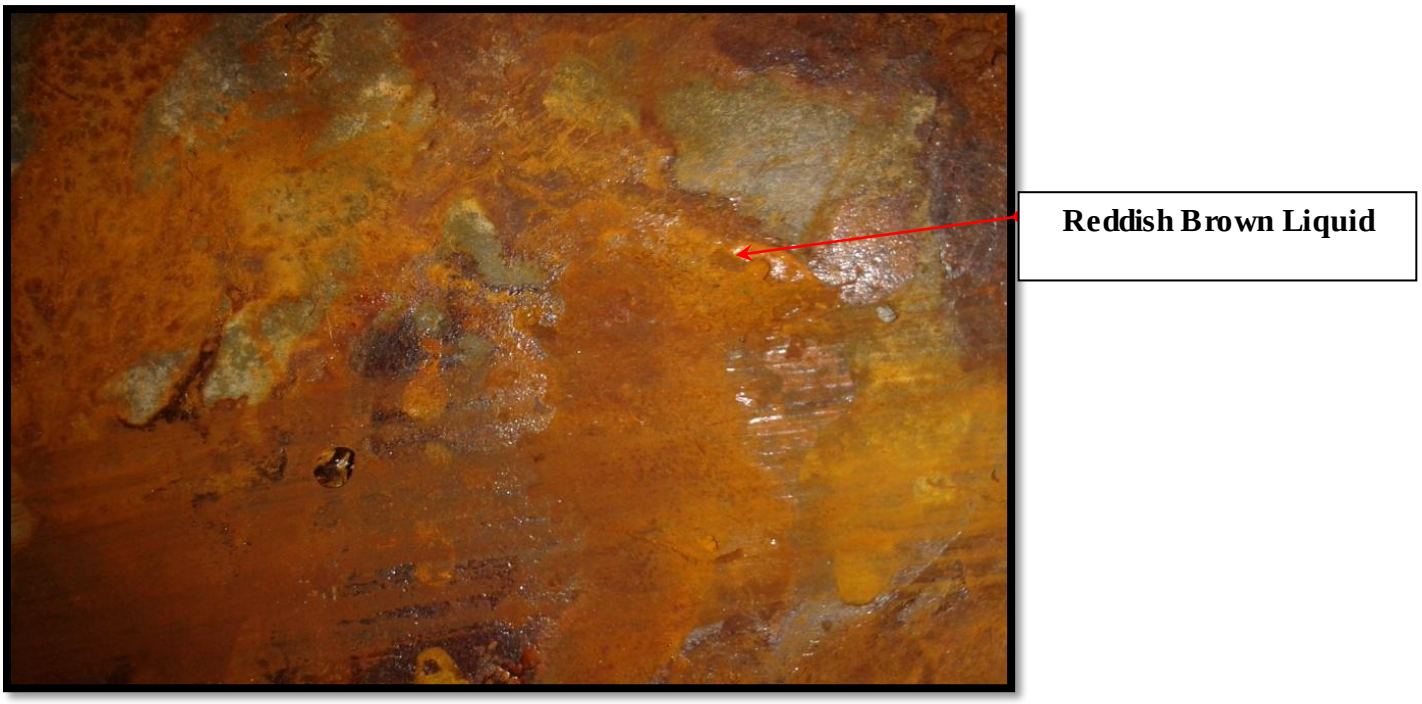

Fig: 5.14 back Side face of C-18 Beam

It was concluded from the above results that with the increase in exposure period of beams to corrosion, deterioration of beam increases i.e. crack length and width increases, there is also increase in volume of corrosion products with exposure period. Initially crack appear on the beam surface, and then propagates along the direction of reinforcement with time. In addition vertical cracks are also observed due to formation of voluminous net products (6-10 times than that of steel).

5.3 Variations in Potential

The fluctuations in the voltage of the corrosion cell can be useful when comparing the corrosion of individual specimens. After 28 days of curing, each specimen (except for the control) was subjected to accelerated corrosion. The current and voltage that was supplied was monitored on a daily basis. Since the current was constant, the voltage was continuously regulated to compensate for the changing resistance. It was notice that the voltage had undergone

an initial increase -within the first 24 hours, which was followed by a gradual decrease. Given that voltage is directly proportional to resistance -when current is constant (ie. a decrease in resistance would require a reduction in voltage), it can be concluded that there was mounting electrical resistance initially, followed by a progressive reduction. The average voltages during the accelerated corrosion for the beams connected in series were approximately 9.5volts during corrosion period and at initial stage voltage was 15.5 volts at constant current of 0.8A.

It is clear from these observations that there is an initial increase of resistance within the system, which is followed by a decreasing trend. This phenomenon can be attributed to the initial build up of corrosion products that occupy the pores of the concrete, thus blocking the movement of ions and increasing the electrical resistance. Eventually, the tensile stresses developed within the concrete caused by the expanding corrosion products crack the concrete, making a corridor for the transport of ions and escaping corrosion products, which results in the subsiding of resistance.

5.4 Load Deflection Behavior of Corroded Beams

After the corrosion process was completed, all four beams and control beam for load deflection behavior. Beams were loaded in four-point bending until failure and the corresponding load and deflections at midspan and span/4 were measured using LVDTS.

5.4.1 Control Beam (C-0)

The control uncorroded beam (C-0) was tested under four point loading. The setup ensures pure bending in the central third portion of the beam. The beam was as shown in Fig: 5.15 and loads were applied till the failure and beam stop taking further load. It may be noted that the beam sections were under-reinforced and steel as yielded for all the sections. The first crack appears at a load of 19.5KN near the left point load, accompanied by number of flexure cracks at the side face of control beam. As the load on the beam further increased and the beam finally fails at 25.5KN. Almost all cracks were vertical near top and bottom edge, sub cracks were developed connecting to main cracks. So experimentally it was observed that ultimate load for the control beam is 25.5KN with ultimate deflection at mid-span 81mm and at span/4 is 40mm as shown in Fig: 5.15 clearly shows that it is a pure flexure failure. The load deflection response of the control un-corroded beam is shown in Fig: 5.16

Fig: 5.15 Flexure Cracks on side face of C-0 beam

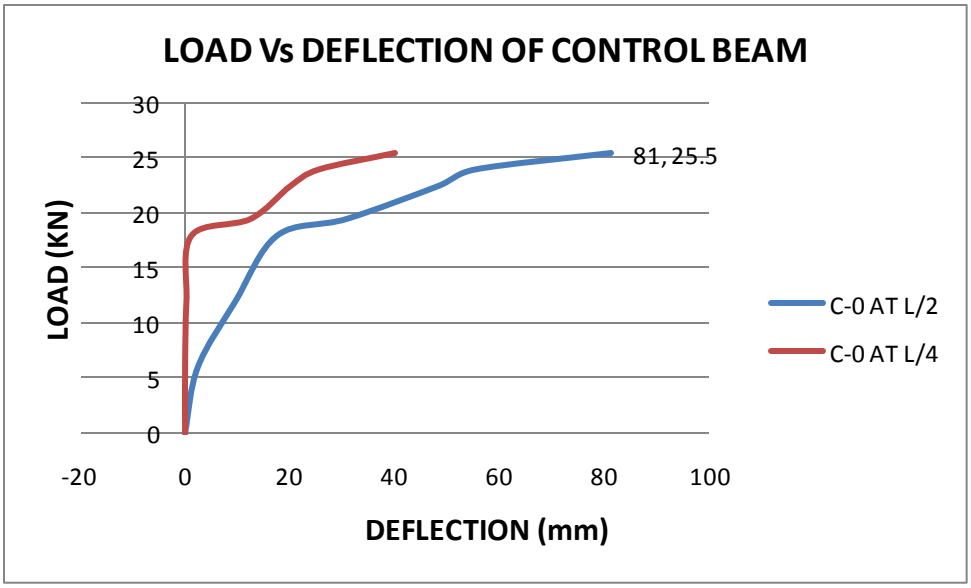

Fig: 5.16 Load-Deflection Curves of C-0 beam

5.4.2 Beams Corroded to 6-Days (C-6)

Fig: 5.17 shows beam with 6 days corrosion having no previous corrosion cracks as discussed earlier was tested under static loading. First crack appeared at a load of 19.02KN at centre of the beam near tension zone. Load is further increased the cracks widened and start progressing towards the compression zone and beam suddenly failed at load of 23.7 KN from extreme tensile face at centre as shown in Fig: 5.18. No additional cracks appear on the surface

of beam. Fig: 5.19 show the load deflection behavior of C-6 beam. P-Δ curves indicated that there is a decrease in load carrying capacity and deflection capacity as compared to control beam. It was noticed from the results that there is decrease in load carrying capacity of C-6 beam was 7.05% as compared to healthy control beam.

Fig: 5.17 Side face of C-6 Beam before loading

Fig: 5.18 C-6 beam showing huge crack at centre after failure

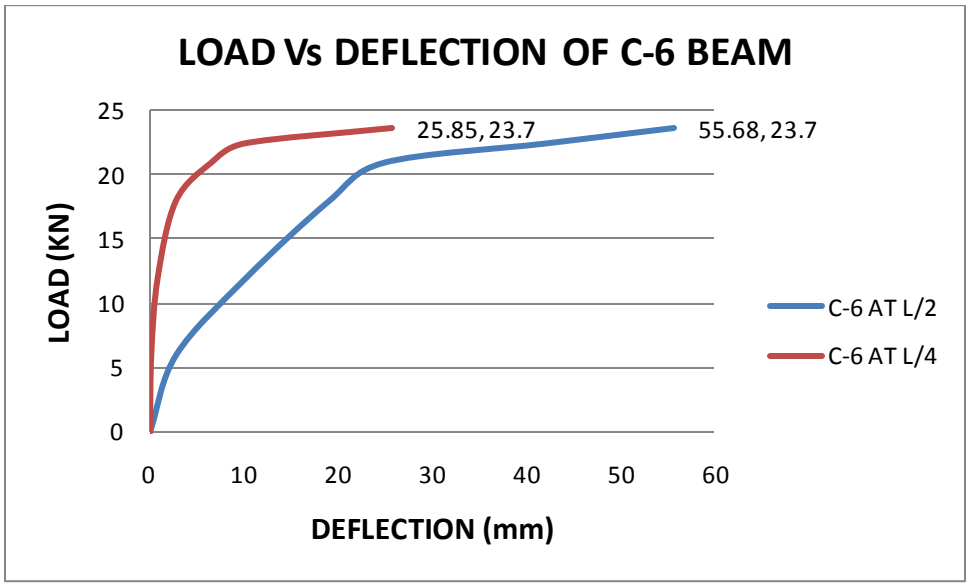

Fig: 5.19 Load-Deflection Curves of C-6 Beam

5.4.3 Beams Corroded to 12-Days (C-12)

Beam undergoing corrosion for 12 days (C-12) shows longitudinal and vertical cracks before loading on front side face as shown in Fig: 5.9. C-12 beam was loaded under two point loading, Fig: 5.20 shows the C-12 beam before loading. First crack appears at a load of 19.68KN near the left point load, then further as the load was increased widening of longitudinal corrosion crack was observed, accompanied by vertical sub cracks generating from longitudinal crack near the tension zone progressing towards the compression zone as shown in Fig: 5.21. And then suddenly beam fails from the extreme tension face resulting in large cracks at soffit of the beam which were progressed from the longitudinal crack on the side face as shown in Fig: 5.22. The ultimate load at which beam fails is 21.6KN and ultimate deflection at centre is 50.002 mm and at span/4 is 23.47mm as shown by load deflection curves of C-12 beam in Fig: 5.23. It was observed from the results that there is a decrease in load carrying capacity and deflection capacity of C-12 beam as compared to C-6 beam and control beam. As compared to healthy beam there is a decrease of 15.29% in load carrying capacity of C-12 beam.

Fig: 5.20 Side face of C-12 Beam before loading

Fig: 5.21 Side face of C-12 Beam showing cracks after failure

Fig: 5.22 C-12 Beam showing Cracks generated at the soffit after failure

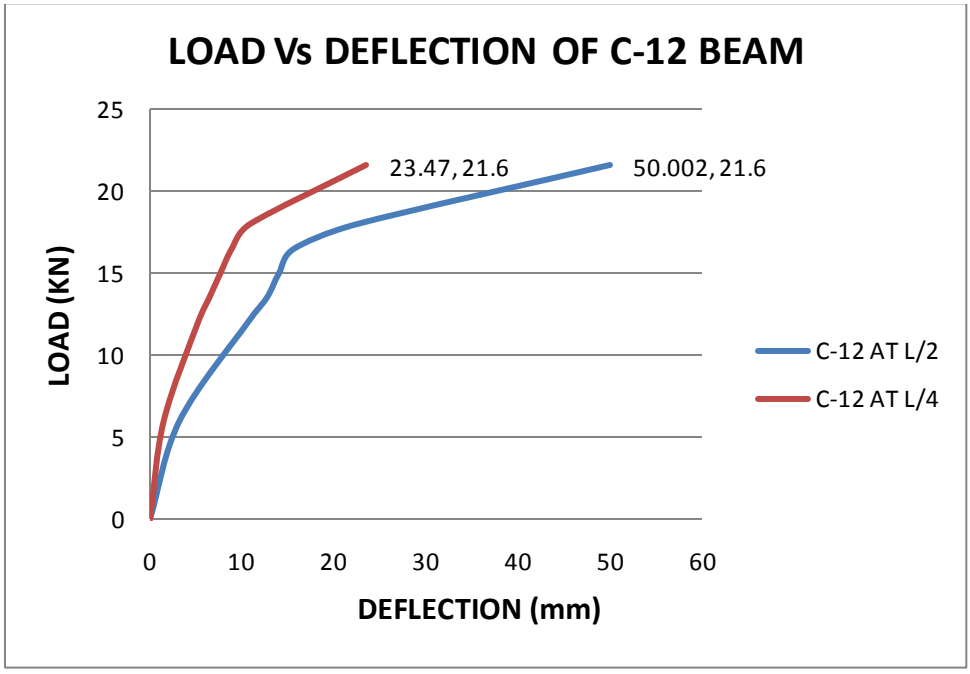

Fig: 5.23 Load-Deflection Curves of C-12 Beam

5.4.4 Beams Corroded to 18-Days (C-18)

Beam undergoing corrosion for 18 days shows longitudinal crack throughout the corrosion region and some vertical cracks on side face before loading as shown in Fig: 5.24. It was observed that first vertical crack appeared at a load of 20.04KN near the centre of beam on side face, with widening of longitudinal crack at the centre and as the load on beam was increased, vertical crack from tension zone propagates towards the compression face till the longitudinal crack and finally beam fails at a load of 20.50KN with a huge crack at centre of beam and further widening of the vertical crack and crushing of concrete from the extreme tensile face as shown in Fig: 5.25.At ultimate load ultimate deflection noted at centre was 45.97mm and at span/4 was 20.68. It was observed from the curves shown in Fig: 5.26 that there is a decrease in load carrying capacity and deflection capacity of C-18 beam as compared to C-6 beam, C-12 beam and control beam. It was noted C-18 beam that there is a decrease of 19.6% in load carrying capacity as compared to healthy beam.

Fig: 5.24 Side face of C-18 Beam before loading

Fig: 5.25 C-18 beam showing large vertical crack near the centre of beam

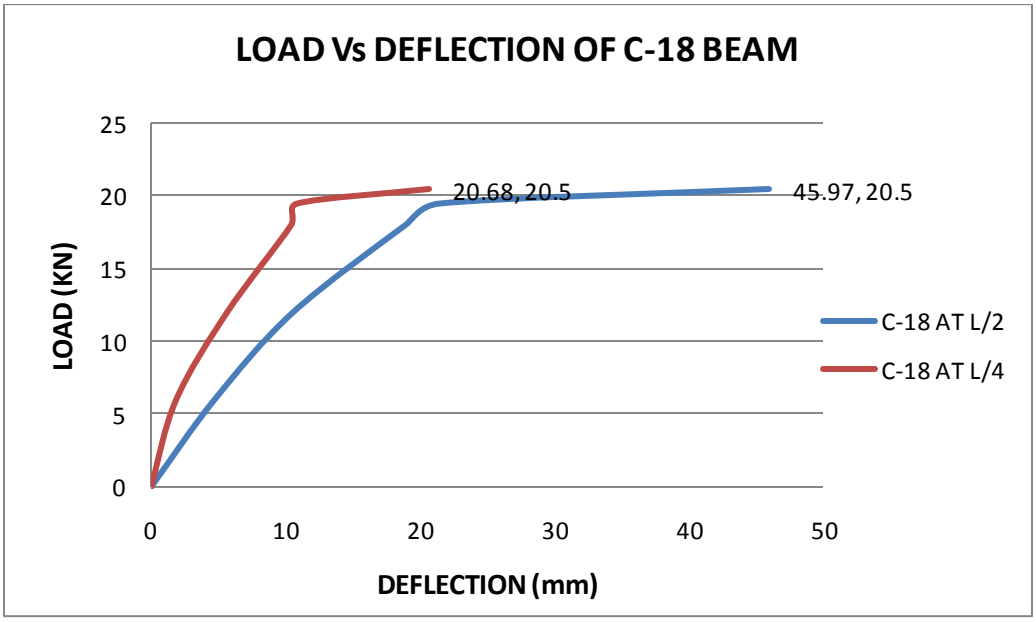

Fig: 5.26 Load-Deflection Curves of C-18 Beam

5.4.5 Beam Corroded to 28 days (C-28)

Beam undergoing corrosion for 28 days has longitudinal and vertical cracks on side face before loading as shown in Fig: 5.27. Deterioration of C-28 beam due to corrosion was to a large extent than the other beams as discussed earlier. It was observed that first crack appear at a load

of 13.08 KN at right side from the centre of beam on side face, with widening of vertical corrosion cracks on both left and right side from the centre as shown in Fig: 5.28 & 5.29. As load increases beam suddenly get fails at a load of 13.5KN without giving any warning as shown in Fig: 5.28. The ultimate deflection at centre is 39.74mm and at span/4 is 18.54mm as shown by curves in Fig: 5.31. It was visually observed that vertical cracks propagate to extreme tension face leaving the bottom face with huge cracks as shown in Fig: 5.30. Load carrying capacity of C-28 beam was decreases to 47.05% as compared to healthy beam.

Fig: 5.27 Side face of C-28 Beam before loading

C-28 Beam showing cracks on left side from centre of side face of beam after failure

Fig: 5.28 Side Face of C-28 beam

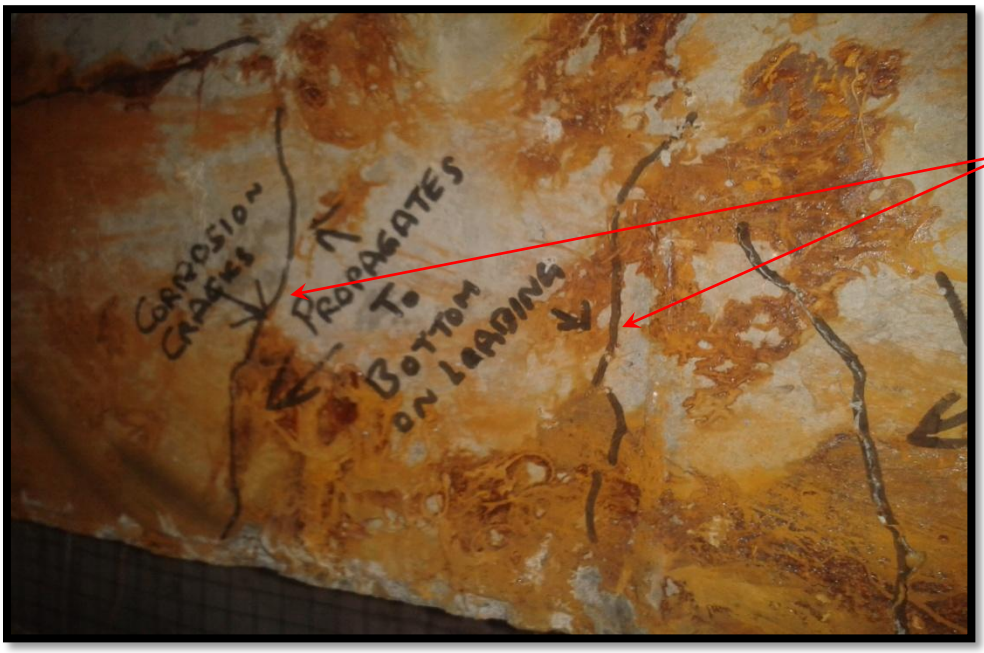

C-28 Beam showing propagation of corrosion cracks towards tension zone on left side from centre on side face of beam after loading

Fig: 5.29 Side face of C-28 beam

Cracks generated at extreme tension face after failure

Fig: 5.30 C-28 Beam showing cracks at soffit after failure

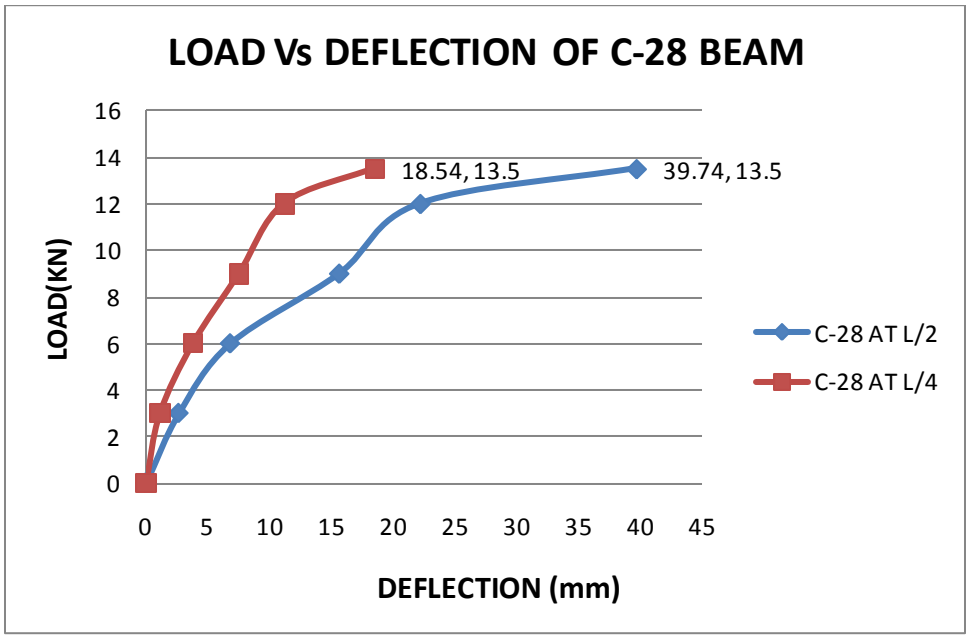

Fig: 5.31 Load-Deflection Curves of C-28 Beam

From the above results, the beam tests show a reduction in both the load-carrying capacity and the deflection capacity with this increase in corrosion level. This is due to the known effects of reductions in steel-concrete bond, reinforcing steel cross-sectional area, and concrete cracking and spalling due to corrosion.

In this study, a decrease in load as well as deflection capacity is regarded as an indication of reduced ductility.

5.5 Comparison of Load-Deflection Curves

Load-deflection curves (LDC's) reveal much information concerning the behavior of RC beams and they are notably altered with the progression of corrosion. Results shown in Fig: 5.32 predicts that

- As the corrosion level increases deflections increases at initial stages.
- The ultimate deflections corresponding ultimate load, however, were reduced with increasing corrosion.
- A higher corrosion level results in decreased stiffness.

- These reductions in stiffness, load carrying capacity and deflection capacity suggest a rise in brittleness.

These phenomena are a result of the combination of the deteriorated bond between the steel and the concrete, the reduction in the cross-sectional area of the reinforcing steel, and the cracking and delamination of the concrete.

As corrosion increased, the failure mode of the beams shifted from predictable ductile flexure failures to more brittle bond-shear failures. Severely corroded beams displayed extremely brittle failures at centre or near the centre, with no forewarning.

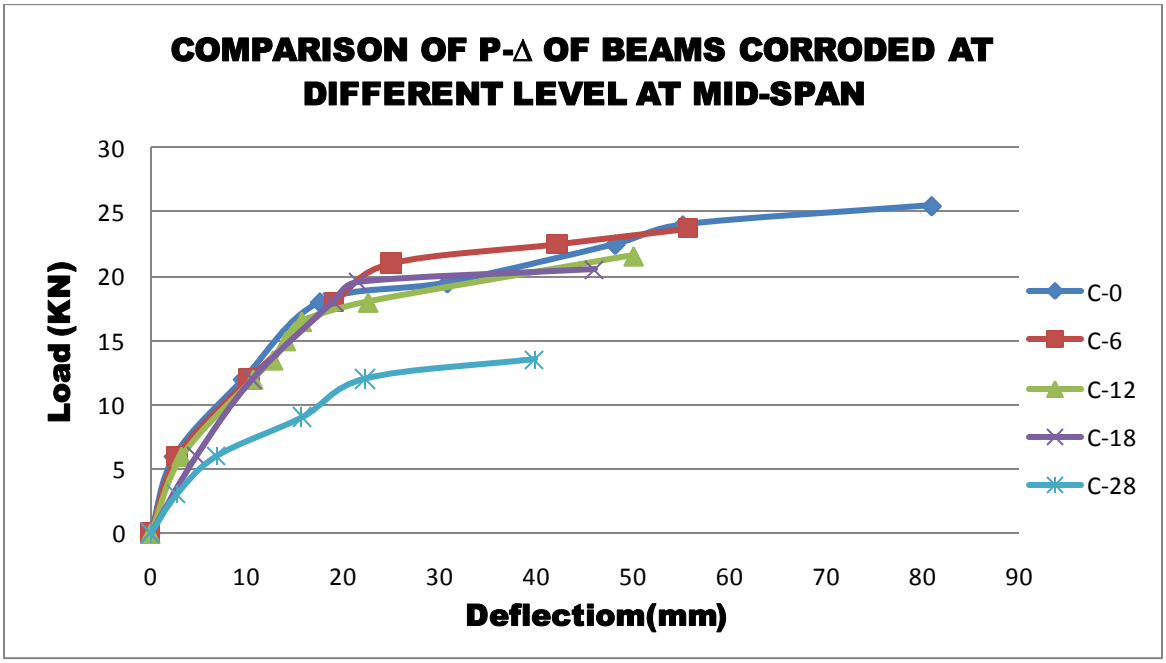

Fig: 5.32 Comparison of P-Δ Curves of beams Corroded at different levels at mid span

The slope of the LDC before failure or the yielding of the reinforcing steel can indicate the stiffness of RC beams. The slope of the LDC was determined by *m* of the equation of the straight line portion of each LDC, in the section of the curve before the yielding of the reinforcing steel or the collapse of the beam, whichever came first.

The slope of the LDC, and the deflection capacity all decrease with increased corrosion intensity, implying a reduction in the stiffness. Bar chart shown in Fig: 5.33 show that as the age of corrosion increases stiffness loss increases. Percent loss in stiffness was found in comparison to stiffness of healthy beam.

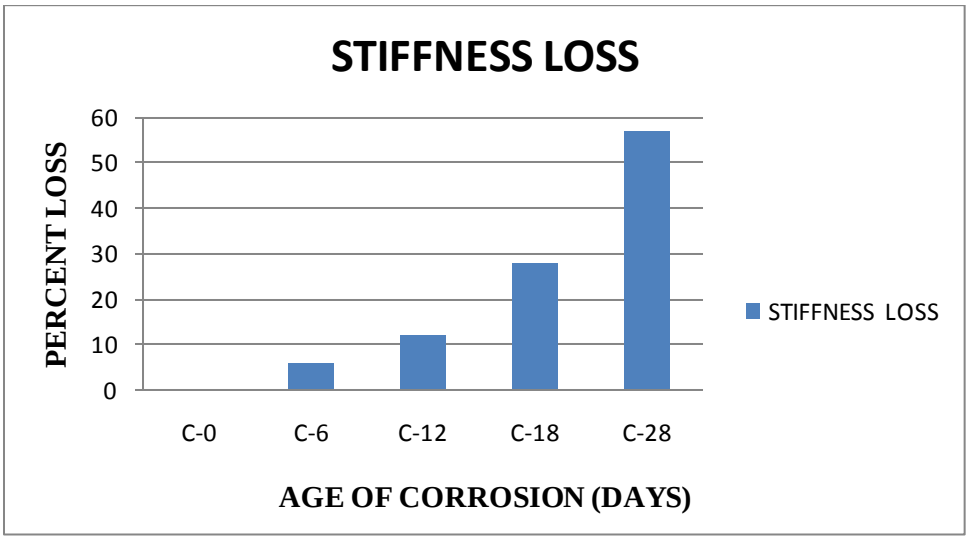

Fig: 5.33 % Loss of Stiffness Vs Age of corrosion

5.6 Mass Loss Determination

Following the mechanical testing, the beams were dismantled with a jackhammer to retrieve the reinforcing steel. Once obtained, centre 1.5m corroded portion of cage was trimmed, cleaned to remove all corrosion products and concrete, and then weighed. The mass loss was then calculated relative to a predetermined benchmark called the control mass. Control mass was calculated for fresh uncorroded bars. The corroded reinforcing bars were characterized by percent mass loss (ML), which was calculated by **eq: 5.1** where *m* denotes mass and the subscript "i" represents the initial or reference mass and "cor" represents the residual mass.

$$ML = \frac{mi - mcor}{mi} X\ 100 \qquad \text{- eq. 5.1}$$

Where,

mi = Initial or Reference Mass

mcor = Residual mass

Fig: 5.34 clearly show that mass loss increases with the increases in corrosion level. It was noticed that beams corroded for 6 days, 12 days 18 days and 28 days has percent mass 11.20%, 18.27%, 21.89%, and 25.34% respectively.

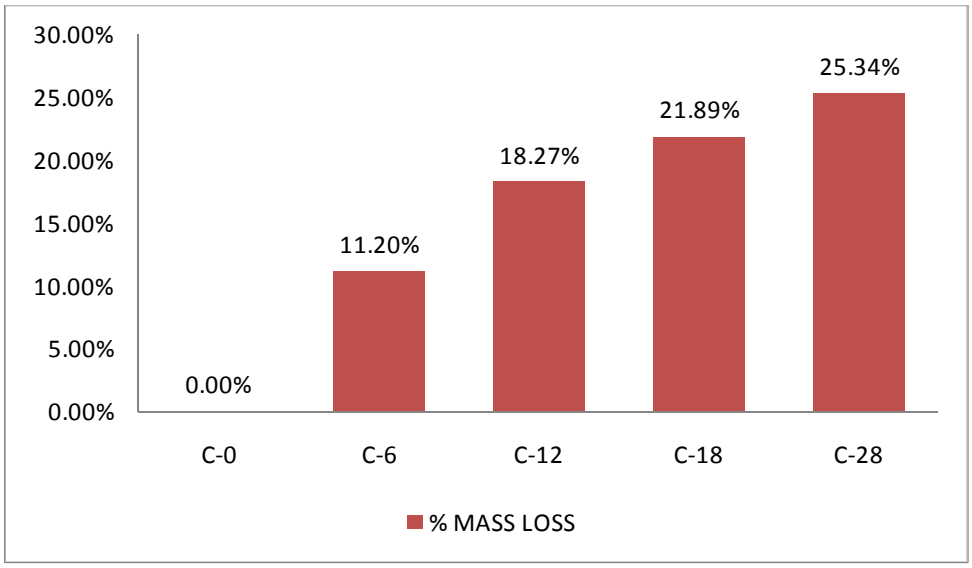

Fig: 5.34 Percent Mass Loss in Bars corroded at different levels

Further percent mass loss was correlated with the ultimate load, ultimate deflections at mid span, and percent stiffness loss in RC beams as discussed below.

- **Correlation b/w Ultimate Load and Percent Mass Loss**

Fig: 5.35 clearly shows that as the percent mass loss increases with increase in corrosion level corresponding ultimate load decreases i.e. load carrying capacity of RC beams decreases with age of corrosion.

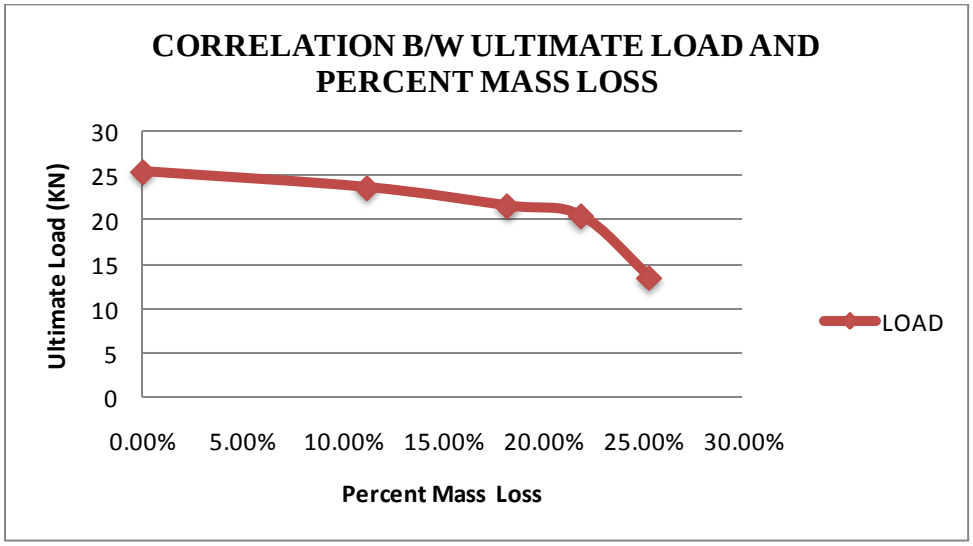

Fig: 5.35 Correlation b/w Ultimate Load and Percent Mass Loss

- **Correlation b/w Ultimate Deflections and Percent Mass Loss**

Fig: 5.26 clearly show that ultimate deflection capacity also decreases with increase in percent mass loss as the corrosion level increases. It shows that there is a great decrease in deflection capacity even at initial stages i.e. from 0 to 6 days of corrosion.

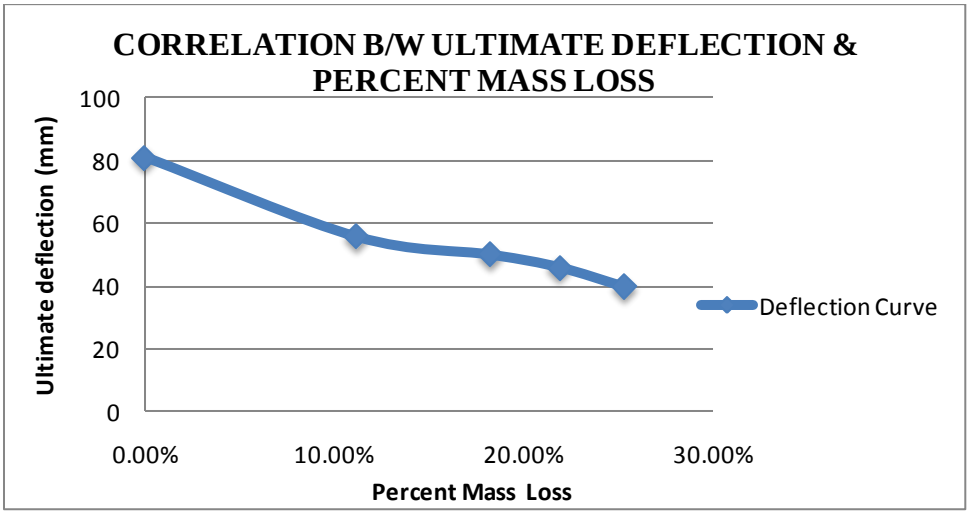

Fig: 5.36 Correlation b/w Percent Mass Loss and Ultimate Deflections

- **Correlation b/w Percent Stiffness Loss and Percent Mass Loss**

Fig: 5.37 shows that percent stiffness loss increases with increase in percent mass loss. It shows that there is small loss in stiffness at initial level of corrosion but as the corrosion level increases from 0 to 28 days loss in stiffness increases.

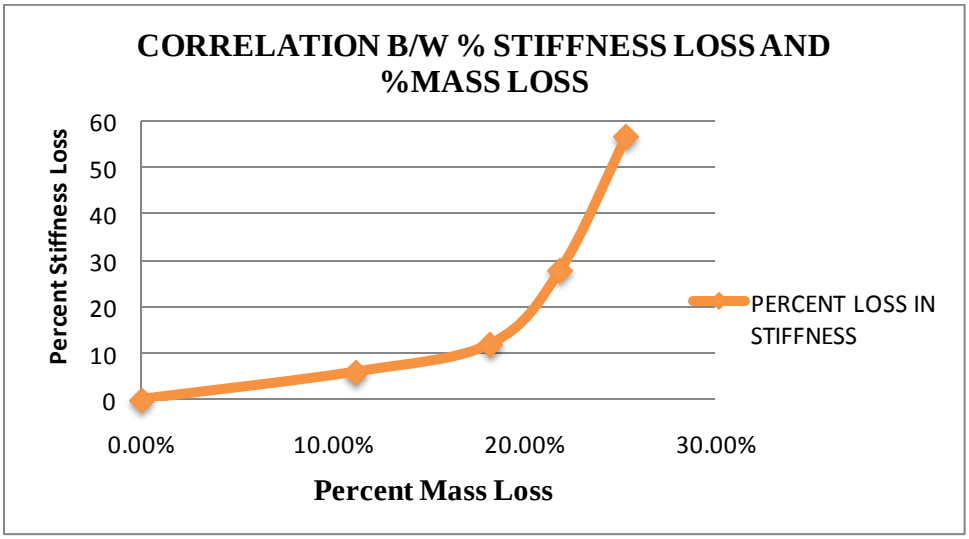

Fig: 5.37 Correlation b/w Percent Stiffness Loss and Percent Mass Loss

5.7 Ultrasonic Testing Results

After finding the percent mass loss of centre 1.5m portion of corroded area, the tension and compression bars were extracted from the corroded portion and trimmed to equal length of 500mm for ultrasonic testing. Extracted bars were visually observed for deterioration due to corrosion, and it was found that with the increase in exposure time of the beams to corrosion, damage to the bars increases, comparison of healthy bar with corroded bar is shown in Fig: 5.34 & 5.35. The extracted bars from the beam subjected to 28 days corrosion shows huge pits on its surface as shown in Fig: 5.36. The type of corrosion found in the more severely corroded bars can be classified as pitting.

After the visual observations of the extracted bars, they were tested both in pulse echo (P/E) and pulse transmission (P/T). As discussed earlier in P/E single transducers is used to send the pulse in the testing bar and same is used for receiving. And in P/T two transducers are used, one act as transmitter to send the pulse wave and other act as receiver. Both the transducers are used on the opposite ends of the bar which is to be tested.

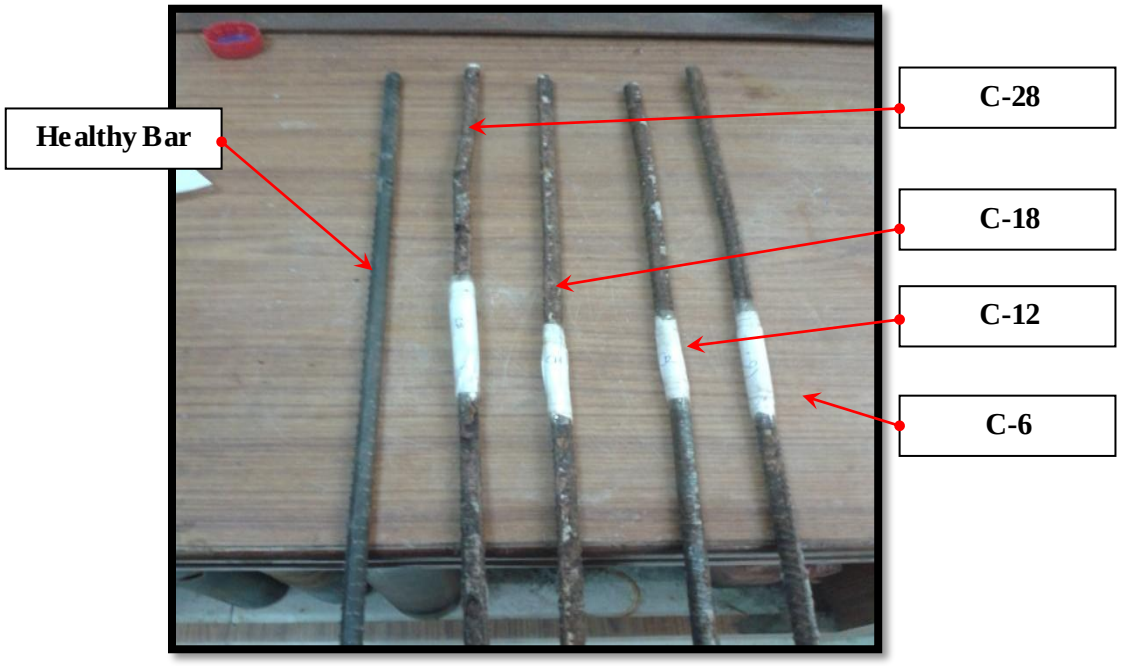

Fig: 5.38 8mm Corroded bars.

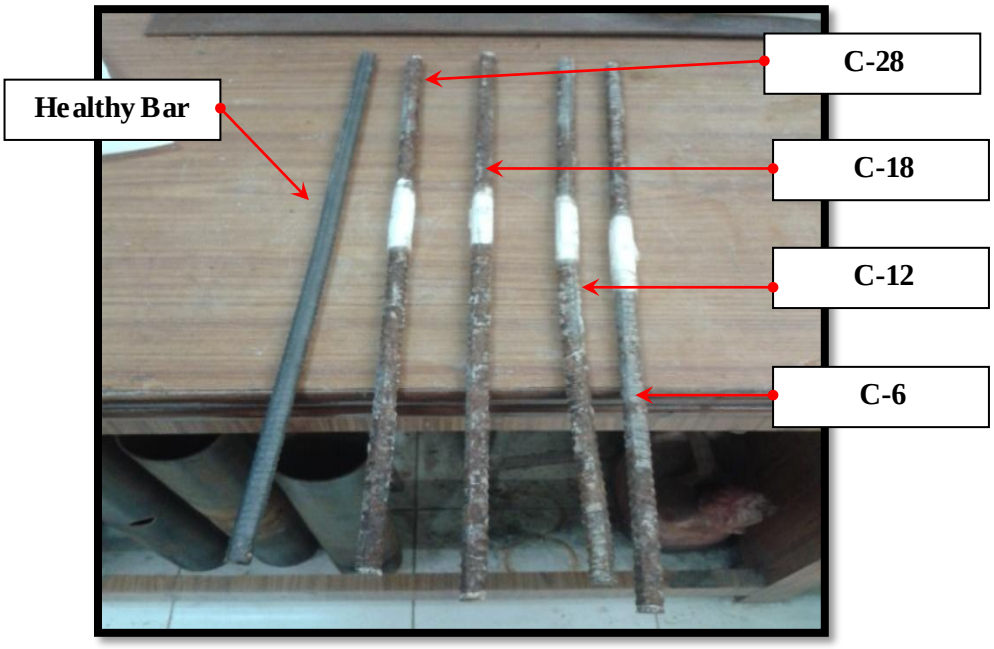

Fig: 5.39 10mm Corroded bars.

Fig: 5.40 Closure View of Pit formation

5.7.1 Pulse Echo Investigations

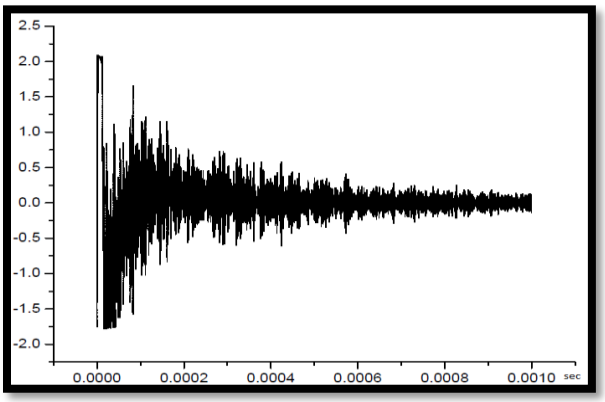

(a) Healthy Bar (C-0)

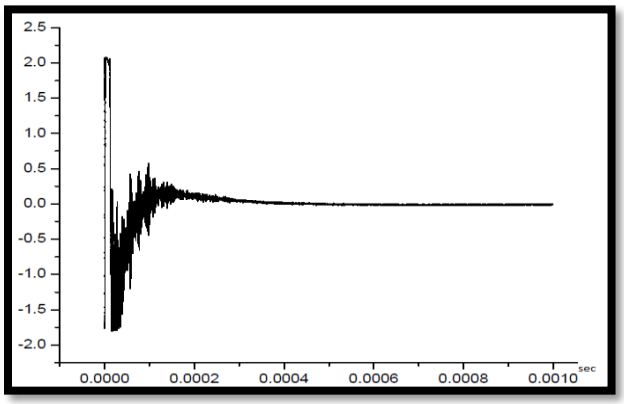

(b) 6 Days Corrosion (C-6)

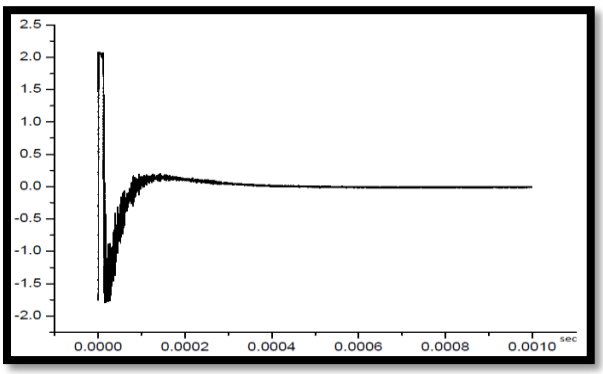

(C) 12 Days Corrosion (C-12)

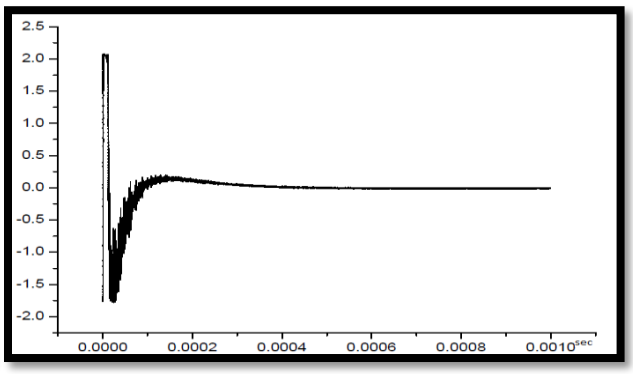

(d) 18 Days Corrosion (C-18)

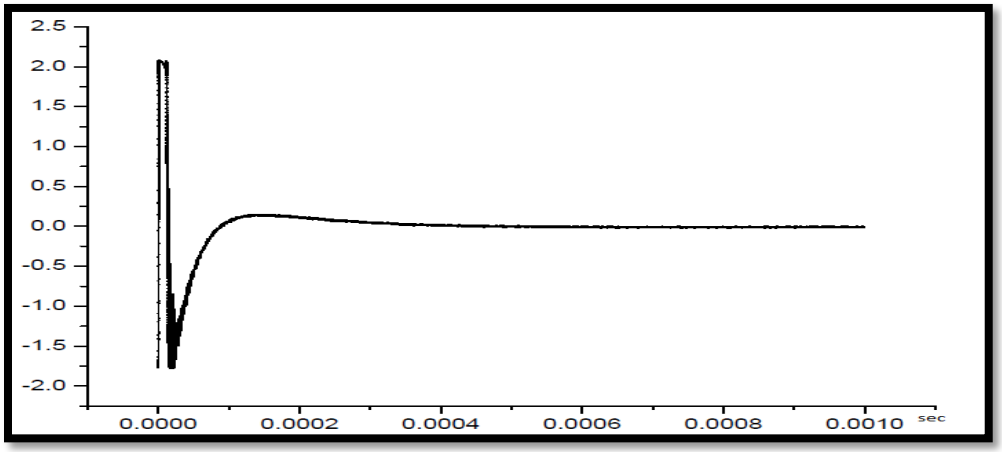

(e) 28 Days Corrosion (C-28)

Fig: 5.41 Pulse Echo (P/E) signatures of 10mm bar

5.7.2 Pulse Transmission Investigations

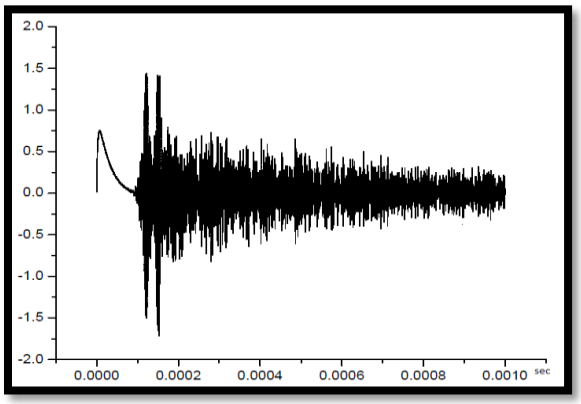

(a) Healthy Bar (C-0)

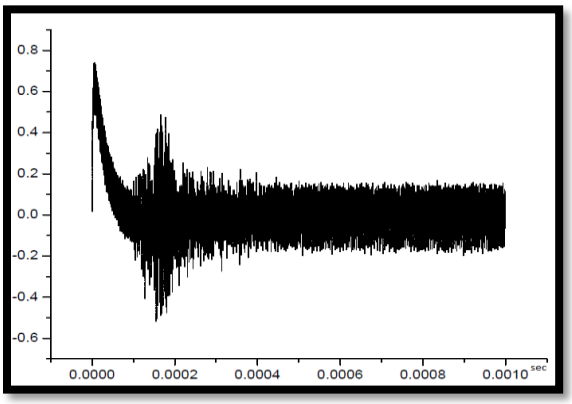

(b) 6 Days Corrosion (C-6)

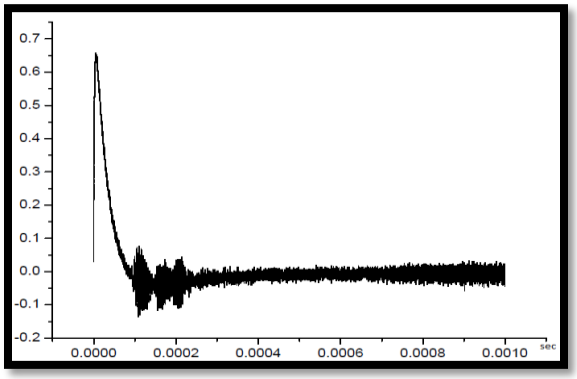

(C) 12 Days Corrosion (C-12)

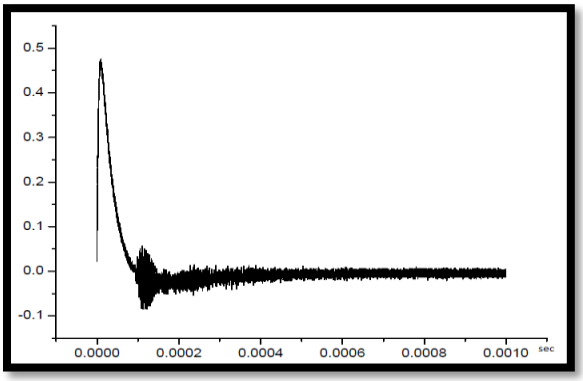

(d) 18 Days Corrosion (C-18)

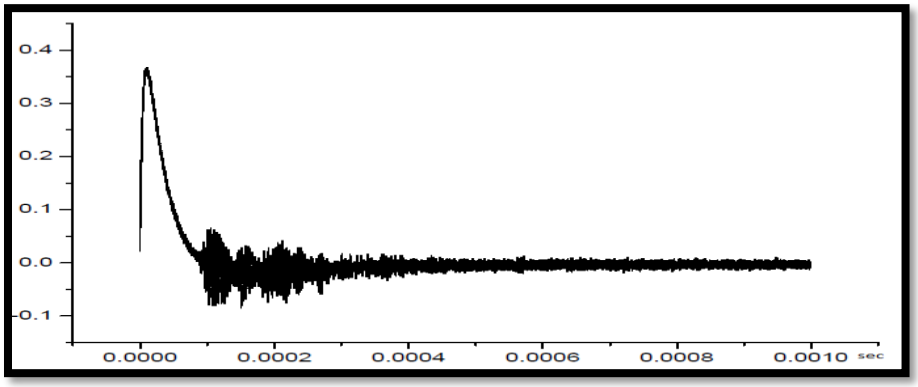

(e) 28 Days Corrosion (C-28)

Fig: 5.42 Pulse Transmission (P/T) signatures of 10 mm bar

It was observed during ultrasonic testing on bars in air, that recorded signatures for pulse echo and pulse transmission shows a decrease in amplitude with the increase in age of corrosion. By studying the relative change in amplitude of the input pulse and transmitted pulse severity of damage can be calibrated.

By observing the peak to peak voltage trend of transmitted peak as shown in Fig: 5.41 to 5.42, it can be said that by increasing the age of corrosion from 0-days to 28-days, the magnitude of transmitted peak decreases. For the bars which are exposed to 28days of corrosion, while taking P/E signatures and P/T, peak was observed but of very small. This is because as the damage in bars increased, more energy is reflected back and less of it travels through the bar to reach the other end. Hence, relative signal attenuation of the transmitted pulse can relate to the extent of the damage in the bar. Thus, peak-to-peak voltage amplitudes of reflected and transmitted peaks in pulse echo and transmission methods closely relate to the extent of damage.

Graphs shown in Fig: 5.43 & 5.44 are plotted using peak values of the voltage from the P/E and P/T signatures. The trend of lines obtained from the peak values for 8mm and 10mm bars clearly shows that there is decrease in amplitude as the corrosion level increases. In P/T 70.24% decrease in amplitude was recorded at initial stages i.e. C-0 to C-6 in case of 10mm bar. This is result is of great importance as it makes the ultrasonic testing fit for detecting small damages.

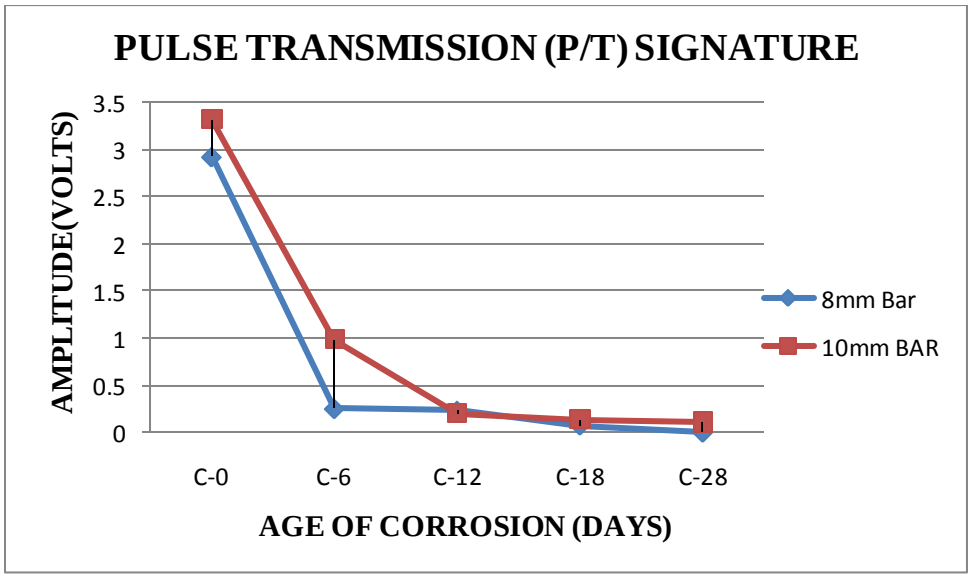

Fig: 5.43 Amplitude Vs Age of Corrosion plot for P/T

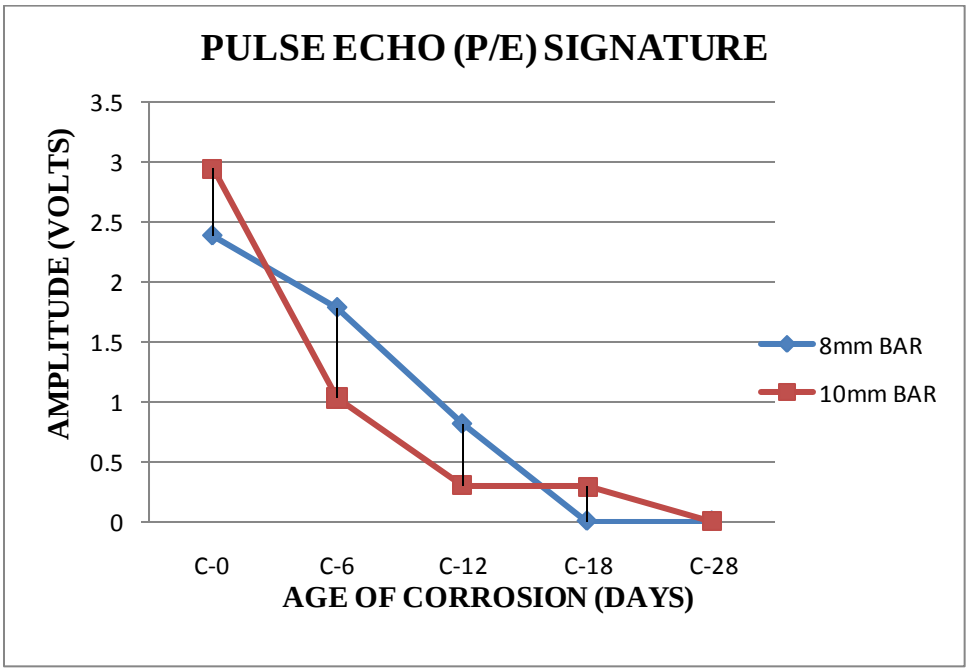

Fig: 5.44 Amplitude Vs Age of Corrosion plot for P/E

The most likely cause of these phenomena is that corrosion affects the waveguide. In the fresh bar the diameter is uniform throughout the length. Thus, a smooth waveguide forms. Corrosion reduces the diameter of the bar non-uniformly. Thus, the waveguide is disturbed and scattering takes place from the rough surface. Moreover corrosion is characterized by large pitting as discussed above that further restricts the passage of waves.

It can be concluded that ultrasonic testing is sensitive enough to detect the damage even at early stages of corrosion i.e. six days of corrosion. It is clear from the trends of line from the Fig: 5.43 & 5.44 that there is great decrease in amplitude voltage from 0 to 6 days of corrosion. So it can be said that RC structures subjected to even 6 days of corrosion shows large defects in the reinforcing bars.

5.8 Closing Remarks

This chapter highlights the results obtained from the experiments done during the thesis work. It shows results of visual observations of RC beams subjected to different levels of corrosion and its effect on load deflection behavior when the RC beams were tested under static

four point loading. From the results it was observed that there is decrease in ultimate load, deflection capacity, stiffness as the corrosion level increases. Mass loss determination was also done which show that percent mass loss increases with increase in corrosion level. Further ultrasonic testing on bars shows dercrease in voltage amplitude with increase in age of corrosion. It shows that even 6-days corrosion can cause severe damages to the bars in RC structures.

CHAPTER – 6
CONCLUSIONS

From the reinforced concrete beams subjected to accelerated corrosion at different levels i.e. 6 days, 12 days, 18days, & 28 days, all beams were visually inspected and it was observed that as exposure time of the beams to corrosion increases deterioration increases. Following results are observed:

- For C-6 Beam shows only reddish brown corrosion patches on the centre 1.5 m portion of beam which was intentionally corroded and which act as a cathode. No cracks were developed on the surface of the beam.
- For C-12 beam small cracks were seen on the surface of beam of smaller length and width and increase in volume of corrosion product was noticed.
- For C-18 beam, increase in length and width of crack was noticed and corrosion liquid of reddish brown colour was seen oozing out from the cracks.
- For C-28 beams, it was observed that the cracks has covered full longitudinal length at middle 1.5m portion of RC beam and corrosion products generated were of dark reddish brown colour of increased volume that other beam with lot of corrosion liquid oozes out from the cracks.

This reddish brown product is a results of rusting of reinforcement in the beams and crack generation is because of tensile stresses generated due to increased volume of bar at cathode area, as we all know concrete is weak in tension so it results in cracking.

After completing the corrosion process beams were subjected to static four- point loading and load-deflection behavior of the beams were observed. Load-deflection curves (LDC) reveal much information concerning the behavior of RC beams and they are notably altered with the progression of corrosion. Static Load test shows the following results:

- As the exposure time of RC beams to corrosion environment increases load carrying capacity of beams decreases.
- Stiffness loss increases with increase in corrosion level.
- Deflection Capacity decreases with the increase in corrosion level.

It was observed from the load deflection behavior of RC beams, ultimate load carrying capacity of C-28 beam reduces almost to half in comparison to C-0 beam. For C-28 beam 47.05% reduction in load carrying capacity and 56.8% loss in stiffness were noticed. This is mainly due to reduction in bar diameter, loss of bond between concrete and steel. Most important effect noticed for RC beams testing under static loading was failure mode of beams shifted from ductile to brittle failure.

Percent mass loss of the corroded bars was calculated and it was observed that mass loss increases with increase in age of corrosion. Maximum mass loss of 25.34% was calculated for C-28 beam. Further percent mass loss was correlated with stiffness, ultimate load and deflection. The following results were noticed:

- Percent Stiffness loss increases with increase in percent mass loss.
- Ultimate load decreases with increase in percent mass loss.
- Ultimate deflection capacity also decreases with increase in percent mass loss.

Ultrasonic testing methods were used to monitor defects in reinforcing bars subjected to varying level of corrosion. It was observed during ultrasonic testing of bars in air, that recorded signatures for pulse echo and pulse transmission shows a decrease in amplitude with the increase in age of corrosion. Results shows that by using ultrasonic methods, even small damages can be easily detected like while taking signatures for pulse transmission 70.24% drop in amplitude voltage was encountered from 0 to 6 days of corrosion of RC beams. Which reveals that for RC structures exposed to 6 days of corrosion can face heavy damages to the reinforcing bars.

REFERENCES

- Andrade, C., Alonso, M. C., and Gonzalez, J. A.,(1990**). An initial effort to use the corrosion rate measurements for estimating rebar durability.** *Corrosion rates of steel in concrete*, ASTM, West Conshohocken, Pa., 29–37.

- Almusallam, A. A., Al-Gahtani, A. S., Abdur Rauf Aziz, and Rasheeduz zafar. (1996b). **Effect of reinforcement corrosion on bond strength**. *Constr. Build. Mat.*, 10(2), 123–129.

- Andrade C, Garcés P, Martínez I., (2008). **Galvanic currents and corrosion rates of reinforcements measured in cells simulating different pitting areas caused by chloride attack in sodium hydroxide**. Corrosion Sci;50:2959-64.

- A.A. Torres-Acosta, M.J. Fabela-Gallegos, A. Muñoz-Noval,D. Vázquez-Vega,J.R. Hernandez-Jimenez,and M. Martínez-Madrid., (2004). **Influence of Corrosion on the Structural Stiffness of Reinforced Concrete Beams.** Nace International.

- Aal H, Assem Adel A., (2003). **Bond of reinforcement in concrete with different types of corroded bars.** Theses and dissertations. Paper 133.

- Abdullah A. Almusallam., (2000**). Effect of degree of corrosion on the properties of reinforcing steel bars.** Department of Civil Engineering, King Fahd University of Petroleum and Minerals, Dhahran 31261, Saudi Arabia.

- Bonacci, J., et al.,(1998). **Laboratory simulation of corrosion in reinforced concrete and repair with CFRP wraps.** *Proc., Canadian Society of Civil Engineering Annual Conf.*, Canadian Society of Civil Engineering, Ottawa, IIIb, 653–662.

- Broomfield, J. P., (1997**). Corrosion of steel in concrete: understanding, investigation, and repair,** E&FN Spon, London.

- Ballim, Y., J.C. Reid., (2003). **Reinforcement corrosion and the deflection of RC beams—an experimental critique of current test methods**. School of Civil and Environmental Engineering, University of the Witwatersrand, Private Bag 3, WITS, 2050 Johannesburg, South Africa.

- El Maaddaway T, Soudki K., (2003). **Effectiveness of impressed current technique to simulate corrosion of steel reinforcement in concrete**. J Mater Civil Eng 2003; 15(1):41-7.

- G. Malumbela, Mark Alexander, Pilate Moyo., (2009). **Steel corrosion on RC structures under sustained service loads -A critical review.** Department of Civil Eng., University of Cape Town, Private Bag X3, Rondebosch, 7700, South Africa.

- G. Malumbela, P. Moyo & M. Alexander., (2009). Structural behaviour of beams under simultaneous load and steel corrosion. University of Cape Town, South Africa.

- Iyer, S., (2002). **Evaluation of ultrasonic C-scan imaging to detect corrosion and voids in post-tensioning tendons.** M.S. Thesis, The Pennsylvania State University.

- Joyce, T. A. (2008). **The Effects of Steel Reinforcement Corrosion on The Flexural Capacity and Stiffness of Reinforced Concrete Beams**. MASc Thesis, Ryerson University, Toronto.

- Jones, R., S. Pitt, M. Tan, C. Wallbrink, W.K. Chiu., (2006). **Interaction of ultrasonic waves with structural damage: A diffraction analogy.**

- Kivell, A. Palermo and A. Scott., (2011). **Effects of Bond Deterioration due to Corrosion in Reinforced Concrete.** Department of Civil and Natural Resources Engineering, University of Canterbury, Christchurch, 8140, New Zealand.

- Liang, M., Po-Jen Su., (2001). **Detection of the corrosion damage of rebar in concrete using impact-echo method.** Department of Harbor and River Engineering, National Taiwan Ocean University, Number 2, Pei-Ning Road, Keelung 20224, Taiwan, ROC.

- Nicholas J. Carino., (1999). Nondestructive Technique to investigate corrosion status in concrete structures. Journal of Performance of constructed facilities. J. Perform. Constr. Facil. 1999.13:96-106.
- Okude, N., Kunieda, M., Tomoki Shiotani and Hikaru Nakamura., (2009). **Flexure Behaviour of RC beams with rebar corrosion and damage evaluation by Acoustic Emmission**.

- Phuvoravan, K., **Effect of Steel Corrosion Level on Flexural Behaviour of Reinforced concrete beam.** Lecturer, Faculty of Engineering, Kasetsart University, Bangkok, Thailand, fengkpp@ku.ac.th.
- Sharma, S., and Mukherjee, A., (2011). **Monitoring corrosion in Oxide and Chloride Environments Using Ultrasonic Guided Waves**. Journal of materials in Civil Engineering.

- Sharma, S., and Mukherjee, A., (2010). **Longitudinal Guided Waves for Monitoring Chloride Corrosion in Reinforcing Bars in Concrete.** Structural Health Monitoring, Sage Publications.

- Sharma, S., (2010). **Monitoring of Damage in Reinforcement in concrete.** Thesis, (Doctor of Philosophy) Department of Civil Engineering Thapar University, Patiala, India.

- Toongoenthong, K., and Maekawa, K., (2005). **Multi-mechanical approach to structural performance assessment of corroded RC members in shear**. Journal of Advanced Concrete Technology, 3(1), 107-122.

- Smith, Roger W., (2007). **The effects of corrosion on the performance of reinforced concrete beams**. Master Thesis. Toronto, Canada, Paper 149.

- Torres-Acost, A. A., Navarro-Gutierrez, S., and Terán-Guillén, J. (2007). **Residual flexure capacity of corroded reinforced concrete beams.** Engineering Structures, Vol. 29, No. 6, pp. 1145-1152.

- Vermani, G., (2008**). Damage Detection in Reinforcing Steel Bars using Ultrasonic wave propagation.** Masters Thesis, Thapar University, Patiala, India.

- Vidal T, Castel A, Francois R., (2004). **Analyzing crack width to predict corrosion in reinforced concrete**. Cement Concrete Res ;34:165-74.

- Wang Y, Zhu XQ, Hao H, Ou JP., (2009) **Guided wave propagation and spectral element method for debonding damage assessment in RC structures**. J Sound Vib;324:751–72.

- Webster, M, P., (2000). **The Assessment of Corrosion damaged concrete structures.** A Thesis submitted to The University of Birmingham for the degree of Doctor of Philosophy.

- Ye Lu, Jianchun Li, Lin Ye, Dong Wang., (2013**). Guided waves for damage detection in rebar-reinforced concrete beams.** Construction and Building Materials 47 (2013) 370–378.